

Characterization of putative G1/S transcription complex factors Swi6p, Swi4p and
Mbp1p in the fungal pathogen *Candida albicans*

Yaolin Chen

A Thesis

in

The Department

of

Biology

Presented in Partial Fulfillment of the Requirements
for the Degree of Master of Science (Biology) at
Concordia University
Montreal, Quebec, Canada

March 2013

©Yaolin Chen, 2013

CONCORDIA UNIVERSITY

School of Graduate Studies

This is to certify that the thesis prepared

By: Yaolin Chen

Entitled: Characterization of putative G1/S transcription complex factors Swi6p, Swi4p and Mbp1p in the fungal pathogen *Candida albicans*

and submitted in partial fulfillment of the requirements for the degree of

Master of Science (Biology)

complies with the regulations of the University and meets the accepted standards with respect to originality and quality.

Signed by the final examining committee:

_____ Selvadurai Dayanandan _____ Chair

_____ Malcolm Whiteway _____ Examiner

_____ Reginald Storms _____ Examiner

_____ Vladimir Titorenko _____ External Examiner

_____ Catherine Bachewich _____ Supervisor

Approved by _____ Selvadurai Dayanandan _____
Chair of Department or Graduate Program Director

Date

Dean of Faculty

ABSTRACT

Characterization of putative G1/S transcription complex factors Swi6p, Swi4p
and Mbp1p in the fungal pathogen *Candida albicans*

Yaolin Chen

The G1/S transition governs cell proliferation in many systems, and involves essential transcription complexes such as SBF and MBF in *Saccharomyces cerevisiae*, or MBF in *Schizosaccharomyces pombe*. SBF and MBF are composed of the regulatory subunit Swi6p and the DNA-binding elements Swi4p (SBF) or Mbp1p (MBF). The fungal pathogen *Candida albicans* contains orthologues of *SWI6*, *SWI4* and *MBP1*. Previous genetic, DNA expression and bioinformatic data suggest that Swi4p and Swi6p may be core components of a single MBF-like complex. However, direct evidence is lacking, and the role of Mbp1p is unclear. In order to determine the composition and mechanisms of action of the putative G1/S transcription complex in *C. albicans*, and identify other factors important for G1/S control, we determined physical interactions between Swi6p, Swi4p and Mbp1p using co-immunoprecipitation, systematically affinity-purified each protein and identified interacting factors through mass spectrometry, and investigated putative Swi4p targets using genome wide location analysis (ChIP-chip). We show that Swi6p physically interacts with Swi4p and Mbp1p, and Swi4p may bind Mbp1p. Affinity purifications did not identify many additional interacting proteins, suggesting that Swi6p, Swi4p and Mbp1p may be the core complex

factors. Finally, ChIP-chip analysis identified putative Swi4p targets including G1 cyclins, cell wall-associated factors, and regulators of hyphal growth, consistent with the *swi4Δ/Δ* phenotype. Unexpectedly, few putative Swi4p target promoters contained the conserved MBF binding site (ACGCGT). Rather, 8.6% contained a canonical SBF-binding (CNCGAAA) motif, and 43.0% contained a related motif, CACAAAA. Although the ChIP-chip data require confirmation by qPCR, the results suggest that Swi4p may be involved in regulating G1/S progression and hyphal development, but may not exclusively function through the conserved MBF-binding element. In summary, our results provide new insights on G1/S regulation in *C. albicans*, which have important implications for controlling cell proliferation and development in the pathogen.

Acknowledgements

First, I would like to sincerely thank my supervisor Dr. Bachewich for providing the wonderful opportunity to do the research work and learn about *C. albicans*. Your enthusiasm and rigorous attitude for work is truly impressed. Thank you very much for your knowledge and patient guidance through these years.

I would also like to thank my former committee members, Dr. Zerges and Dr. Piekny for your time and guidance. And thank my new committee members, Dr. Whiteway, Dr. Storms and Dr. Titorenko, for your kindly being my committee for my thesis and defense.

To my lab colleague Amandeep, thank you for all your help. It's a great pleasure to have worked with you. You are really helpful and have answered so many of my questions, and if you charge for it, you must be a millionaire. Also, thanks to other lab members Amin, Amir, Stephanie, Sara and Jim. Although we worked only for a short period, we had a great time together.

Also, I would like to thank Dr. Bonneil from Proteomic Centre of University of Montreal, who helped do the mass spectrometry; and Dr. Weber and Dr. Raymond from University of Montreal, in whose lab we did the ChIP-chip experiment.

Table of Contents

List of Figures	vi
List of Tables	viii
List of Acronyms	ix
1. Introduction.....	1
1.1 Eukaryotic Cell Cycle.....	1
1.1.1 General overview.....	1
1.1.2 The G1/S transition.....	2
1.1.3 The relationship between G1/S phase and Development	7
1.2 <i>Candida albicans</i>	8
1.2.1 An opportunistic fungal pathogen.....	8
1.2.2 Virulence-determining traits: Morphogenesis	9
1.2.3 Virulence-determining trait: Cell proliferation.....	11
1.2.4 Relationship between the Cell cycle and Morphogenesis: the importance of G1 phase	15
1.2.5 Summary:.....	17
1.3 Objectives	17
2. Materials and Methods.....	18
2.1 Strains, oligonucleotides and plasmids.....	18
2.2 Medium and growth conditions	22
2.3 Construction of strains	23
2.3.1 <i>SWI4</i>	23
2.3.1.1 <i>SWI4-HA</i>	23

2.3.3 <i>MBP1</i>	27
2.3.4 Complementary strains	32
2.4 <i>Escherichia coli</i> transformation	36
2.5 Transformation of <i>C. albicans</i>	37
2.6 Genomic DNA (gDNA) extraction	37
2.7 PCR screening	38
2.8 Protein Extraction	42
2.8.1 Protein extraction by bead-beating.	42
2.8.2 Protein extraction by lyophilisation.	42
2.9 Western Blotting	43
2.10 Co-Immuoprecipitation	44
2.11 Two Step Affinity Purification	45
2.12 ChIP-chip	47
2.13 Cell imaging	49
3. Results	50
3.1 Physical interactions between Swi6p, Swi4p and Mbp1p	50
3.1.1 Swi6p physically interacts with Swi4p <i>in vivo</i>	50
3.1.2 Swi6p physically interacts with Mbp1p <i>in vivo</i>	51
3.1.3 Swi4p and Mbp1p may interact.	52
3.2 Affinity purification of Swi6p, Swi4p and Mbp1p and mass spectrometry analyses of putative interacting proteins.	55
3.2.1 Swi6p-intertacting proteins	56
3.2.2 Swi4p-intertacting proteins	57
3.2.3 Mbp1p-intertacting proteins	58

3.2.4 Swi6p-interacting proteins in cells blocked in G1 phase.....	58
3.3 Mbp1p is expressed at lower levels than Swi4p or Swi6p.....	60
3.4 Identification of possible Swi4p targets using genome-wide location analysis (ChIP-chip).	61
3.4.1 Global ChIP-chip results.....	61
3.4.2 Comparison of location and expression data reveals some overlap and underscores putative Swi4p targets.....	63
3.4.3 A large proportion of Swi4p-enriched loci do not contain the predicted MCB element.....	65
4. Discussion.....	102
4.1 Physical interactions between Swi6p, Swi4p and Mbp1p: implications for G1/S transcription complex composition.....	103
4.2 Systematic affinity purifications of Swi6p, Swi4p and Mbp1p reveal few other predominant interacting proteins.	105
4.3 ChIP-chip analysis identifies putative Swi4p targets involved in G1/S progression and filamentous growth.....	106
4.4 Swi4p may not function exclusively through the conserved MCB element.....	108
References:.....	110
Appendix I: Full list of Orbitrap LC/MS and Swi4p ChIP-chip data (See excel files in attached CD).	116
Appendix II: Identification of additional factors that contribute to G1/S regulation using a directed approach: Characterization of orf19.5961 (See word file in attached CD).	116

List of Figures

Figure 1 : Comparison of G1/S transcription regulation in yeast and metazoan	4
Figure 2: Signaling pathway during yeast-hyphal transition	11
Figure 3: The putative G1/S circuit in <i>C. albicans</i> compared to <i>S. cerevisiae</i>	13
Figure 4. One-step PCR strategy for tagging a gene with HA, TAP or MYC.....	67
Figure 5. Two-step PCR strategy for tagging a gene with HA, TAP or MYC.....	68
Figure 6. Western blot and growth curve confirming proper expression and function of Swi6p-TAP.	69
Figure 7. Confirmation of a <i>swi4Δ/SWI4-HA</i> strain.	70
Figure 8. PCR and Western blot confirmation of tagging <i>SWI4</i> with HA in a strain carrying <i>SWI6-TAP</i>	71
Figure 9. Co-immunoprecipitations demonstrate interactions between Swi4p and Swi6p.	72
Figure 10. PCR and Western blot confirmation of an <i>mbp1Δ/MBP1-TAP</i> strain.	73
Figure 11. PCR and Western blot confirmation of a <i>swi6Δ/SWI6-HA</i> strain.	74
Figure 12. Growth curve of strains carrying a single copy of <i>SWI6-HA</i> or <i>MBP1-TAP</i> . .	75
Figure 13. PCR and Western Blot confirmation of a <i>swi6Δ/SWI6-HA, MBP1/MBP1-TAP</i> strain.....	76
Figure 14. Co-immunoprecipitations demonstrate physical interactions between Mbp1p and Swi6p.....	77

Figure 15. PCR and Western Blot confirmation of an <i>MBP1/MBP1-TAP swi4Δ/SWI4-HA</i> strain.....	78
Figure 16. Co-immunoprecipitation of Swi4p and Mbp1p using IgG sepharose beads. ...	79
Figure 17. Confirmation of a <i>swi4Δ/SWI4-MYC</i> strain.	80
Figure 18. PCR and Western Blot confirmation of a <i>swi4Δ/SWI4-MYC MBP1/MBP1-TAP</i> strain.....	81
Figure 19. Co-immunoprecipitations on Swi4p-MYC and Mbp1p-HA using anti-HA beads.	82
Figure 20. Co-immunoprecipitations of Swi4p and Mbp1p using anti-HA beads.	83
Figure 21. Confirmation of a <i>swi4Δ/SWI4-TAP</i> strain.....	84
Figure 22: Tandem affinity purification of Swi6p, Mbp1p, and Swi4p	85
Figure 23. PCR and Western confirmation of tagging of <i>SWI6</i> with TAP in a <i>cln3Δ/MET3::CLN3</i> strain.....	91
Figure 24: Protein expression levels of Swi4p, Swi6p and Mbp1p under yeast and hyphal growth conditions.....	94
Figure 25: Genome-wide location analysis of Swi4p-HA.....	95
Figure 26: Compariosn of ChIP-chip location and DNA expression data.....	99
Figure 27: Motifs enriched in promoters of genes bound by Swi4p-HA.	100

List of Tables

Table 1: <i>Candida albicans</i> strains used in this study.....	18
Table 2: Oligonucleotides used in this study	20
Table 3: Plasmids used in this study	22
Table 4: Orbitrap LC/MS analysis of putative Swi6p-interacting proteins	86
Table 5: Orbitrap LC/MS analysis of putative Swi4p-interacting proteins.	87
Table 6: 1 st Orbitrap LC/MS analysis of putative Mbp1p-interacting proteins.	89
Table 7: Orbitrap LC/MS analysis of putative Mbp1p-interacting proteins from larger cultures.....	90
Table 8: Orbitrap LC/MS analysis of putative Swi6p-interacting proteins in cells blocked in G1 phase.	92
Table 9. Select Swi4p-enriched targets	96
Table 10: GO slim analysis of Swi4p-enriched targets	98
Table 11. Swi4p-HA enriched promoters containing SCB (CNCGAAA) or MCB(ACGCGT) elements	101

List of Acronyms

bp	base pair(s)
BSA	Bovine Serum Albumin
cAMP	Cyclic adenosine monophosphate
CDC	Cell division cycle
CDK	Cyclin-dependent kinase
ChIP	Chromatin Immunoprecipitation
DAPI	4', 6'-diamidino-2-phenylindole dihydrochloride
DNA	Deoxyribonucleic acid
dNTP	Deoxyribonucleotide triphosphate
EDTA	Ethylenediaminetetraacetic acid
FBS	Fetal Bovine Serum
gDNA	Genomic DNA
HDAC	Histone deacetylase
hr	Hour(s)
kb	kilo base pair(s)
L	Litre(s)
LiAc	Lithium acetate
MAP	Mitogen-activated protein
MBF	<i>MluI</i> binding factor
MCB	<i>MluI</i> cell cycle box
-MC	SD medium lacking methionine and cysteine.
+MC	SD medium supplemented with 2.5mM methionine and 0.5mM cysteine.
min	Minute(s)
ml	Milliliter(s)
nt	nucleotides
O.D.	Optical Density
PCR	Polymerase chain reaction
qPCR	Quantitative PCR
PEG	Polyethylene glycol
Rcf	Relative Centrifugal Force
RNA	Ribonucleic acid
rpm	Rotations per minute
SBF	Swi4-Swi6 cell cycle box binding factor
SCB	Swi4/6 cell cycle box
SD	0.67% yeast nitrogen base without amino acids, 2% glucose
SDS	Sodium Dodecyl Sulfate
sec	Second(s)
ssDNA	Salmon Sperm DNA
TRIS	Tris(hydroxymethyl)aminomethane
YPD	1% yeast extract, 2% peptone, 2% dextrose

1. Introduction

1.1 Eukaryotic Cell Cycle

1.1.1 General overview

The cell cycle comprises a series of events that allow cells to duplicate [1]. In many systems, the cell cycle consists of several phases, including G1, S, G2, M phase, as well as cytokinesis. Genetic material is replicated during S-phase, then segregated into two identical daughter cells during M phase and cytokinesis. The S and M-phases are separated by two gap phases (G1 and G2) that are associated with cell growth in many organisms [2].

Proper cell cycle progression has crucial implications for cell growth and development, as well as diseases such as cancer. It is thus important to understand how it is regulated [1]. The cell cycle is controlled at many different levels that include both transcriptional and post-translational mechanisms [3]. One central and conserved regulator of cell cycle progression includes the cyclin-dependent kinases (CDKs) [4]. These kinases associate with phase-specific cyclins to mediate transitions between cell cycle stages. For example, in metazoans, Cyclin D/Cdk4–6 promotes G1 progression, cyclin E/Cdk2 governs the G1/S transition, cyclin A/Cdk 2 promotes S phase progression and the S/G2 transition, while cyclin B/Cdk1 governs the G2/M transition [5]. The cell ensures that all previous processes have been completed correctly before permitting progression to the next phase, and achieves this through utilizing different checkpoints. Major checkpoints exist at the G1/S, G2/M and metaphase-to-anaphase transitions [6].

For example, in response to DNA damage, a checkpoint pathway is activated that ultimately impinges on and inhibits Cdk/Cyclin B, which in turn prevents the G2/M transition and provides time for repair [7, 8].

1.1.2 The G1/S transition

a. Mammalian cells

The G1/S transition is called the Restriction Point in metazoans [9, 10] and represents the phase when many cells commit to mitotic cell division [11]. Entry into a new cell cycle involves a burst in transcription of G1/S-associated genes. Upstream of this circuit lies CDK activity, including CDK4/cyclin D. Mitogenic growth factors induce activation of cyclin D, which associates with the catalytic subunit CDK4/CDK6. This CDK/cyclin complex then phosphorylates Retinoblastoma protein (pRb). pRb is hypophosphorylated in G0 and early G1, and in this form represses a heterotrimeric G1/S transcription factor complex called E2F. The E2F family of transcription factors are important for cell cycle entry [12]. Three members of this family, E2F-1, E2F-2 and E2F-3a, are activators of G1/S transcription, while others act as suppressors [13]. For example, E2F-1 is directly involved in the DNA synthesis and repair, cell proliferation and apoptosis [14, 15]. The E2F consensus binding site is “TTTCGCGC” [16] and is present in the promoters of target genes including cyclin E, cyclin A, cyclin D1, Cdc2 kinase, DNA polymerase A, thymidine kinase, and factors essential for DNA replication, including Cdc6, ORC1, and MCM, for example [17]. E2F remains inactive when bound

by pRb [18]. Phosphorylation of pRb by cyclin D-Cdk4/6 during G1 phase results in its disassociation from E2F, thus activating E2F target genes. Some important E2F target genes, such as cyclin E and cyclin A, associate with Cdk2 and further target pRb for hyperphosphorylation in a positive feedback manner [19] (Fig. 1).

b. Saccharomyces cerevisiae

The G1/S circuitry shows some conservation from yeast to man. For example, in the model budding yeast *Saccharomyces cerevisiae*, an upstream regulatory component is the CDK Cdc28p, which associates with the G1 cyclin Cln3p. Cdc28p/Cln3p phosphorylates and antagonizes Whi5p, which is a functional analogue of mammalian pRb but has no sequence similarity [20]. Whi5p in turn antagonizes SBF, which is the functional equivalent of mammalian E2F but also has no sequence homology [21]. SBF, as well as another complex, MBF, are required for G1/S transcription in this organism. SBF and MBF are composed of ankyrin-repeat proteins and have homologues in most fungi where known. SBF is composed of the transcriptional activator Swi6p and a DNA binding factor, Swi4p, which binds SCB (Swi4/6 cell cycle binding box) elements [22]. In early G1, SBF binds to target promoters but is maintained in a repressed state by association with Whi5p. Phosphorylation of Whi5p and SBF complexes by Cdc28p/Cln3p results in Whi5p dissociation from SBF promoters and nuclear export, which permits SBF-dependent transcription and cell cycle entry [23, 24]. Transcriptional repression of SBF targets when cells exit G1 phase is promoted by B-type cyclin associated with Cdc28p. This activity leads to dissociation of the SBF transcription factor from promoters [25] (Fig. 1).

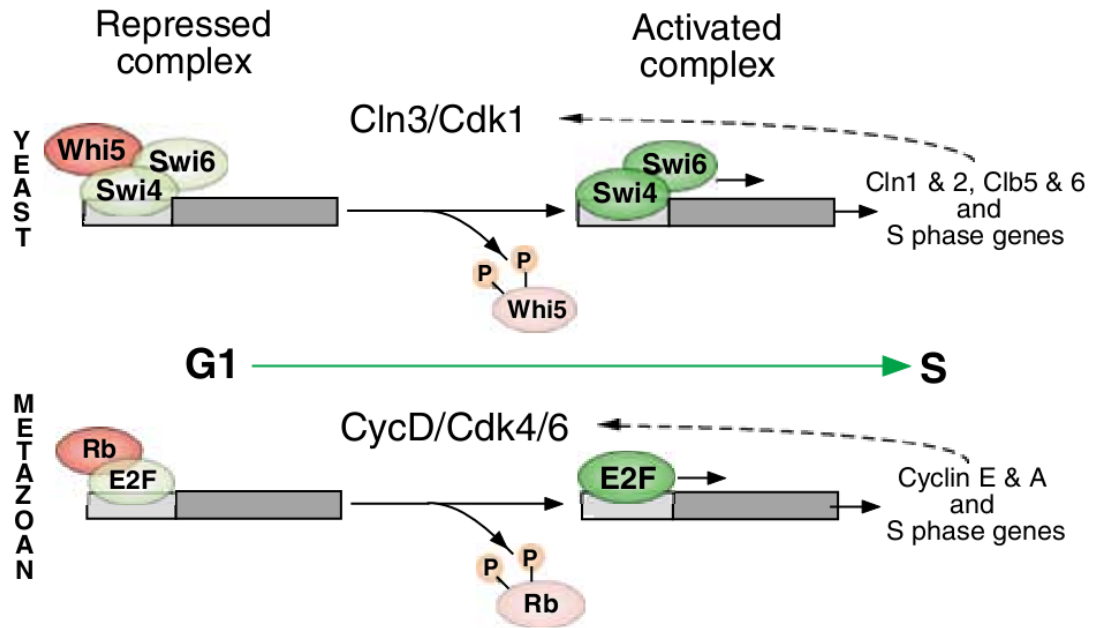


Figure 1: Comparison of G1/S transcription regulation in yeast and metazoans [26].

MBF is also composed of the activator Swi6p and a different DNA binding factor, Mbp1p, which binds MCB (*Mlu* cell cycle box) elements in promoters of target genes [22]. Unlike SBF, MBF confines the expression of its targets to the G1 phase by repressing transcription outside of G1 phase rather than by promoting transcriptional activation [27]. Nrm1p is a cofactor that assists MBF function, and is also a downstream target. As Nrm1p accumulates during the G1/S transition, it binds to MBF and acts as a transcriptional co-repressor for MBF target genes [28]. In response to genotoxic stress, the S-phase checkpoint protein kinase Rad53p [29] can directly phosphorylate Nrm1p as cells go through S-phase, resulting in its disassociation from MBF and maintenance of expression of MBF target genes [30].

SBF and MBF targets were identified through ChIP-chip analyses [31], and fall into two classes. SBF targets are associated with cell morphogenesis, spindle pole body duplication and other growth-related functions, and include the G1 cyclins *CLN1/2*, *PCL1/2*, as well as other factors such as *GIN4* and *FKS1/2*, for example. On the other hand, MBF targets are involved in the control of DNA replication and repair, and include factors such as *POL2*, *CDC2*, *RNR1* and *CLB5/6*, for example [26]. SBF and MBF can also bind each other's target domain sequence, contributing to some overlap in function. Indeed, absence of *MBP1* or *SWI4* was not lethal due to some redundancy [32]. However, absence of *SWI4* and *SWI6*, or *SWI4* and *MBP1* is lethal and results in a G1 phase arrest [32, 33]. Thus, the complexes are essential for growth. Intriguingly, some SBF/MBF targets don't contain the canonical binding sequences, including G1/S activators *PLM2*, *DUN1*, *EXG1*, and *ERP3*. However, these are cell cycle-regulated with or without *SWI4* and *MBP1* [32], suggesting that there is some Swi4p and Mbp1p-independent regulation of G1/S transcription, albeit via unknown mechanisms.

SBF/MBF activity is also regulated by Bck2p and Stb1p [34]. Bck2p is specific to *S. cerevisiae*, and can activate G1/S transcription independent of Cdc28p [35]. A *cln3Δ* strain will transiently arrest in G1 phase, followed by resumption of budding due to the presence of Bck2p [36]. *BCK2* and *CLN3* redundantly activate transcription of the SBF and MBF target genes but in two different ways; Cln3p acts through SBF and MBF while Bck2p only partly depends upon these factors [37]. Stb1p is a component of both SBF and MBF via binding Swi6p during G1 phase. It has been proposed to contribute to

G1 phase transcription via influencing the histone deacetylase (HDAC) component Sin3p at promoters of G1/S genes [38, 39].

c. Schizosaccharomyces pombe

G1/S circuitry has also been well defined in the fission yeast model *Schizosaccharomyces pombe* with some important variations compared to the situation in *S. cerevisiae*. The CDK Cdc2p associates with some G1 cyclins, including Cig1p, Cig2p and Puc1p [40]. However, evidence supporting a role for Cdc2p/cyclin in activating the G1/S transcription complex, MBF, is lacking. Alternatively, the cyclin Pas1p associated with the cyclin-dependent kinase Pef1p is thought to activate the MBF complex in *S. pombe* [41].

In *S. pombe*, there is only a single MBF complex that mediates G1/S transcription. It is composed of the activating factor Cdc10p and at least two DNA binding elements, Res1p and Res2p [27]. Res1p and Res2p bind to Cdc10p at their C termini and to DNA via their N termini [42]. Res1p and Swi4p, as well as Res2p and Mbp1p, are homologous in their N-terminal regions while Cdc10p and Swi6p are homologous in their C-terminal regions [43, 44]. The DNA-binding activity of MBF is required for controlling several genes important for entry into S phase, including *CDC22*, which encodes the regulatory subunit of ribonucleotide reductase [45], *CDC18*, which encodes a component of the S phase checkpoint [46], and *CDT1*, which is necessary for DNA replication [47]. The promoters of these genes contain the MCB *MluI* cell cycle box, ACGCGT, which is recognized by Res1p and Res2p [44]. Xu *et al.* (2005)

identified 747 cell cycle-regulated genes in *S.pombe*, and out of the 31 G1 phase cluster genes, 20 contained one or more MCB motifs in their promoters [48].

As in *S. cerevisiae*, SpNrm1p is a co-factor of MBF, and functions to help repress G1-specific genes outside of G1 phase [28]. Recently, SpYox1p was identified to be another MBF regulatory component in fission yeast [49]. Similar to *NMRI*, *YOX1* is a target gene of MBF and accumulates during the G1/S transition. Yox1p binds Res2p indirectly via Nrm1p, and contributes to the repression of MBF-regulated genes once cells are out of G1/S phase [49, 50].

1.1.3 The relationship between G1/S phase and Development

G1 phase is a critical control point lying at the interface of the cell cycle and development. Approximately this time in the cell cycle, cells either commit to mitosis and will proliferate, or exit the cell cycle to allow development. For example, mammalian embryonic cells actively divide but exit the cell cycle in G0 in order to differentiate [51]. In *S. cerevisiae*, the developmental processes of meiosis, conjugation tube formation and filamentous growth are also associated with a block in G1 phase, in part through down-regulation of the G1 cyclin Cln3p [52, 53]. In contrast, mutations leading to stabilization of Cln3p result in premature expression of G1-specific genes, small cell size and resistance to G1-phase arrest by mating pheromone [54].

However, some G1/S regulators play direct roles in development, independent of their cell cycle function [55]. For example, E2F1 activates genes including Neogenin, a cell surface protein induced in non-dividing neural cells immediately before terminal differentiation, WASF1, a signal transmission factor specially expressed in the brain, and SGEF, a tissue-specific expressed protein [56]. Furthermore, E2F3 is critical for normal development since only one-quarter of the expected frequency of *e2f3* mutant mice arise [57], and pRB plays a positive role in activation of muscle-specific genes and is necessary for completing the muscle differentiation and myogenic basic helix-loop-helix-dependent transcription [58]. To date, however, G1/S regulators in yeast such as *S. cerevisiae* have not demonstrated cell-cycle-independent functions in development as in metazoans.

1.2 *Candida albicans*

1.2.1 An opportunistic fungal pathogen

Candida albicans is one of the most common fungal pathogens in humans. As a commensal, it lives in the human gastrointestinal and urogenital tracts without harmful effects. However, it is also an opportunistic pathogen that can cause both mucosal and systemic infections in immune-compromised hosts, such as individuals with organ transplants or HIV infection. Disseminated candidiasis, or invasion of the blood stream from a mucosal infection, results in infection of organs, including the kidney, heart, and brain. These systemic infections are associated with high mortality, up to 45% [59, 60].

Common drug treatments include the azoles, which target ergosterol biosynthesis and are typically fungistatic, or the more potent echinocandins, which disrupt the cell wall through targetting (1, 3)-glucan synthesis and are thus fungicidal [61, 62]. However, due to serious side effects and increasing drug resistance, new drug targets and therapeutic strategies are needed [63]. To this end, we require a more comprehensive understanding of the regulatory biology of *C. albicans*.

1.2.2 Virulence-determining traits: Morphogenesis

One aspect of *C. albicans* biology that is important for virulence is its ability to switch between different cell types. *C. albicans* exists in multiple cell forms, including white phase yeast, the less common but mating competent opaque form of yeast, pseudohyphae, true hyphae and chlamydo spores [64]. The yeast form has a specific contribution to the promotion of pathogenesis. For example, they are easier to disseminate in the circulatory system, and produce their own repertoire of secreted aspartyl proteases, which have important relevance for virulence [65]. The filamentous forms, on the other hand, are believed to be better for tissue penetration during infection [66]. This feature is important for colonizing organs such as the kidney and for escaping from macrophage engulfment [67]. Hyphae also express many other specific factors important for virulence, including additional proteases and cell adhesion factors [68]. The ability to switch between the different cell types and have plasticity in form within the host is essential for virulence; mutants locked in one cell form lose pathogenicity [69].

Thus, differentiation is an crucial virulence-determining trait, and it is important to understand its regulation [70].

The yeast-to-hyphal switch represents one of the most studied cell differentiation events in *C. albicans*. The change in cell fate is activated by environmental cues. While yeast growth is favored at 30°C, hyphal growth requires a higher temperature of 37°C in combination with other inputs, including serum, high pH or other factors [71]. These cues are mediated by a variety of environmental signaling pathways, the most characterized of which involve MAPK or cAMP signaling pathways (Fig. 2). Important downstream transcription factors include Efg1p, which is a member of APSES (Asm1p, Phd1p, Sok2p Efg1p and StuAp) family of fungal proteins that regulate differentiation [72]. Negative regulation is mediated in part by the transcriptional repressors Nrg1p, Rfg1p and their co-repressor Tup1p (Fig. 2). Ultimately the pathways control the physical switch to hyphal growth as well as co-expression of hyphal-specific genes (HSG's), many of which are virulence factors [73].

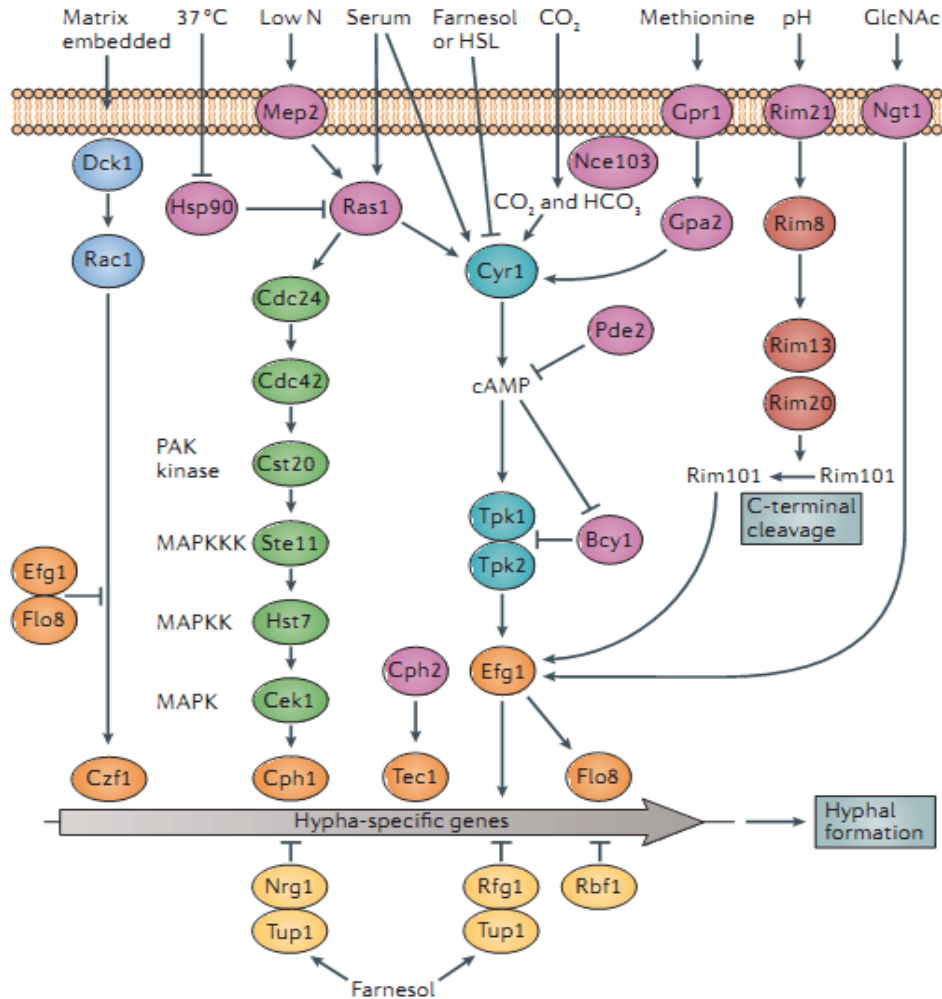


Figure 2: Signaling pathway during yeast-hyphal transition [73].

1.2.3 Virulence-determining trait: Cell proliferation

Another aspect of *C. albicans* biology that is important for pathogenesis is its ability to proliferate. However, we currently have a poor understanding of cell cycle regulation in this organism, particularly the circuitry mediating the G1/S transition and commitment to cell division. This is due in part to the difficulty in synchronizing *C. albicans* cells and the diploid nature of the organism, which in turn hinders traditional

genetic mutational analyses. Nonetheless, Cote *et al.* (2009) were able to synchronize opaque form yeast cells in G1 phase through treatment with pheromone and over-expression of a CDK inhibitor Far1p [74]. Upon release from the block, cells progressed through the cell cycle with a significant degree of synchrony to allow detection of periodic DNA expression patterns. Approximately 500 genes showed transcriptional modulation corresponding to G1/S, S/G2, G2/M, and M/G1 transitions [74]. The expression patterns showed similarity but also many differences to the situations in *S. cerevisiae* and *S. pombe*. Importantly, a large number of genes modulated at G1/S were novel. Furthermore, of the G1/S-modulated genes, only an MCB motif was significantly enriched in the promoters, in contrast to both SCB and MCB motifs in *S. cerevisiae* G1/S-modulated genes. Therefore, genes in *S. cerevisiae* controlled independently by SBF or MBF were proposed to be under the regulation of a single MCB element in *C. albicans*, as in *S. pombe* [74].

Despite this information, only a few factors have been functionally linked to G1 phase regulation in *C. albicans*. For example, an orthologue of the G1 cyclin Cln3p appears to influence G1 phase progression, since its depletion in *C. albicans* yeast cells resulted in large, unbudded cells with a single nucleus [75, 76]. In contrast to the situation in *S. cerevisiae*, however, Cln3p is essential; Cln3p-depleted yeast cells do not resume budding [37, 76]. Rather, the cells switched to the hyphal and pseudohyphal growth mode, suggesting an underlying link between G1 phase and hyphal development in *C. albicans* [76] (Fig. 3).

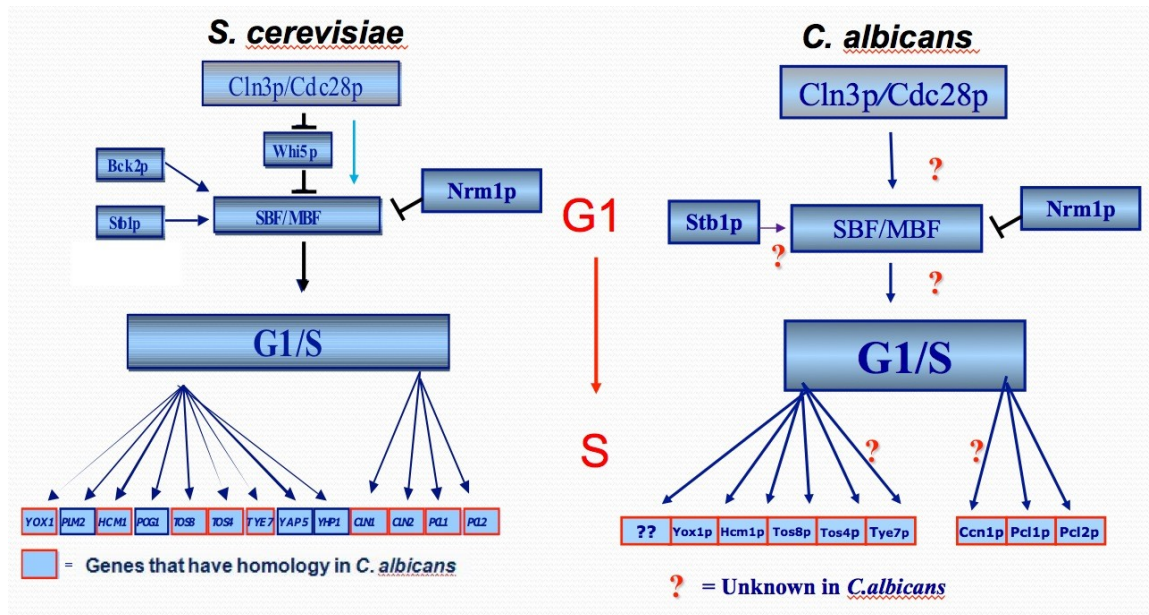


Figure 3: The putative G1/S circuit in *C. albicans* compared to *S. cerevisiae*

C. albicans also contains orthologues of the G1/S transcription factor complex proteins Swi4p, Swi6p and Mbp1p, which are 38, 27 and 29% identical at the protein level to their counterparts in *S. cerevisiae*. Intriguingly, all contain ankyrin-repeat domains and Kila-N DNA-binding domains, while Swi6p in *S. cerevisiae* lacks the latter motif (Candida Genome Database <http://www.candidagenome.org/> and Saccharomyces Genome Database <http://www.yeastgenome.org/>). A recent investigation of function demonstrated that absence of *SWI4* or *SWI6*, but not *MBP1*, in *C. albicans* resulted in cell enlargement, suggesting a delay in G1 phase, and production of filaments [77]. These results underscored a potential link between G1 phase and hyphal development. Intriguingly, cells lacking both *SWI6* and *SWI4* were still viable, did not arrest in G1 phase, and showed enhanced filamentous growth [77]. Similarly, cells lacking *MBP1* and *SWI4* were also viable, enlarged, but resembled the *SWI4* deletion strain. In contrast,

absence of both DNA binding elements in *S. cerevisiae* or *S. pombe* is lethal [78]. Swi6p/Swi4p function was further linked to G1/S regulation since cells lacking these factors showed modulation of some G1/S-associated, periodically expressed genes, including the G1 cyclins *CCN1* and *PCL2*, as well as other factors [77]. Collectively the data supports a model proposing that Swi4p and Swi6p constitute the main players in a G1/S transcription complex in *C. albicans*, which may be the functional equivalent of an MBF, due to the lack of SCB elements in the genome. The role of Mbp1p, however, is less clear [74, 77].

Orthologues of other factors important for G1/S progression in *S. cerevisiae*, including Whi5p, Bck2p and Nrm1p, were considered missing in *C. albicans*. This underscores differences in the circuitry and the need to explore G1/S regulation in the pathogen itself. A recent report identified CaNrm1p, which has very limited sequence homology to Nrm1p in *S. cerevisiae*, yet complements *whi5Δ* and *nrm1Δ* phenotypes [79]. When deleted in *C. albicans*, the cells showed a mild decrease in cell size and increase in hydroxyurea resistance, similar to *whi5Δ* and *nrm1Δ* cells, respectively, in *S. cerevisiae* [79]. In addition, CaNrm1p physically interacted with CaSwi4p in *C. albicans*, and may function through CaSwi4p and CaSwi6p [79]. It thus may be a functional orthologue of Nrm1p in *S. cerevisiae*.

Swi4p and Swi6p function have also been linked to the PKC cell wall integrity pathway in *C. albicans*, as in *S. cerevisiae*. This pathway constitutes key cellular response during resistance to drugs that target the cell membrane, such as azoles [80].

Activation of the pathway leads to a MAPK-dependent modulation of Swi4p and Swi6p, as well as other targets, which are thought to act in part by modulating expression of genes important in cell wall remodeling. Although the targets of Swi4p and Swi6p are not clear in *C. albicans*, these factors influence ergosterol biosynthesis inhibitor tolerance in *S. cerevisiae*, which could provide a mechanism for responding to drug-induced cell wall and membrane damage [81, 82]. Thus, knowledge of the mechanisms of action by which Swi4p and Swi6p function in *C. albicans* has important implications in many contexts.

1.2.4 Relationship between the Cell cycle and Morphogenesis: the importance of G1 phase

In many organisms, development is coordinated with G1 phase of the cell cycle, and cell cycle factors can influence differentiation (**section 1.1.3**). Moreover, in yeast, G1 cyclins are associated with polarized growth of the yeast bud: activation of Cdc28p by the G1 cyclins Cln1p and Cln2p, but not Cln3p, promotes apical growth, while activation of Cdc28p by the mitotic cyclins Clb1p and Clb2p leads to isotropic growth [73, 83]. In *C. albicans*, however, the relationship between G1 phase and hyphal development is complex. For example, hyphal growth is not associated with an extended G1 phase [84], and there is conflicting information on whether hyphal initiation from yeast cells can occur at cell cycle stages later than G1 phase [85, 86]. However, orthologues of G1 cyclins influence hyphal growth. The *C. albicans* homologue of Cln2p in *S. cerevisiae*,

Hgc1p, is specifically required for hyphal induction; it is not expressed in yeast cells but essential for hyphal formation [87]. Hgc1p interacts with the CDK Cdc28p to promote hyphal morphogenesis, and it might also play an important role in preventing cell separation by sequestering some polarity proteins from the site of cytokinesis [87]. Furthermore, the Cln1p cyclin homologue CaCln1p is also needed for maintaining hyphal growth [88].

However, this data does not necessarily support a link between G1 phase and hyphal development; Hgc1p has no known cell cycle or G1 phase function, and yeast cells lacking Ccn1p show only slightly slower growth. The strongest line of evidence supporting a link between G1 phase and hyphal growth in *C. albicans* includes work on the G1 cyclin Cln3p. Depletion of Cln3p in yeast induced a G1 phase arrest and development of hyphae and pseudohyphae in the absence of hyphal-inducing conditions, in a manner that was dependent on hyphal signaling pathway components Efg1p and Ras1p [73, 76]. Intriguingly, hyphae resumed their cell cycles, despite absence of Cln3p, suggesting differential regulation of the cell cycle in yeast vs hyphae [75]. In contrast, arresting or slowing other cell cycle phases in *C. albicans* yeast results in elongated buds or pseudohyphae, respectively [85]. The facts that cells lacking Swi4p and Swi6p also form some true hyphae, and that Nrm1p represses some hyphal specific genes, further underscores the existence of link between G1 phase and hyphal development, although the mechanisms remain unclear. A G1 phase-dependent bias for hyphal initiation could exist [75-77, 79, 84], but strong environmental inducers such as serum

may be able to override this relationship, allowing hyphal formation at other cell cycle stages [89].

1.2.5 Summary:

Elucidating the regulation of the G1/S transition in *C. albicans* has crucial implications for understanding how cell proliferation in the pathogen is controlled, and determining the mechanisms linking this cell cycle stage with hyphal development. A framework for G1/S regulation is emerging, but some important questions remain. Homologues of Swi4p, Swi6p and Mbp1p exist in *C. albicans* and were genetically linked to G1/S control, but evidence that they act as a complex, and whether one or more complexes are required, is lacking. Furthermore, the precise binding sequence of the G1/S regulatory complex(es) and identity of specific targets has not been explored. Finally, current data suggests that factors other than Swi6p, Swi4p and Mbp1p contribute to G1/S regulation in *C. albicans*, but their identity remains unknown.

1.3 Objectives

The major aims of this thesis include: 1) Determine physical interactions between Swi6p, Swi4p and Mbp1p in order to elucidate their potential for forming a complex(es); 2) Identify interacting factors of Swi6p, Swi4p and Mbp1p in order to address their function, possible regulation, and identify additional factors that may contribute to G1/S control; and 3) Identify direct binding targets of Swi4p, Swi6p and Mbp1p in order to confirm their roles in G1/S regulation and elucidate their precise mechanisms of action.

2. Materials and Methods

2.1 Strains, oligonucleotides and plasmids

Strains, oligonucleotides and plasmids used in this study are listed in Tables 1, 2 and 3, respectively.

Table 1: *Candida albicans* strains used in this study

Strain	Genotype	Parent/Source
SC5314	Wild type	[90]
BWP17	<i>ura3::imm434/ura3::imm434, his1::hisG/his1::hisG, arg4::hisG/arg4::hisG</i>	[91]
AM202.2	<i>SWI6-TAP-URA3/SWI6</i>	BWP17
AM201.5	<i>SWI6-TAP-ARG4/swi6::URA3</i>	BWP17
AH110	<i>SWI4-HA-HIS1/SWI4, SWI6-TAP-ARG4/swi6::URA3</i>	AM201.5
BH415	BWP17 (<i>pBS-CaARG4, pBS-CaURA3</i>)	BWP17
BH420	BWP17 (<i>pRM100, pBS-CaARG4</i>)	BWP17
BH440	BWP17 (<i>pBS-CaHIS1, pBS-CaURA3</i>)	BWP17
BH101	<i>swi6::HIS1/SWI6</i>	BWP17
BH114	<i>swi4::hisG/SWI4</i>	BWP17
BH120	<i>swi6::HIS1/swi6::URA3</i>	BWP17
BH137	<i>mbp1::HIS1/MBP1</i>	BWP17
BH180	<i>swi4::HIS1/SWI4</i>	BWP17
BH185	<i>swi4::URA3/swi4::HIS1</i>	BWP17
BH201	<i>CLN3-HA-HIS1/CLN3</i>	BWP17
BH261	<i>mbp1::HIS1/mbp1::URA3</i>	BWP17
ROm101	<i>MBP1-TAP-URA3/MBP1</i>	BWP17
YC101	<i>SWI4-HA-HIS1/SWI4</i>	BWP17

YC113	<i>SWI4-HA-HIS1/swi4::hisG</i>	BH114
YC122	<i>SWI4-MYC-URA3/SWI4, CLN3-HA-HIS1/CLN3</i>	BH201
YC131	<i>SWI4-MYC-URA3/swi4::HIS1</i>	BH180
YC161	BH185 (<i>pBS-ARG4-SWI4</i>)	BH185
YC171	BH185 (<i>pBS-ARG4</i>)	BH185
YC193	<i>SWI4-TAP-URA3/swi4A::HIS1</i>	BH180
YC201	BH120 (<i>pBS-ARG4-SWI6</i>)	BH120
YC216	<i>SWI6-HA-URA3/swi6::HIS1</i>	BH101
YC221	<i>SWI6-TAP-URA3 / SWI6, cln3::hisG / MET::CLN3-ARG4</i>	BH253
YC231	BH120 (<i>pBS-ARG4</i>)	BH120
YC301	<i>MBP1-MYC-ARG4/MBP1, SWI6-TAP-URA3/SWI6</i>	AM202.2
YC311	<i>MBP1-MYC-ARG4/MBP1</i>	BWP17
YC323	BH261 (<i>pBS-ARG4-MBP1</i>)	BH261
YC341	<i>MBP1-MYC-ARG/mbp1::HIS1</i>	BH137
YC351	<i>MBP1-HA-URA3/mbp1::HIS1</i>	BH137
YC367	<i>MBP1-TAP-URA3/mbp1::HIS1</i>	ROm101
YC372	<i>MBP1-TAP-URA3/MBP1, swi4::hisG/SWI4-HA-HIS1</i>	YC113
YC381	BH261 (<i>pBS-ARG4</i>)	BH261
YC396	<i>MBP1-TAP-ARG4 / MBP1, SWI6-HA-URA3 / swi6::HIS1</i>	YC216
YC415	<i>MET::ORF19.5961-ARG4/ORF19.5961</i>	BWP17
YC422	<i>MET3:: ORF19.5961-ARG4/orf19.5961 ::URA3</i>	BH415
YC441	<i>orf19.5961 ::URA3/ ORF19.5961</i>	BWP17
YC451	<i>orf19.5961 ::URA3/orf19.5961::HIS1</i>	YC441
YC602	<i>MBP1/MBP1-HA-ARG4, SWI4-MYC-URA3/swi4::HIS1</i>	YC131

Table 2: Oligonucleotides used in this study

Oligo	Sequence 5'-3'
YC 1F	AGTAATGCTAACCAAAGCAATAAATTTGCC
YC 1R	AATGTAAACATGTAGTCCCGGAATTAGTTT
YC 2F	CACTGTAAATCACACCAACTCAATTAACTCCCCTTTAGTAAGATTTTTC
YC 2R	GGCAAATTTATTGCTTTGGTTAGCATTACTCATGTTTTCTGGGGAGGGT GAAGCAATCTCCTCAATTGACTACAATACAGATTACATACTCCAACAAAGTTT
YC 3R	AAGAGAACACTTTAATAATCTGAACATTTTAACTATTGCTCATAGACAGGCGC AGCGGTCGGGCTGA
YC 4R	TGACCAATAATACCGCCACA
YC 5F	TCCTGTTCCAACAACACCAA
YC 6F	CAAAAATTTGCGGTGTGTTG
YC 6R	ATATCCTGGTGGCGTGCTTA
YC 7F	GAAGCCCTATTTTGAGAATA
YC 7R	GCCTGCGTCCTGAAATAAAA
YC 8F	AAGTGGCGGTAGCAGGAGTG
YC 8R	TTACAGTTTCTTTGGTTGTA
YC 9F	AATGAGACAACAGTTAACTC
YC 9R	TGAAGGTGTTGAACTATAAG
YC 10F	AGTGATATTAACGTATTTCAAAGTGTTGAG
YC 10R	TTTTTTGACCAATGATTCTTCCATAGCATC
YC 11F	ATATACATAAATGTCTACACATAAGCTTCT
YC 11R	TTAGTTTGTFTGGCAAGATCATTATTAAGG
YC 12F	GATGCTATGGAAGAATCATTTGGTCAAAAAAGGTTCGACGGATCCCCGGGGA
YC 12R	AGAAGCTTATGTGTAGACATTTATGTATATAGGCGCAGCGGTCTGGGCTGA
YC 13F	GGTGGTCTCGAGGACTAAGTCGACACAATGAG
YC 13R	GGTGGTGGTACCAGTTCTAGATCCTCGCAGAT
YC 14F	GGTGGTCTCGAGTCCGGATCCCTAACTTTGGT
YC 14R	GGTGGTGGTACCCGGCGCTAAACTCCTATCTG
YC 15F	GGTGGTCTCGAGAAGTTGTTGATTCCCTTCACT
YC 15R	GGTGGTACATGTACTATTGCTCATAGACTTAG
YC 16F	TTGCAACCCAAGCCTTTGAA
YC 16R	CCAACAAGTATATGCGAACA
YC 17F	CAATAAAGTTCCGACAACCTG

YC 17R	TCAACTTGGCTGGTTGGTAA
YC 16R'	TTGGTCCTTCCAGAGTGACA
YC 18F	TACATTGATACGAGACAGAA
YC 18R	GTCATCTATCTCAACAATGG
YC 19F	GGTGGTCTCGAGAGTAACAGTGTAACCAATTA
YC 19R	GGTGGTGGTACCCATCGGCACTCATTCTATCG
YC 20F	GCTCTGGTAGTGGTAAATCA
YC 20R	TCGACCCCTGATGAGCCTGTA
YC 21F	ACGAAAGAGAAGTATCTGGAGATGAATCAA
YC 21R	CGTCATACCTTCAGTTAATGATTCGGCAAT
YC 22F	ATTGCCGAATCATTAACTGAAGGTATGACGGGTCGACGGATCCCCGGGT
YC 22R	TTGTTCCGATTTAATTTCCCCCATCTATCGTCGATGAATTCGAGCTCGTT
YC 23F	ACTCCTGATACGCAACGAAC
YC 24R	CTGTGCAATAACTTTCTGTC
CaNAS6F1	TCATCGTCACAATCACATCCACAATCAAAC
CaNAS6R1	AGTTAATTGAGTTGGGTGTGATTTACAGTG
CaNAS6F2	CACTGTAAATCACACCCAACTCAATTAACTTATAGGGCGAATTGGAGCTC
CaNAS6R2	GTTGATACTACTTACTTACTTCCCTAACAAATGACGGTATCGATAAGCTTGA
CaNAS6F3	ATTGTTAGGAAGTAAGTAAGTAGTATCAAC
CaNAS6R3	TTCCTGCTATGCTTTGTGGAATAGTTAACA
CaNAS6F4	ATTGAAGAAAGACGAGATTC
CaNAS6R4	AGATGGAGATAGTTGGTTTC
SWI4F1	TAAATATAGAAAATTGCTTAGTTTGAGTTGTGGTGTTAAAGTTGAAGAAATTG ACAGTTTAATTGATGGAATTGCCGAATCATTAACTGAAGGTATGACGGGTCG ACGGATCCCCGGGT
SWI4R1	GACCCAAAGCACAATAAGAAAATGAGCATAAGAGAATTCATTAAGTAGCAG TTATACATTGCCAGTACGATAATTCAAACATAATATTACAATTATTCTAATCG ATGAATTCGAGCTCGTT
SWI6F1	TTCTAAGTTTAAGAAAGTTGTCAGCATATGTACAAATGTTGGTGTAACGAA GTTGATGAATTTTTAGACGGGTTGTTGGAAGCAGTGGAAGGACAACAGGGTC GACGGATCCCCGGGT
SWI6R1	ATTCAGGAATAGCTGCGGCGCTAAACTCCTATCTGGGTTTGGTATAGAGAGC CATATAAAACAATACACGGGGAATTAGAAGTATACATGTGTTCCGATTATCGA TGAATTCGAGCTCGTT
AG4F	GGTCGACGGATCCCCGGGTATACCCATACGATGTTCCCTGAC
AG4R	TCGATGAATTCGAGCTCGTT

Table 3: Plasmids used in this study

Plasmid	Description	Parent/Source
pBS-Ca <i>URA3</i>	pBluescript Ca <i>URA3</i>	A.J.P. Brown
pBS-Ca <i>HIS1</i>	pBluescript Ca <i>HIS1</i>	C. Bachewich
pBS-Ca <i>ARG4</i>	pBluescript Ca <i>ARG4</i>	H. Huang
pFA- <i>MET3</i> -Ca <i>ARG4</i>	<i>MET3</i> promoter – Ca <i>ARG4</i>	[92]
pFA-HA-Ca <i>HIS1</i>		[92]
pFA-HA-Ca <i>URA3</i>		[92]
pFA-TAP-Ca <i>URA3</i>		[92]
pFA-TAP-Ca <i>ARG4</i>		[92]
pFA-MYC-Ca <i>URA3</i>		[92]
pFA-MYC-Ca <i>ARG4</i>		[92]

2.2 Medium and growth conditions

The majority of strains were grown at 30°C in YPD medium containing 1% yeast extract, 2% peptone and 2% glucose. For conditional strains, cells were grown at 30°C in synthetic complete (SC) medium containing 0.67% yeast nitrogen base, 2% glucose and amino acids supplemented with or without 2.5 mM methionine and 0.5 mM cysteine for repression and induction of the *MET3* promoter, respectively [93]. In order to study cells under hyphal-inducing conditions, 10% fetal bovine serum (Hyclone) was added to growth medium, and cells were incubated at 37°C. All media were supplemented with 100 mg/L of uridine, histidine or arginine to allow optimal growth of *URA3*⁺, *HIS1*⁺ or *ARG4*⁺ auxotrophs, except when being selected [94]. Strains were incubated overnight in YPD medium at 30°C, diluted into fresh medium to an O.D._{600nm} of 0.2, and incubated until the O.D._{600nm} reached 0.8-1.0. In the case of the *MET3p-CLN3* conditional strain,

cells were incubated overnight at 30°C in SC medium lacking methionine, then diluted into fresh SC medium containing 2.5mM methionine and 0.5mM cysteine and incubated for 4 h to block cells in G1 phase. *E. coli* cells were incubated at 37°C in 2 x YT medium containing 1% yeast extract, 1.6% tryptone 0.5% NaCl and NaOH to pH 7.0. 100 µg/ml Ampicillin was included for selection.

2.3 Construction of strains

2.3.1 *SWI4*

2.3.1.1 *SWI4-HA*

In order to tag *SWI4* at the 3' end with the hemagglutinin (HA) epitope, oligonucleotides AG4F and AG4R were used to amplify a 1.7 kb fragment containing an *HA-HIS1* cassette from plasmid pFA-HA-HIS1. The PCR reaction mix was composed of 0.6 µM oligonucleotides, 0.4 mM dNTPs, 100 ng of template, 3.75U of Expand Long Template Polymerase (Roche), and 1X Buffer 3. The reaction conditions were as follows: 94°C for 4 min, followed by 25 cycles of 94°C for 30 sec, 44°C for 30 sec, 68°C for 1 min, 40 sec, followed by a 7 min extension at 68°C and storage at 4°C. This fragment was purified and used as the template with oligonucleotides SWI4F1 and SWI4R1 to amplify a final 1.9 kb fragment that contained an *HA-HIS1* cassette and 100 bp sequences homologous to either side of the STOP codon of *SWI4*. The PCR reaction mix was composed of 0.6 µM oligonucleotides, 0.4 mM dNTPs, 100 ng of template, 3.75U of Expand Long Template Polymerase (Roche), and 1X Buffer 3. The reaction conditions

were as follows: 94°C for 4 min, followed by 25 cycles of 94°C for 1 min, 42°C for 1 min, 68°C for 1 min, 55 sec, followed by a 7 min extension at 68°C and storage at 4°C. The final product was cleaned using a PCR purification kit (OMEGA) and 4 µg were transformed into strain BWP17, resulting in strain YC101 (*SWI4-HA-HIS1/SWI4*). Another 4 µg were transformed into strain BH114, resulting in strain YC113 (*SWI4-HA-HIS1/swi4Δ::hisG*).

2.3.1.2 *SWI4-MYC*

In order to tag *SWI4* at the 3' end with the MYC epitope, oligonucleotides SWI4F1 and SWI4R1 were used in a one step PCR reaction to amplify a 1.9kb fragment that contained a *MYC-URA3* cassette from plasmid pFA-MYC-URA3, 100 bp homology to *SWI4* starting upstream from the stop codon, and 100 bp homology to the 3' end of *SWI4*. The PCR reaction mix was composed of 0.6 µM oligonucleotides, 0.4 mM dNTPs, 100 ng of pFA-MYC-URA3 as template, 3.75U of Expand Long Template Polymerase (Roche), and 1X Buffer 3. The reaction conditions were as follows: 94°C for 4 min, followed by 25 cycles of 94°C for 1 min, 42°C for 1 min, 68°C for 1 min, 55 sec, followed by a 7 min extension at 68°C and storage at 4°C. The cleaned product was transformed into strain BH201, resulting in strain YC122 (*SWI4-MYC-URA3/SWI4, CLN3-HA-HIS1/CLN3*), or strain BH180, resulting in strain YC131 (*SWI4-MYC-URA3/swi4Δ::HIS1*).

2.3.1.3 *SWI4-TAP*

A 2-step fusion PCR method was utilized to tag *SWI4* with *TAP-URA3*. First, a 752 bp fragment corresponding to the 5' flank of *SWI4*, located just before the stop codon, was PCR amplified from gDNA with oligonucleotides YC21F and YC21R. The thermocycling conditions included: 94°C for 3 min, followed by 25 cycles of 94°C for 30 sec, 50°C for 30 sec, 68°C for 50 sec, and a final elongation at 68°C for 7 min. The reaction mix was composed of a final concentration of 0.6 µM of oligonucleotides, 0.4 mM dNTPs, 100 ng of gDNA as template, 3.75U of Expand Long Template Polymerase, and 1X Buffer 3. A 763 bp fragment corresponding to the 3' flank of *SWI4*, starting 3 bp after the stop codon, was similarly amplified using oligonucleotides BH14F and BH14R and the following thermocycling conditions: 94°C for 3 min, followed by 25 cycles of 94°C for 30 sec, 50°C for 30 sec, 68°C for 50 sec, and a final elongation at 68°C for 7 min. The reaction mix composition was similar to that used for the 5' flank. In order to amplify the 2181 bp *TAP-URA3* cassette fragment from plasmid pFA-TAP-URA3, oligonucleotides YC22F and YC22R were used, which contain homology to the plasmid plus additional 30 bp sequences that are the reverse complement of oligonucleotides YC21R and BH14F, respectively. The following thermocycling conditions were used: 94°C for 3 min, followed by 25 cycles of 94°C for 30 sec, 43°C for 30 sec, 68°C for 2 min, and a final elongation at 68°C for 7 min. The reaction mix was composed of a final concentration of 0.6 µM of oligonucleotides, 0.4 mM dNTPs, 100 ng of pFA-TAP-URA3 as template, 3.75U of Expand Long Template Polymerase, and 1X Buffer 3. In order to create the final construct for transformation, oligonucleotides YC21F and YC14R were

used at a concentration of 0.45 μ M with a 1:2:1 (50ng:100ng:50ng) amount of these three PCR fragments, in a reaction including 0.5 mM of dNTPs, 3.75U of Expand Long Template Polymerase, and 1X Buffer 3. The following thermocycling conditions were used: 94°C for 3 min, followed by 10 cycles of 94°C for 10 sec, 50°C for 30 sec, and 68°C for 3 min, 40 sec, followed by 15 cycles of 94°C for 10 sec, 50°C for 30 sec, 68°C for 4 min with a 20 sec auto-segment extension, and a final elongation at 68°C for 7 min. The final 3696 bp product was cleaned and transformed into strain BH180, resulting strain YC193 (*swi4 Δ ::HIS1/SWI4-TAP-URA3*).

2.3.2 *SWI6*

2.3.2.1 *SWI6-HA*

In order to tag *SWI6* at the 3' end with the hemagglutinin (HA) epitope, oligonucleotides SWI6F1 and SWI6R1 were used to amplify a 1.7 kb fragment that contained an *HA-URA3* cassette from plasmid pFA-HA-URA3, 100 bp homology to *SWI6* starting upstream from the stop codon, and 100 bp homology to the 3' end of *SWI6*. The PCR reaction mix was composed of 0.6 μ M oligonucleotides, 0.6 mM dNTPs, 100 ng of pFA-HA-URA3 as template, 3.75U of Expand Long Template Polymerase (Roche), and 1X Buffer 3. The reaction conditions were as follows: 94°C for 4 min, followed by 25 cycles of 94°C for 1 min, 42°C for 1 min, 68°C for 1 min, 50 sec, followed by a 7 min extension at 68°C and storage at 4°C. The cleaned product was transformed into strain BH101, resulting in strain YC216 (*SWI6-HA-URA3/swi6 Δ ::HIS1*).

2.3.2.2 *SWI6-TAP*

In order to tag *SWI6* at the 3' end with TAP epitope, oligonucleotides SWI6F1 and SWI6R1 were used to amplify a 2381 bp fragment containing a *TAP-URA3* cassette from plasmid pFA-TAP-URA3, 100 bp homology to *SWI6* starting upstream from the stop codon, and 100 bp homology to the 3' end of *SWI6*. The PCR reaction mix was composed of 0.6 μ M oligonucleotides, 0.6 mM dNTPs, 100 ng of pFA-TAP-URA3 as template, 3.75U of Expand Long Template Polymerase (Roche), and 1X Buffer 3. The reaction conditions were as follows: 94°C for 4 min, followed by 25 cycles of 94°C for 1 min, 42°C for 1 min, 68°C for 2 min, followed by a 7 min extension at 68°C and storage at 4°C. The final 2381 cleaned bp product was transformed into strain BH253, resulting in strain YC221 (*SWI6-TAP-URA3/SWI6, cln3 Δ ::hisG /MET::CLN3-ARG4*).

2.3.3 *MBP1*

2.3.3.1 *MBP1-MYC*

In order to tag *MBP1*, a 2-step fusion PCR method was utilized. First, a 646 bp fragment corresponding to the 5' flank of *MBP1*, located just before the stop codon, was PCR amplified from gDNA with oligonucleotides YC10F and YC10R. The thermocycling conditions included: 94°C for 3 min, followed by 25 cycles of 94°C for 30 sec, 47°C for 30 sec, 68°C for 30 sec, and a final elongation at 68°C for 7 min. The reaction mix was composed of a final concentration of 0.6 μ M of oligonucleotides, 0.4 mM dNTPs, 100 ng of gDNA as template, 3.75U of Expand Long Template Polymerase, and 1X Buffer 3. A 340 bp fragment corresponding to the 3' flank of *MBP1*, starting 40

bp after the stop codon, was similarly amplified using oligonucleotides YC11F and YC11R and the following thermo-cycling conditions: 94°C for 3 min, followed by 25 cycles of 94°C for 30 sec, 46°C for 30 sec, 68°C for 30 sec, and a final elongation at 68°C for 7 min. The reaction mix composition was similar to that used for the 5' flank. In order to amplify the 3033 bp *MYC-ARG4* cassette fragment from plasmid pFA-MYC-ARG4, oligonucleotides YC12F and YC12R were used, which contain homology to the plasmid plus additional 30 bp sequences bearing homology to oligonucleotides YC10R and YC11F, respectively. The following thermocycling conditions were used: 94°C for 3 min, followed by 25 cycles of 94°C for 30 sec, 54°C for 30 sec, 68°C for 3 min, and a final elongation at 68°C for 7 min. The reaction mix was composed of a final concentration of 0.6 μM of oligonucleotides, 0.4 mM dNTPs, 100 ng of pFA-MYC-ARG4 as template, 3.75U of Expand Long Template Polymerase, and 1X Buffer 3. In order to create the final construct for transformation, oligonucleotides YC10F and YC11R were used at a concentration of 0.45 μM with a 1:2:1 (50ng:100ng:50ng) amount of these three PCR fragments, in a reaction including 0.5 mM of dNTPs, 3.75U of Expand Long Template Polymerase, and 1X Buffer 3. The following thermocycling conditions were used: 94°C for 3 min, followed by 10 cycles of 94°C for 10 sec, 47°C for 30 sec, and 68°C for 4 min, followed by 15 cycles of 94°C for 10 sec, 47°C for 30 sec, 68°C for 4 min with a 20 sec auto-segment extension, and a final elongation at 68°C for 7 min. The cleaned construct was transformed into strain AM202.2, resulting in strain YC301 (*MBP1-MYC-ARG4/MBP1, SWI6-TAP-URA3/SWI6*), strain BWP17, resulting in

strain YC311 (*MBPI-MYC-ARG4/MBPI*), or strain BH137, resulting in strain YC341 (*MBPI-MYC-ARG/mbp1Δ::HIS1*).

2.3.3.2 *MBPI-HA*

In order to tag *MBPI* with HA, the 2 step fusion PCR strategy was utilized as described above. A 646 bp fragment corresponding to the 5' flank of *MBPI*, located just before the stop codon, was PCR amplified from gDNA with oligonucleotides YC10F and YC10R, using the following thermocycling conditions: 94°C for 3 min, followed by 25 cycles of 94°C for 30 sec, 47°C for 30 sec, 68°C for 30 sec, and a final elongation at 68°C for 7 min. The reaction mix was composed of a final concentration of 0.6 μM of oligonucleotides, 0.4 mM dNTPs, 100 ng of gDNA as template, 3.75U of Expand Long Template Polymerase, and 1X Buffer 3. A 340 bp fragment corresponding to the 3' flank of *MBPI*, located 40 bp after the stop codon, was similarly amplified using oligonucleotides YC11F and YC11R and the following thermocycling conditions: 94°C for 3 min, followed by 25 cycles of 94°C for 30 sec, 46°C for 30 sec, 68°C for 30 sec, and a final elongation at 68°C for 7 min. The reaction mix composition was similar to that used for the 5 flank. To amplify the 2380 bp *HA-URA3* cassette fragment from plasmid pFA-HA-URA3, oligonucleotides YC12F and YC12R were used, which contain homology to the plasmid plus additional 30 bp sequences homologous oligonucleotides YC10R and YC11F, respectively. The following thermocycling conditions were used: 94°C for 3 min, followed by 25 cycles of 94°C for 30 sec, 54°C for 30 sec, 68°C for 2 min 15 sec, and a final elongation at 68°C for 7 min. The reaction mix was composed of a final concentration of 0.6 μM of oligonucleotides, 0.4 mM dNTPs, 100 ng of pFA-HA-

URA3 as template, 3.75U of Expand Long Template Polymerase, and 1X Buffer 3. The final PCR construct for transformation was created using oligonucleotides YC10F and YC11R at a concentration of 0.45 μ M with a 1:2:1 (50ng:100ng:50ng) amount of the three PCR fragments, in a reaction including 0.5 mM of dNTPs, 3.75U of Expand Long Template Polymerase, and 1X Buffer 3. The following thermocycling conditions were used: 94°C for 3 min, followed by 10 cycles of 94°C for 10 sec, 48°C for 30 sec, and 68°C for 3 min 20 sec, followed by 15 cycles of 94°C for 10 sec, 48°C for 30 sec, 68°C for 3 min 20 sec with a 20 sec auto-segment extension, and a final elongation at 68°C for 7 min. The final cleaned 3366 bp product was transformed into strain BH137, resulting in strain YC351 (*MBP1-HA-URA3/mbp1 Δ ::HIS1*).

2.3.3.3 MBP1-TAP

To tag *MBP1* with TAP, a strategy similar to MYC-tagging was utilized, with the exception of utilizing plasmid pFA-TAP-URA3 or pFA-TAP-ARG4 with oligonucleotides YC12F and YC12R. The 2796 bp *TAP-URA3* cassette fragment was amplified using the following thermocycling conditions: 94°C for 3 min, followed by 25 cycles of 94°C for 30 sec, 54°C for 30 sec, 68°C for 2 min 30 sec, and a final elongation at 68°C for 7 min. To amplify the 3405 bp *TAP-ARG4* cassette fragment from plasmid pFA-TAP-ARG4, oligonucleotides YC12F and YC12R were used with the following thermocycling conditions: 94°C for 3 min, followed by 25 cycles of 94°C for 30 sec, 54°C for 30 sec, 68°C for 3 min, and a final elongation at 68°C for 7 min. The final 3782 bp construct for transformation of *TAP-URA3* was created with oligonucleotides YC10F and YC11R and a 1:2:1 (50ng:100ng:50ng) amount of the three PCR fragments, with

following thermocycling conditions: 94°C for 3 min, followed by 10 cycles of 94°C for 10 sec, 48°C for 30 sec, and 68°C for 3 min 45 sec, followed by 15 cycles of 94°C for 10 sec, 48°C for 30 sec, 68°C for 3 min 45 sec with a 20 sec auto-segment extension, and a final elongation at 68°C for 7 min. The cleaned product was transformed into strain YC113, resulting in strain YC372 (*MBP1-TAP-URA3/MBP1, swi4Δ::hisG/SWI4-HA-HIS1*). The final 4391 bp *TAP-ARG4* product was created with oligonucleotides YC10F and YC11R and a 1:2:1 (50ng:100ng:50ng) amount of the three PCR fragments, with following thermocycling conditions: 94°C for 3 min, followed by 10 cycles of 94°C for 10 sec, 48°C for 30 sec, and 68°C for 4 min 20 sec, followed by 15 cycles of 94°C for 10 sec, 48°C for 30 sec, 68°C for 4 min 20 sec with a 20 sec auto-segment extension, and a final elongation at 68°C for 7 min. The product was transformed into strain YC216, resulting in strain YC396 (*MBP1-TAP-ARG4/MBP1, SWI6-HA-URA3/swi6Δ::HIS1*).

2.3.3.4 *MBP1* deletion

The 2-step fusion PCR strategy was utilized to delete one copy of *MBP1*. A 790 bp fragment corresponding to the 5' flank, starting 812 bp upstream of the *MBP1* start codon, was amplified from gDNA using oligonucleotides BH7F and BH7R, and the following thermocycling conditions: 94°C for 3 min, followed by 25 cycles of 94°C for 30 sec, 51°C for 30 sec, 68°C for 45 sec, and a final elongation at 68°C for 7 min. A 799 bp fragment corresponding to the 3' flank of *MBP1*, starting 161 bp downstream of the stop codon, was then amplified using oligonucleotides BH9F and BH9R and the following thermocycling conditions: 94°C for 3 min, followed by 25 cycles of 94°C for 30 sec, 50°C for 30 sec, 68°C for 45 sec, and a final elongation at 68°C for 7 min. A 1348 bp

HIS1 cassette fragment was then amplified from plasmid pBS-CaHIS1 using oligonucleotides BH8F and BH8R, which contained homology to the plasmid plus 30 bp homology to oligonucleotides BH7R and BH9F, respectively, to allow for PCR fusion. The following thermocycling conditions were used: 94°C for 3 min, followed by 25 cycles of 94°C for 30 sec, 42°C for 30 sec, 68°C for 1 min 15 sec, and a final elongation at 68°C for 7 min. The reaction mix was composed of a final concentration of 0.6 µM of oligonucleotides, 0.4 mM dNTPs, 100 ng of pBS-CaHIS1 as template, 3.75U of Expand Long Template Polymerase, and 1X Buffer 3. In order to create the final 2938 bp construct for transformation, 0.45 µM of oligonucleotides BH7F and BH9R were used with a 1:2:1 (50ng:100ng:50ng) ratio of the three fragments, in a reaction including 0.5 mM of dNTPs, 3.75U of Expand Long Template Polymerase, and 1X Buffer 3. The following thermocycling conditions were used: 94°C for 3 min, followed by 10 cycles of 94°C for 10 sec, 51°C for 30 sec, and 68°C for 2 min 50 sec, followed by 15 cycles of 94°C for 10 sec, 51°C for 30 sec, 68°C for 2 min 50 sec with a 20 sec auto-segment extension, and a final elongation at 68°C for 7 min. 5 µg of the cleaned construct was transformed into strain Rom101, resulting in strain YC367 (*MBP1-TAP-URA3/mbp1Δ::HIS1*).

2.3.4 Complemented strains

In order to construct the complement for strains BH185 (*swi4* Δ/Δ), BH120 (*swi6* Δ/Δ) and BH261 (*mbp1* Δ/Δ), a single copy of the corresponding ORF plus 1000 bp of 5' upstream sequence was reintroduced back into the strains.

For *swi4Δ/Δ* cells, a 4925 bp fragment that contained 1430 bp upstream of the *SWI4* start codon, the *SWI4* ORF, and 282 bp downstream of the stop codon, was amplified with oligonucleotides YC13F and YC13R. The PCR reaction mix was composed of a final concentration of 0.6 μM of oligonucleotides, 0.4 mM dNTPs, 100 ng of BWP17 gDNA as template, 3.75U of Expand Long Template Polymerase (Roche), and 1X Buffer 3. The reaction conditions were as follows: 94°C for 3 min, followed by 25 cycles of 94°C for 30 sec, 43°C for 30 sec, 68°C for 5 min, a 7 min extension at 68°C, and storage at 4°C. The PCR product was digested with *Xho I* and *Acc65 I*, utilizing 1X BSA, 1X Buffer 3, 40 U *Xho I* (NEB), 20 U *Acc65 I* (NEB) and 1.73 μg of purified PCR product. The reaction was incubated at 37°C overnight. In addition, 1.0 μg of plasmid pBS-ARG4 was similarly digested. The digestion products were purified using Pure Mini Kit I (OMEGA), and used for ligations. The ligation reaction mix was composed of a final concentration of 1X Ligase buffer, 200 U T4 DNA Ligase enzyme (BioLabs), 5.0 ng digested pBS-ARG4 and varied amounts of digested PCR product (0 ng, 5 ng, 10 ng, 20 ng, 40 ng) in a total volume of 10 μl. The reactions were incubated at 16°C overnight. The ligations were transformed into *E.coli* and random colonies were inoculated into 3.0 ml 100 μg/ml Amp contained LB medium. The samples were incubated at 37°C overnight, and plasmid DNA was extracted using the Plasmid Mini Kit I (OMEGA). Purified plasmid was then digested with *Kpn I*, which sits in pBS-ARG4. The reactions were composed of 1X BSA, 1X Buffer 1, 20 U *Kpn I* (NEB), 100 ng of purified plasmid, and incubated at 37°C for 3 h. Positive integrations were confirmed by visualization of a

9925 bp vs. 5000 bp band on a DNA gel. Since no proper restriction enzyme site was found within the 1430 bp of *SWI4* promoter sequence, 4.0 µg of uncut, positive plasmid was directly transformed into strain BH185, resulting strain YC161 (BH185 (*pBS-ARG4-SWI4*)).

For *swi6Δ/Δ* cells, a 3236 bp fragment that contained 850 bp upstream of the *SWI6* start codon, the *SWI6* ORF, and 163 bp downstream of the stop codon, was amplified with oligonucleotides YC14F and YC14R. The PCR reaction mix was composed of a final concentration of 0.6 µM of oligonucleotides, 0.4 mM dNTPs, 100 ng of BWP17 gDNA as template, 3.75U of Expand Long Template Polymerase (Roche), and 1X Buffer 3. The reaction conditions were as follows: 94°C for 3 min, followed by 25 cycles of 94°C for 30 sec, 55°C for 30 sec, 68°C for 3 min 30 sec. Then give it a 7 min extension at 68°C and stored at 4°C. The PCR product was digested with *Xho I* and *Acc65 I*, utilizing 1X BSA, 1X Buffer 3, 40 U *Xho I* (NEB), 20 U *Acc65 I* (NEB) and 1.73 µg of purified PCR product. The reaction was incubated at 37°C overnight. In addition, 1.0 µg of plasmid pBS-ARG4 was similarly digested. The digestion products were purified and used for ligations. Ligations mixes were as described for *SWI4* above. Purified plasmids from *E. coli* transformants were digested with *Kpn I*, which sits in pBS-ARG4. The reactions were composed of 1X BSA, 1X Buffer 1, 20 U *Kpn I* (NEB), 100 ng of purified plasmid, and incubated at 37°C for 3 h. Positive integrations were confirmed by the presence of a 8236 bp vs 5000 bp band on a DNA gel. Then the positive integration was digested with *Nco I*, utilizing 1X BSA, 1X Buffer 3, 40 U *Nco I* (NEB), and 4 µg of

confirmed construction, and incubated at 37°C overnight. This cut is within the 850 bp 5' sequence, allowing integration at the promoter of *SWI6*. The cut construct was transformed into strain BH120, resulting in strain YC201 (BH120 (*pBS-ARG4-SWI6*)).

For *mbp1ΔΔ* cells, a 3963 bp fragment that contained 1160 bp upstream of the *MBP1* start codon, the *MBP1* ORF, and 245 bp downstream of the stop codon, was amplified with oligonucleotides YC15F and YC15R. The PCR reaction mix was composed of a final concentration of 0.6 μM of oligonucleotides, 0.4 mM dNTPs, 100 ng of BWP17 gDNA as template, 3.75U of Expand Long Template Polymerase (Roche), and 1X Buffer 3. The reaction conditions were as follows: 94°C for 3 min, followed by 25 cycles of 94°C for 30 sec, 40°C for 30 sec, 68°C for 4 min. Then give it a 7 min extension at 68°C and stored at 4°C. The PCR product was digested with *Xho I* and *Afl III*, utilizing 1X BSA, 1X Buffer 3, 40 U *Xho I* (NEB), 20 U *Afl III* (NEB) and 2.0 μg of purified PCR product. The reaction was incubated at 37°C overnight. In addition, 1.0 μg of plasmid pBS-ARG4 was similarly digested. The digestion products were purified, and ligated as described above. Purified plasmid was digested with *EcoR V*, which sits in pBS-ARG4. The reactions were composed of 1X BSA, 1X Buffer 1, 20 U *EcoR V* (NEB), 100 ng of purified plasmid, and incubated at 37°C for 3 h. Positive integrations were confirmed by the presence of a 8963 bp vs 5000 bp band on a DNA gel. Then the positive integration was digested with *Blp I*, utilizing 1X BSA, 1X Buffer 3, 40 U *Blp I* (NEB), and 4 μg of confirmed construction, and incubated at 37°C overnight. This digests the product within the 1160 bp 5' sequence, allowing integration at the promoter

of *MBP1*. The cut construct was cleaned and transformed into strain BH261, resulting in strain YC323 (BH261 (*pBS-ARG4-MBP1*)).

2.4 *Escherichia coli* transformation

Subcloning Efficiency DH5 α Chemically Competent cells (F- ϕ 80*lacZ* Δ M15 Δ (*lacZYA-argF*) U169 *recA1 endA1 hsdR17*(rk-, mk+) *phoA supE44 thi-1 gyrA96 relA1* λ -; Invitrogen) were stored at -80°C. 50 μ l were gently thawed and mixed with 10 μ l of ligation product. Cells were incubated for 30 min on ice, heat shocked for 2 min in a 42°C water bath, then placed on ice for an additional 5 min. 940 μ l of 2 x YT medium was immediately added, and the cells were incubated at 37°C for 1 hour with shaking at 225 rpm. The transformed cells were then centrifuged, 900 μ l of the media was removed, and the remaining 100 μ l was plated on 2 x YT agar plates containing 100 μ g/ml of Ampicillin. Plates were incubated at 37°C overnight. The following day, random colonies were inoculated to 3.0 ml 100 μ g/ml Ampicillin contained LB medium. The samples were incubated at 37°C overnight, and plasmid DNA was extracted using the Plasmid Mini Kit I (OMEGA). Purified plasmids were then digested with specific restriction enzymes (NEB).

2.5 Transformation of *C. albicans*

A lithium acetate one-step transformation protocol was utilized for transformation of *C. albicans* [95-97]. To prepare the One-Step-Buffer (OSB), 25 μ l of salmon sperm DNA (10 mg/ml stock, Invitrogen) was first boiled for 10 min, cooled on ice for 5 min, then added to 200 μ l of sterilized 1 M Lithium Acetate. Subsequently, 25 μ l of 4.0 M DTT was added, followed by 800 μ l of 50% PEG 4000 (Sigma). The mixture was vortexed for 1 min, and 100 μ l of OSB solution was combined with 200-300 μ l of washed, stationary phase cells that had been centrifuged from culture. Approximately 4-5 μ g of transforming DNA in a maximum volume of 10 μ l was added. The reaction mix was vortexed for 1 min and incubated overnight at 30°C. The following day, the mixture was heat-shocked for 1 h at 43°C and plated on selective solid medium. After 2-3 days, transformants were streaked to single colony three times on fresh selective medium prior to screening. For increased transformation efficiency in the regulated *CLN3* strains, cells were grown overnight in SC medium lacking methionine and cysteine, then transferred into rich YPD medium for 2 h prior to collection.

2.6 Genomic DNA (gDNA) extraction

In order to extract gDNA [98], cells were inoculated into 5 ml of YPD medium or SC medium lacking methionine and cysteine, incubated at 30°C overnight, and then centrifuged for 5 min at 3000 rpm. The supernatant was discarded and the pellet was

washed once with 0.5 ml sterile distilled water. The cell pellet was re-suspended in 1 ml of sorbitol buffer (1M sorbitol, 0.1M EDTA) mixed with 10 μ l of lyticase (10U/ μ l) (Sigma) and 2 μ l of 4.0 M DTT. The mixture was incubated at 37°C for 1.5 h, centrifuged for 1 min at 13500 rpm, and the supernatant was discarded. The pellet was re-suspended in 200 μ l Tris-EDTA solution (50 mM Tris, 20 mM EDTA), 1% final SDS and incubated at 65°C for 30 min. After this incubation, 100 μ l of 5.0 M potassium acetate (KAc) was added and the solution was gently mixed to avoid shearing DNA. The mixture was incubated on ice for 60 min, centrifuged for 10 min at 13500 rpm, and the supernatant transferred to a new Eppendorf tube. An equal amount of 100% isopropanol was added to the supernatant, and after mixing for 1 min, the DNA pellet was collected by centrifuging at 13500 rpm for 1 min. The DNA pellet was then washed with 70% ethanol, air-dried, and re-suspended into 100 μ l of TE buffer (1 mM EDTA, 10 mM Tris-HCl pH 8.0) with 2 μ l of RNaseA (10 mg/ml, Molecular Bioproducts). DNA was incubated at 37°C for 30 min and stored at 4°C. Genomic DNA was quantified with a fluorometer (Hoefer DQ300) using Hoechst Dye (Invitrogen).

2.7 PCR screening

PCR screening reaction mixes were composed of 0.6 μ M of oligonucleotides, 0.4 mM of dNTPs, 100 ng of gDNA as template, 3 mM of MgCl₂, 1X Taq Buffer with (NH₄)₂SO₄ and 1 U Taq DNA Polymerase (Fermentas). In order to confirm strains

YC101 (*SWI4-HA-HIS1/SWI4*) and YC113 (*SWI4-HA-HIS1/swi4Δ::hisG*), oligonucleotides SWI4SF1, which locates 171 bp upstream of stop codon of *SWI4*, and CaHIS1R, which locates inside the plasmid pFA-HA-HIS1, were utilized to amplify a 1035 bp product. The reaction conditions were as follows: 95°C for 3min, 30 cycles of 95°C for 30 sec, 45°C for 30 sec, 72°C for 1 min 5 sec, followed by a 7 min extension at 72 °C and storage at 4 °C . Strains YC122 (*SWI4-MYC-URA3/SWI4, CLN3-HA-HIS1/CLN3*) and YC131 (*SWI4-MYC-URA3/swi4Δ::HIS1*) were confirmed using oligonucleotides SWI4SF1, (located 171 bp upstream of stop codon of *SWI4*) and CaMYCR (located inside pFA-MYC-URA3) which produced a 371 bp product. The reaction conditions were as follows: 95°C for 3min, 30 cycles of 95°C for 30 sec, 48°C for 30 sec, 72°C for 30 sec, followed by a 7 min extension at 72°C and storage at 4°C . Strain YC193 (*swi4Δ::HIS1/SWI4-TAP-URA3*) was confirmed using oligonucleotides YC23F (located 1086 bp upstream of stop codon of *SWI4*), and AG3R (located inside the plasmid pFA-TAP-URA3), which amplified a 1166 bp product. The reaction conditions were as follows: 95°C for 3min, 30 cycles of 95°C for 30 sec, 46°C for 30 sec, 72°C for 1 min 15 sec, followed by a 7 min extension at 72°C and storage at 4°C . Strain YC216 (*SWI6-HA-URA3/swi6Δ::HIS1*) was confirmed using oligonucleotides CaURA3F (located inside pFA-HA-URA3) and SWI6SR (located 310 bp downstream of stop codon of *SWI6*), which amplified a 898 bp product. The reaction conditions were as follows: 95°C for 3min, 30 cycles of 95°C for 30 sec, 42°C for 30 sec, 72°C for 1 min, followed by a 7 min extension at 72°C and storage at 4°C . Strain YC221 (*SWI6-TAP-URA3/SWI6*,

cln3Δ::hisG/ MET::CLN3-ARG4) was confirmed using oligonucleotides CaURA3F (located inside pFA-HA-URA3) and SWI6SR1 (located 310 bp downstream of stop codon of *SWI6*), which amplified a 898 bp product. The reaction conditions were as follows: 95°C for 3min, 30 cycles of 95°C for 30 sec, 42°C for 30 sec, 72°C for 1 min, followed by a 7 min extension at 72°C and storage at 4°C. Strains YC311 (*MBP1-MYC-ARG4/MBP1*) and YC341 (*MBP1-MYC-ARG/mbp1Δ::HIS1*) were confirmed using oligonucleotides AG30F (located 696 bps upstream of stop codon of *MBP1*) and CaMYCR (located inside pFA-MYC-ARG4), which amplified a 893 bp product. The reaction conditions were as follows: 95°C for 3min, 30 cycles of 95°C for 30 sec, 42°C for 30 sec, 72°C for 1 min, followed by a 7 min extension at 72°C and storage at 4°C. Strain YC351 (*MBP1-HA-URA3/mbp1Δ::HIS1*) was confirmed using oligonucleotides AG30F (located 696 bps upstream of stop codon of *MBP1*) and CaURA3R (located inside pFA-HA-URA3), which amplified a 2254 bp product. The reaction conditions were as follows: 95°C for 3min, 30 cycles of 95°C for 30 sec, 40°C for 30 sec, 72°C for 2 min 20 sec, followed by a 7 min extension at 72°C and storage at 4°C. Strains YC372 (*MBP1-TAP-URA3/MBP1, swi4Δ::hisG/SWI4-HA-HIS1*) and YC396 (*MBP1-TAP-ARG4/MBP1, SWI6-HA-URA3/swi6Δ::HIS1*) were confirmed using oligonucleotides AG30F (located 696 bps upstream of stop codon of *MBP1*) and AG3R (located inside pFA-TAP-URA3) which amplified a 768 bp product. The reaction conditions were as follows: 95°C for 3min, 30 cycles of 95°C for 30 sec, 42°C for 30 sec, 72°C for 50 sec, followed by a 7 min extension at 72°C and storage at 4°C. Strain YC367 (*MBP1-TAP-*

URA3/mbp1Δ::HIS1) was confirmed using oligonucleotides BH32F (located 880 bps upstream of stop codon of *MBPI*) and CaHIS1R (located inside the plasmid pBS-HIS1), which amplified a 1424 bp product. The reaction conditions were as follows: 95°C for 3min, 30 cycles of 95°C for 30 sec, 42°C for 30 sec, 72°C for 1 min 30 sec, followed by a 7 min extension at 72°C and storage at 4°C. Strain YC161 (BH185 (*pBS-ARG4-SWI4*)) was confirmed using oligonucleotides YC18F (located 1500 bp upstream of start codon of *SWI4*) and CB120R (located 200 bp downstream of the start codon of *SWI4*), which amplified a 1700 bp product. The reaction conditions were as follows: 95°C for 3min, 30 cycles of 95°C for 30 sec, 42°C for 30 sec, 72°C for 1 min 50 sec, followed by a 7 min extension at 72°C and storage at 4°C. Strain YC201 (BH120 (*pBS-ARG4-SWI6*)) was confirmed using YC17f (located which 985 bp upstream of *SWI6*) and YC17R (located 330 bp downstream of *SWI6*), which amplified a 1336 bp product. The reaction conditions were as follows: 95°C for 3min, 30 cycles of 95°C for 30 sec, 42°C for 30 sec, 72°C for 1 min 30 sec, followed by a 7 min extension at 72°C and storage at 4°C. Strain YC323 (BH261 (*pBS-ARG4-MBPI*)) was confirmed using YC16F (located 1240 bp upstream of start codon of *MBPI*) and YC16R (located 55 bp downstream of start codon of *MBPI*), which amplified a 1315 bp product. The reaction conditions were as follows: 95°C for 3min, 30 cycles of 95°C for 30 sec, 44°C for 30 sec, 72°C for 1 min 30 sec, followed by a 7 min extension at 72°C and storage at 4°C.

2.8 Protein Extraction

2.8.1 Protein extraction by bead-beating.

To prepare the cell pellet for protein extraction, cells were inoculated into 2 ml of YPD medium or SC minimal medium without methionine and cysteine, and incubated overnight at 30°C. The overnight culture was then diluted into 20 ml of YPD or SC (-MC) medium to an OD_{600nm} of 0.2, and incubated at 30°C until the culture reached an OD_{600nm} of 0.8-1.0. After centrifuging the culture for 5 min at 3000 rpm and removing the supernatant, the pellet was immersed in liquid nitrogen or dry ice and stored at -80°C. The pellets were thawed on ice then re-suspended in 20 µl of RIPA buffer (10 mM sodium phosphate, 1% Triton X-100, 0.1% SDS, 10 mM EDTA, 150 mM NaCl, pH 7.0, 5 µg/ml Leupeptin, 5 µg/ml Aprotin and 1mM AEBSF) and 200 µl of glass beads (Sigma, 425-600) were added. Cells were agitated in a Mini bead-beater (Biospec, Mini-Beadbeater-8) for 45 sec, followed by 2 min on ice, for a total of 3 trials. The crude extract was washed with 200 µl of RIPA buffer, and final extracts were obtained by centrifugation at 13,500 rpm for 10 min at 4°C, followed by 13,500 rpm for 1 hour at 4°C. The supernatant was transferred to a new Eppendorf tube and frozen at -80°C [99].

2.8.2 Protein extraction by lyophilisation.

An alternative method for protein extraction [100] involved lyophilizing the cell pellets for 24 h in a freeze dryer (ThermoSavant, Modulyo D). The following day, the freeze-dried cell pellet was ground to fine powder in a mortar and pestle, to which 1.3 ml of cold HK buffer (25 mM TRIS pH7.5, 0.5% NP40, 300 mM NaCl, 5 mM EDTA pH8.0,

15 mM EGTA pH8.0, 60 mM Beta Gly.PO₄, 500 μM Na Vanadate, 10 mM Na Fluoride, 15 mM pNPP, 1 μg/ml Pepsatin A, 10 μg/ml Leupeptin, 10 μg/ml Trypsin ChymoT inhibitor, 10 μg/ml Aprotinin, 10 μg/ml TPCK, 2 mM TAME, 5 mM Benzamidine, 250 μg/ml PMSF, 1 mM DTT) per 0.1 g dry weight was added. The samples were vortexed at room temperature 3 X 10 sec with a 2 min break on ice in between rounds. The extracts were then centrifuged at 13,500 rpm for 10 min at 4°C, followed by 13,500 rpm for 1 h at 4°C. Then protein contained supernatant was transferred to a new eppendorf tube and frozen at -80°C. Protein concentration was measured using the Bradford assay (Bio-Rad) [101].

2.9 Western Blotting

Approximately 30 μg of protein were analyzed on 7.5% SDS PAGE gels. Proteins were then transferred to PVDF (polyvinyl difluoride) membranes (BIO-RAD) at 30V, 4°C, overnight. The membrane was dried, and incubated in blocking solution (5% milk in 1X TBST with 0.05% Tween-20) for 90 min, washed 3 times with 1X TBST (50 mM Tris, 0.15 M NaCl, 0.05% Tween-20, pH 7.6) for 10 min each, then incubated with primary antibody diluted in TBST for 2 h. Primary antibodies included Mouse monoclonal antibody Clone 12CA5 Anti-HA (Roche Diagnostics, 1:500 dilution), Pierce Anti-TAP Tag Rabbit polyclonal Antibody (Thermo Scientific, 1:1000 dilution) and Anti-c-myc Mouse monoclonal antibody Clone 9E10 IgG (Roche Diagnostics, 1:250 dilution). Membranes were washed 3 times with 1X TBST for 10 min each, and incubated with secondary antibody for 1 h. Secondary antibodies included Goat anti-

rabbit IgG-HRP (Santa Cruz Biotechnology, 1:1000 dilution), Goat anti-mouse IgG (H+L) (Mandel Scientific, 1:500 dilution). After membranes were washed 3 times with 1X TBST for 10 min each, signal was detected using chemiluminescence with ECL (GE Healthcare). For membrane stripping, 15 ml of stripping solution (0.4% SDS, 1.2 mM Tris pH 6.8, 0.25g DTT) was prepared and incubated at 50°C for at least 2 h. Membrane was rinsed with 2X TBST for 10 min, and incubated in stripping solution for 30 min at 50°C. Membranes were then blocked as described above.

2.10 Co-Immuoprecipitation

Overnight cultures of strains were diluted into 1 L of YPD medium and incubated in 30°C until the OD_{600nm} reached 0.8-1.0. The culture was centrifuged for 5 min at 3000 rpm, and the remaining pellet was immersed in liquid nitrogen or dry ice and stored at -80°C. Protein was extracted using the lyophilization method described above. For Co-immunoprecipitation, IgG Sepharose 6 Fast Flow beads (GE Healthcare) or Mono HA 11 Affinity beads (Covance) were used. Prior to use, 60 µl of beads (which included a 40 µl bead volume) were centrifuged at 2500 rpm for 2 min at 4°C. The buffer was removed and the beads were washed 3 times in 500 µl HK buffer. The final washed beads were resuspended in fresh HK buffer to a final volume of 60 µl, and were combined with 40 mg of protein. After incubating overnight at 4°C with rocking, beads were centrifuged at 2500 rpm for 2 min at 4°C and washed 4 times with 500 µl HK buffer. Protein was eluted from the beads by boiling in 50 µl of 1X SDS sample buffer (50 mM Tris pH 6.8, 2% SDS, 0.01% Bromophenol blue, 10% Glycerol, 100mM DTT) for 10 min. After

centrifuging at 13,500 rpm for 2 min at 4°C, the supernatant was removed and beads were boiled in another 40 µl 1X SDS sample buffer for 10 min. Eluted samples were combined and approximately 30 µl was loaded on SDS PAGE gels for Western blotting.

2.11 Two Step Affinity Purification

Affinity purification was carried out according to Rigaut *et al.* (1999) and Liu *et al.* (2010) [100, 102], with some modifications. TAP-tagged and isogenic control strains were inoculated into 20 ml of YPD medium and grown overnight at 30°C. The overnight culture was diluted into 2 L of YPD medium and incubated in 30°C until the OD_{600nm} reached 0.8-1.0. The culture was centrifuged for 5 min at 3000 rpm, and after removing the supernatant, the pellet was frozen in liquid nitrogen or dry ice and stored at -80°C. Protein was extracted using the lyophilization method described above. A 2 L culture typically yielded 200 mg–300 mg of protein. For the first step of the affinity purification, 200 mg–300 mg of protein from tagged and untagged strains were pre-cleared by adding 500 µl of Sepharose 6B (Sigma) beads and rocking at 4°C for 30 min. The beads were removed by centrifuging at 2500 rpm for 2 min at 4°C and the extract was incubated with 500 µl IgG Sepharose 6 Fast Flow (GE Healthcare) for 4 h at 4°C with rocking. After 4 h, the extract and beads were poured into a Poly-Prep Chromatography Column (BIO-RAD). The elute was discarded and beads were washed twice with 10 ml ice cold IPP300 buffer (25 mM Tris-HCl pH 8.0, 300 mM NaCl, 0.1% NP-40), once with 10 ml IPP150 buffer (25 mM Tris-HCl pH 8.0, 150 mM NaCl, 0.1% NP-40) and once with 10 ml TEV CB (25 mM Tris-HCl pH 8.0, 150 mM NaCl, 0.1% NP-40, 0.5 mM EDTA and 1 mM DTT).

After 1 ml TEV CB buffer containing 50 U of Ac-TEV protease (Intrivogen) was added, the column was capped, and rocked overnight at 4°C. The next day, the eluate was collected and beads were washed with another 1 ml TEV CB buffer. To the final 2 ml eluate, 6.0 ml of CBB (25 mM Tris-HCl pH 8.0, 150 mM NaCl, 1 mM Mg acetate, 1 mM Imidazole, 2 mM CaCl₂), 24 µl of 1.0 M CaCl₂ and 300 µl of Calmodulin Sepharose 4B (GE Healthcare) was added. The mixture was rocked for 1 h at 4°C. After centrifugation, beads were washed twice with 1.0 ml CBB (0.1% NP-40), and once with 1.0 ml CBB (0.02% NP-40). Protein was eluted from the beads by two subsequent additions of 1.0 ml CEB (25 mM Tris-HCl pH 8.0, 150 mM NaCl, 0.02% NP-40, 1 mM Mg acetate, 1 mM Imidazole, 20 mM EGTA, 10 mM β-mercaptoethanol). The elutions were combined and protein was precipitated by adding ¼ volume of 50% room temperature Trichloroacetic acid (TCA) (Sigma). The samples were kept on ice for 30 min, then centrifuged at 16,000 g for 10 min at 4°C. The supernatant was removed, and 1.0 ml of -20°C stored 80% acetone was added to wash the precipitate. After centrifuged at 16,000 g for 10 min at 4°C to remove the acetone, the sample was air-dried on ice for approximately 1 h until all acetone evaporated. The pellet was re-suspended in 30 µl 1 X SDS sample buffer, and boiled for 10 min. One quarter of the sample was loaded on an SDS-PAGE gel for silver staining (BIO-RAD). The remainder was run on a separate SDS PAGE gel, until the sample entered the resolving gel, to ensure a compact band of stacked proteins [100]. The gel was stained with Coomassie blue (BIO-RAD), and gel pieces corresponding to tagged and untagged strains were sent for processing and analysis via Orbitrap LC/MS (IRIC,

University of Montreal). Alternatively, the entire TCA precipitate was washed 3 times by acetone and sent for analysis via mass spectrometry (IRIC, University of Montreal).

2.12 ChIP-chip

The ChIP-chip protocol was carried out according to Znaidi *et al.* (2009), Liu *et al.* (2007) and Huang *et al.* (2010) [103-105], in collaboration with Dr. Martine Raymond, IRIC, University of Montreal. Briefly, strains YC113 (*swi4/SWI4-HA*) and untagged strain YC901 were inoculated into 10 ml of YPD and incubated overnight at 30°C. Overnight cultures were diluted to an O.D._{600nm} of 50 ml of YPD medium, and incubated at 30°C until the OD₆₀₀ reached 0.8. In order to cross-link the cells, 1.4 ml of 37% formaldehyde was added. Cultures were rocked on a shaker for 30 min, after which 2.5 ml of 2.5 M glycine was added to inhibit further cross-linking. Cells were centrifuged at 3,600 rpm for 5 min at 4°C to remove the media, after which 40 ml of ice-cold TBS was added. The cells were re-suspended, centrifuged at 3,600 rpm for 5 min at 4°C, and the wash repeated. Final pellets were stored at -80°C. In order to extract the chromatin, cell pellets were re-suspended in 700 µl ice-cold lysis buffer (50 mM HEPES-KOH pH 7.5, 140 mM NaCl, 1 mM EDTA, 1% Triton X-100, 0.1% Na-deoxycholate, 1 mM PMSF, 1 mM Benzamidine, 10 µg/ml Aprotinin, 1 µg/ml Leupeptin, 1 µg/ml Pepstatin) and disrupted in a Mini bead-beater (Biospec, Mini-Beadbeater-8) for 5 min followed by 5 min on ice. The beating was repeated 5 more times or until at least 70% of the cells appeared to have been disrupted under microscope. A hole was punched in the bottom of the eppendorf tube to elute into a new tube. The extract was re-suspended in

700 μ l lysis buffer and sonicated (Branson Sonifier 250) at setting 7, 10 times for 10 sec each, with at least 1 min break on ice between every round. The samples were then centrifuged at 13,500 rpm for 5 min at 4°C and the supernatant transferred to a new 1.5 ml Eppendorf tube. In order to precipitate the tagged protein plus bound chromatin, 30 μ l of anti-HA-coupled-magnetic beads (Covance) were added and the samples rotated overnight at 4°C (Fisher, Hematology Chemistry Mixer 346). The next day, beads were washed twice with 1 ml lysis buffer, twice with 1 ml 360 mM NaCl supplemented lysis buffer, twice with 1 ml wash buffer (10 mM Tris-HCl pH 8.0, 250 mM LiCl, 0.5% NP40, 0.5% Na-deoxycholate, 1 mM EDTA) and once with 1 ml TE (10 mM Tris pH 8.0, 1 mM EDTA). In order to reverse the cross-linking, 50 μ l of TE/SDS (10 mM Tris pH 8.0, 1 mM EDTA, 1% SDS) was added to the beads and the samples were incubated overnight at 65°C. The DNA was then purified by incubating in RNase A and protease K, followed by extraction with phenol/chloroform/isoamyl alcohol and ethanol precipitation. In order to label DNA with Cy3 or Cy5 dyes, DNA fragments were first blunted with T4 DNA polymerase, ligated to linkers, and amplified by ligation-mediated PCR with aminoallyl-modified dUTP. The amplified DNA was then labelled with monoreactive Cy-dye NHS esters that will react specifically with the aminoallyl-modified dUTP. The tagged strain was labelled with Cy5 and the untagged strain labelled with Cy3. Dye-labelled DNA was combined and hybridized to a *C. albicans* whole genome tiled oligonucleotide DNA microarray (NimbleGen Systems Inc) [106]. Slides were scanned with a GenePix 4000B scanner (Molecular Devices). The data was subsequently analyzed in a custom-designed *C. albicans* genome browser (<http://www.candida-montreal.ca/>) based on assembly 19 of

the *C. albicans* genome (<http://www.candidagenome.org/>). Enriched peaks were based on a fold enrichment of 1.6 or higher, and P value of 0.01 or less.

The data was subsequently grouped according to function or process using the GO Slim Mapper tool at CGD (<http://www.candidagenome.org/cgi-bin/GO/goTermMapper>). In order to identify common binding motifs in the data set, enriched promoter binding regions identified from the ChIP-chip data were uploaded into SCOPE (<http://genie.Dartmouth.edu/scope>). The data was also screened for the presence of MCB and SCB sequences using fuzznuc software from EMBOSS (<http://emboss.bioinformatics.nl/>). As a control, 1.5 kb sequences representing intergenic regions from the entire genome were also utilized [103, 104].

2.13 Cell imaging

Cells were visualized by fixing cells in 70% ethanol for 1 h. Nomarski differential interference contrast (DIC) images were obtained with a Leica DM6000B microscope (Leica Microsystems Canada Inc. Richmond Hill, ON) equipped with a Hamamatsu-ORCA ER camera (Hamamatsu Photonics, Hamamatsu City, Japan) using 63X, or 100X objectives and DAPI (460nm) filter sets. Images were captured with Openlab software (Improvision Inc, Perkin Elmer).

3. Results

3.1 Physical interactions between Swi6p, Swi4p and Mbp1p

3.1.1 Swi6p physically interacts with Swi4p *in vivo*.

Previous genetic and DNA expression-based data suggested that Swi4p and Swi6p may comprise the major components of a putative MBF-like complex in *C. albicans* [74, 77, 79]. However, biochemical evidence supporting complex formation between these factors is lacking. In order to determine whether Swi6p and Swi4p physically interact, we performed co-immunoprecipitation. First, a single copy of *SWI6* in strain CB517 (*swi6Δ/SWI6*) was tagged at the C-terminus with a tandem affinity purification (TAP) tag (Protein A and calmodulin-binding peptide, separated by a tobacco etch virus (TEV) protease cleavage site), using a PCR-amplified linear construct (Fig. 4). This procedure resulted in strain AM201.5, and was completed by a previous graduate student, Amin Osmani. In order to confirm that the protein was expressed and functional, a Western blot and growth curve were completed (Fig. 6). These results, together with the fact that yeast cell morphology was normal (data not shown), suggest that the tagged protein was functional. Next, a single copy of *SWI4* in strain BH114 (*swi4Δ::hisG/SWI4*) was tagged using a similar approach (Fig. 4) with three copies of the haemagglutinin (HA) epitope at the C terminus [107]. Transformants were confirmed for correct integration using PCR (Fig. 7A, B). Western blotting and determination of growth rate (Fig. 7C, D) suggested that the protein was expressed and functional. Strain YC113 (*swi4Δ::HIS1/SWI4-HA-URA3*) was used for subsequent analyses. In order to obtain a double-tagged strain, we

next tagged *SWI4* with HA in strain AM201.5, resulting in strain AH110 (*SWI4/SWI4-HA-HIS1*, *swi6Δ::URA3/SWI6-TAP-ARG4*) (Fig. 8). Strains AH110, YC113 (*swi4::hisG/SWI4-HA-HIS1*) and AM201.5 (*swi6::URA3/SWI6-TAP-ARG*) were subsequently used for co-immunoprecipitation. Immunoprecipitation of Swi6p-TAP with IgG sepharose revealed co-purification of Swi4p-HA (Fig. 9). In contrast, Swi4p-HA was not detected when strain YC113 was incubated with IgG sepharose, indicating that the interaction between Swi6p-TAP and Swi4p-HA was specific (Fig. 9). When Swi4p-HA was alternatively precipitated with anti-HA beads, Swi6p-TAP was present in the pull-down from strain AH110, but not AM201.5 (Fig. 9). Thus, the results suggest that Swi6p physically interacts with Swi4p *in vivo*.

3.1.2 Swi6p physically interacts with Mbp1p *in vivo*.

C. albicans also contains an orthologue of *MBP1*, but its function is not clear due to the fact that cells lacking this factor did not show a strong growth or morphology phenotype, unlike $\Delta\Delta swi4$ or $\Delta\Delta swi6$ cells [77]. Since Swi6p in *S. cerevisiae* forms a second complex with Mbp1p to form MBF [31], we tested whether Swi6p in *C. albicans* also interacts with Mbp1p, using co-immunoprecipitation. First, strains carrying a single copy of *MBP1-TAP* or *SWI6-HA* were created to ensure that the proteins were functional. Strain BWP17 was first transformed with a construct to tag *MBP1* at the C-terminal with TAP. This tagging was done by a previous lab member, Reuben Ostrofsky, and confirmed by Western blotting (Fig. 10A). The resulting strain ROm101 was next transformed with an *MBP1* deletion construct (Fig. 10B). Absence of the untagged allele

was confirmed by PCR (Fig. 10C), and Western blotting demonstrated the expression of Mbp1p-TAP (Fig. 10D). Next, a strain carrying a single copy of *SWI6* tagged at the C-terminal with HA was constructed, and confirmed via PCR and Western blotting (Fig. 11). The resulting strains YC367 (*mbp1::HIS1/MBP1-TAP-URA3*) and YC216 (*swi6::HIS1/SWI6-TAP-URA3*) grew in a normal manner (Fig. 12), further demonstrating that the tagged proteins were functional. We next transformed strain YC216 with a construct to tag *MBP1* at the C-terminal with TAP (Fig. 13). The resulting strain YC396 was confirmed by PCR and Western blotting (Fig. 13). In order to determine whether Swi6p interacted with Mbp1p, strains YC396 (*MBP1/MBP1-TAP-ARG4, swi6::HIS1/SWI6-HA-URA3*), YC216 (*swi6::HIS1/SWI6-HA-URA3*) and YC367 (*mbp1::HIS1/MBP1-TAP-URA3*) were utilized for co-immunoprecipitation. Precipitation of Mbp1p-TAP with IgG-Sepharose pulled down Swi6-HA (Fig. 14). Moreover, when Swi6-HA was precipitated with anti-HA beads, Mbp1p-TAP was present in the pull-down (Fig. 14). In contrast, neither protein was pulled down when immunoprecipitations were performed with single-tagged strains YC216 or YC367, respectively. Thus, Swi6p specifically also interacts with Mbp1p *in vivo* (Fig. 14).

3.1.3 Swi4p and Mbp1p may interact.

Since Swi6p separately interacts with Swi4p and Mbp1p in *S. cerevisiae* to form SBF (Swi6p/Swi4p) and MBF (Swi6p/Mbp1p), respectively, and *C. albicans* contains close orthologues of all three factors, it is possible that there are also two major G1/S transcription factor complexes in this organism. Alternatively, *C. albicans* may contain a single complex, as seen in *S. pombe*, which includes Swi4p, Swi6p and possibly Mbp1p.

In support of the latter, Cote *et al.* (2009) demonstrated an enrichment of MBF, but not SBF, binding sites in promoters of genes that were modulated at G1/S phase [74]. Furthermore, absence of Mbp1p had little effect on growth of *C. albicans* yeast cells, in contrast to absence of Swi4p or Swi6p [77]. If *C. albicans* contained a single major G1/S regulatory complex that included Swi6p, Swi4p and possibly Mbp1p, we predict that Swi4p and Mbp1p might also physically interact. To test this hypothesis, strain YC113 (*swi4::hisG/SWI4-HA-HIS1*) was transformed with a construct to TAP-tag *MBP1*, utilizing a fusion PCR scheme (Fig. 5). Strains were confirmed via PCR and Western blotting (Fig. 15), and co-immunoprecipitation was carried out with strains YC372 (*swi4::hisG/SWI4-HA-HIS1, MBP1/MBP1-TAP-URA3*) and YC113. When Mbp1p-TAP was precipitated with IgG sepharose, Swi4p-HA was present in the immune complex, and Swi4p-HA did not co-purify with IgG Sepharose in a strain lacking Mbp1p-TAP (Fig. 16A), suggesting that Swi4p-HA and Mbp1p-TAP interact. However, Mbp1p-TAP and Swi4p-HA are similar in size, unlike the situation with tagged proteins in the previous co-immunoprecipitation experiments. Therefore, it is possible that the bands corresponding to the original precipitated protein, and reflect non-specific cross-reaction with antibodies. Indeed, antibodies can cross-react with the Protein A epitope in the TAP tag. We did not observe any cross reaction between the anti-HA antibody used for Western blotting and TAP-tagged proteins in crude protein extracts (Figs. 9, 14). However, cross-reaction may take place if the TAP-tagged protein were significantly enriched. In order to test this possibility, the co-immunoprecipitation was repeated with the inclusion of strain YC367 (*mbp1::HIS1/MBP1-TAP-URA3*) for comparison. When a Western blot containing the

IgG sepharose precipitate was incubated with anti-HA antibody, strong cross-reaction was observed with Mbp1p-TAP (Fig. 16B). Thus, the identity of the band observed for Swi4p-HA in Fig. 16A is not conclusive.

In order to test for an interaction between Swi4p and Mbp1p in the absence of potential non-specific cross-reaction with antibodies, and with a greater distinction in protein size, we tagged Swi4p with the MYC epitope and Mbp1p with HA (Figs. 17, 18). First, the single copy of *SWI4* in strain BH180 was tagged with 5 copies of the MYC epitope, resulting in strains YC131 (*swi4::HIS1/SWI4-MYC-URA3*) (Fig. 17). The strain was confirmed via PCR (Fig. 17B) and Western blotting demonstrated expression of the tagged protein at the expected size (Fig. 17C). However, a subsequent analysis of the oligonucleotides that were utilized for creating the MYC-tagging construct showed that two nucleotides were missing, which would result in the MYC sequence being out of frame. Since a band was observed on the Western blot, albeit more faint than when Swi4p was tagged with HA, we subsequently tagged *MBP1* in this strain with HA, resulting in strain YC602 (*swi4::HIS1/SWI4-MYC-URA3 MBP1/MBP1-HA-ARG4*) (Fig. 18). Western blotting demonstrated expression of Mbp1p-HA (Fig. 18C) and also expression of Swi4p-MYC (Fig. 18D). Strains YC602 and YC131 were subsequently used for co-immunoprecipitation. Immunoprecipitation of Mbp1p-HA with anti-HA agarose did not result in co-purification of Swi4p-MYC (Fig. 19). This suggests that Mbp1p and Swi4p may not interact. However, the error in the construct for tagging with MYC, coupled with the relative weakness of the putative Swi4p-MYC band, question the validity of this result.

We thus went back to strain YC372 (*swi4::hisG/SWI4-HA-HIS1, MBP1/MBP1-TAP-URA3*) but alternatively precipitated with anti-HA agarose. In this case, Mbp1p-TAP was co-purified (Fig. 20A). Importantly, the anti-TAP antibody did not cross-react with Swi4p-HA, even when enriched (Fig. 20B). Thus, Swi4p may interact with Mbp1p.

3.2 Affinity purification of Swi6p, Swi4p and Mbp1p and mass spectrometry analyses of putative interacting proteins.

In the model yeast systems *S. cerevisiae* and *S. pombe*, G1/S transcription complexes SBF and MBF, or MBF, respectively, are essential for cell proliferation. Absence of the DNA binding units Swi4p and Mbp1p, Res1p, Res2p or Cdc10p, prevents growth [42, 43, 108, 109]. Additional components that contribute to G1/S transcriptional regulation and SBF/MBF function in *S. cerevisiae*, including Whi5p, Nrm1p, Msa1p and Msa2p, were identified via tandem affinity purification of the components, and Multi-dimensional Protein Identification Technology (MudPIT) [23, 110]. Since absence of both Swi4p and Mbp1p in *C. albicans* was not lethal [77], in contrast to the situations in *S. cerevisiae* and *S. pombe*, we predicted that G1/S regulation likely involves additional core factors [77]. In order to identify additional putative regulators of G1/S progression, as well as further elucidate the mechanisms by which Mbp1p, Swi4p and Swi6p may be functioning, we systematically tandem-affinity purified each protein and identified interacting factors using mass spectrometry.

In order to tandem-affinity purify the proteins, we utilized the TAP tag consisting of protein A and calmodulin-binding protein [102]. Strains AM201.5

(*swi6::URA3/SWI6-TAP-ARG4*) and YC367 (*mbp1::HIS1/MBP1-TAP-URA3*) were previously constructed. We thus created a strain carrying a single copy of *SWI4* tagged with TAP (Fig. 21). A Western blot (Fig. 21C), growth curve (Fig. 21D) and cell phenotype assay (data not shown) confirmed that Swi4p-TAP was expressed and functional. Strains YC193 (*swi4::HIS1/SWI4-TAP-URA3*), AM201.5 (*swi6::URA3/SWI6-TAP-ARG4*), YC367 (*mbp1::HIS1/MBP1-TAP-URA3*) and isogenic, untagged control strains BH440 (*URA3+*, *HIS1+*) or BH415 (*URA3+*, *ARG4+*) were incubated in YPD medium and collected at an O.D._{600nm} of 0.8–1.0. Following protein extraction and two-step affinity purification, silver-stained gels of the samples demonstrated that more protein was pulled out of the tagged vs untagged strains (Fig. 22). The affinity purification was then repeated and TCA-precipitated samples were run on an SDS PAGE gel until they just entered the resolving gel [100]. Gels were stained with Coomassie blue, and single gel pieces corresponding to tagged and untagged strains were sent for processing and analysis via Orbitrap LC/MS (IRIC, University of Montreal). Alternatively, the entire TCA precipitate was washed 3 times by acetone and sent for analysis via mass spectrometry.

3.2.1 Swi6p-intertacting proteins

Analysis of Swi6p-TAP affinity purified samples obtained from exponentially growing cells demonstrated abundant peptides corresponding to Swi6p (28), Swi4p (52) and Mbp1p (22) (Table 4). The remaining factors were represented by fewer peptides, many of which had ribosome-related or other functions. Notably, no other cell-cycle-associated factor was identified, in contrast to physical associations of Swi6p in *S.*

cerevisiae with Cdc28p, Whi5p, the G1 cyclin Cln3p and histones, for example [23, 111]. The results support our previous co-immunoprecipitation data that demonstrated Swi6p physically interacts with Swi4p and Mbp1p. The absence of enriched, additional proteins suggests that Swi4p and Mbp1p may be the predominant binding partners of Swi6p, albeit under the growth conditions used.

3.2.2 Swi4p-intertacting proteins

When Swi4p was affinity purified from exponential-growing cells, the most abundant peptides (142) corresponded to Swi4p, followed by Swi6p (85). Additional factors were present at 20 peptides or less, and were associated with ribosome organization/function, and various metabolic processes (Table 5). Notably, and unlike that found for Swi4p in *S. cerevisiae* (<http://www.yeastgenome.org/>), many peptides also corresponded to regulatory particles of the 26S proteasome, the ribonucleotide reductases Rnr1p and Rnr21p that have crucial functions at G1/S [112], and both α and β -tubulin. Moreover, Cdc46p, whose orthologue in *S. cerevisiae* is a component of the MCM complex that primes origins of replication in G1 phase [113], was enriched. The interaction data was further distinguished from that of Swi4p in *S. cerevisiae* in that no CDK, cyclins, MAPK or Whi5p-/Nrm1p-like factor was identified. However, similar to that found with Swi4p in *S. cerevisiae*, Mbp1p was not present, further questioning whether these factors directly interact. In conclusion, the results suggest that Swi6p is the predominant binding partner of Swi4p.

3.2.3 Mbp1p-interacting proteins

When Mbp1p was affinity-purified from exponential-growing cells, the yield of enriched peptides was much lower than that obtained with Swi4p-TAP or Swi6p-TAP (Table 6). While Mbp1p was present at 50 peptides, Swi6p was detected at 4 peptides, and Nrm1p (*orf19.6022*) was detected at 6 peptides. Swi4p was not present, in agreement with the Swi4p-interacting data in Table 5. In order to enhance detection of Mbp1p-interacting proteins, we repeated the procedure but increased the amount of input protein from 240 mg to 550 mg. Table 7 demonstrates that more factors were identified, but the yield and number of peptides was still much lower than that obtained during Swi4p or Swi6p affinity purifications. Mbp1p was present at only 2 peptides, while Swi6p was present at 3 peptides. The remaining factors were predominantly associated with ribosomal functions. Swi4p was not detected, nor was Nrm1p. This data supports the notion that Mbp1p interacts with Swi6p and suggests an additional interaction with Nrm1p. However, the results further question a direct interaction with Swi4p.

3.2.4 Swi6p-interacting proteins in cells blocked in G1 phase

The lack of detection of additional interacting factors for Swi6p, Swi4p and Mbp1p did not allow for significant additional insights on protein function/regulation. The absence of detection may be due to the fact that purifications were performed in asynchronous, exponential-growing cells. Attempts to identify additional SBF and MBF interactors in *S. cerevisiae* via tandem affinity purification utilized cells blocked in or entering late G1 phase [23], although the results were similar regardless of the phase.

Thus, in order to enhance detection of additional binding proteins, we tagged Swi6p with TAP in a strain that carried a single copy of the G1 cyclin *CLN3* under control of the conditional *MET3* promoter [93]. This approach allows G1 phase arrest and cell synchronization upon repression of *CLN3* [76]. Strain YC221 (*SWI6-TAP-URA3/SWI6 cln3::hisG/MET3p-CLN3-ARG4*) was confirmed via PCR screening and Western blotting (Fig. 23), and grown overnight at 30°C in inducing (-MC) medium. The untagged parental strain, BH253 (*cln3::hisG/MET3p-CLN3-ARG4*), was included as a control. The next day, cells were diluted into repressing (+MC) medium and collected after a 4 h incubation, which resulted in a homogeneous block in G1 phase [76]. After affinity purification of Swi6p-TAP and analysis of the precipitates using mass spectrometry, the most abundant peptide (48) corresponded to Swi4p (Table 8), similar to that found when Swi6p was purified from exponential-growing cells (Table 4). Swi6p was present at 6 peptides. The majority of additional abundant peptides corresponded to those with ribosomal-associated functions. Intriguingly, a significantly enriched peptide corresponded to the polo-like kinase Cdc5p, which plays important roles in mitotic progression in *C. albicans*, although the mechanisms remain unclear [114]. Cdc5p does not interact with Swi6p in *S. cerevisiae*. Intriguingly, Mbp1p was also not detected, unlike with that found in exponential-growing cells. These results suggest that Swi4p is the predominant binding factor of Swi6p in G1 phase-arrested cells, and that Mbp1p may not interact during this time. However, this remains to be confirmed by co-immunoprecipitation. The absence of Mbp1p could also be related to technical issues.

Overall, these results provide the first systematic identification of putative Swi4p, Swi6p and Mbp1p-interacting factors in *C. albicans*. The data demonstrate that Swi6p and Swi4p preferentially bind each other, while Swi6p can additionally interact with Mbp1p. Surprisingly, few other factors show strong or abundant interactions. Additional components are predicted to exist, but the absence of consistent identification suggests that they may play co-regulatory functions under specific conditions and/or have weaker interactions.

3.3 Mbp1p is expressed at lower levels than Swi4p or Swi6p

Despite demonstrating a physical interaction with Swi6p, the role of Mbp1p in G1/S regulation is still not clear. It does not appear to be playing a major role in growth control, since its absence in *C. albicans* did not have a major effect on growth, unlike absence of Swi4p or Swi6p [77]. Further, cells lacking *SWI4* and *MBP1* were viable, unlike the situation in *S. cerevisiae*. It is possible that Mbp1p may play a more dominant role in growth control in different cell forms or under different conditions. Indeed, the Res2p component of MBF in *S. pombe* becomes the predominant DNA binding component of MBF during premeiotic DNA replication [44]. In order to gain additional insights on regulation and function of Swi4p, Swi6p and Mbp1p, we compared protein expression levels in yeast and hyphal cells. Strains YC193 (*swi4::HIS1/SWI4-TAP-URA3*) AM201.5 (*swi6::HIS1/SWI6-TAP-ARG4*) and YC367 (*mbp1::HIS1/MBP1-TAP-URA3*) were incubated in YPD medium at 30°C until an OD_{600nm} of 1.0 was reached. Yeast cells were collected, and protein was extracted for Western blot analysis. For hyphal-inducing conditions, overnight cultures of yeast cells were diluted into YPD medium containing

10% serum, incubated at 37°C for 2 h, collected and processed for Western blotting. Under yeast growth conditions, Swi6p was expressed approximately twice that of Swi4p (Fig. 24), while Mbp1p was expressed at a lower level. In comparison, Swi4p and Mbp1p in *S.cerevisiae* are present in equal amounts while Swi6p is at a slightly higher level [115]. Our result may explain the lower yields of peptides recovered in the Mbp1p affinity purification investigation. Intriguingly, under hyphal conditions, the relationships between expression levels were maintained, but Mbp1p was at an even lower level than in yeast conditions (Fig. 24). These results highlight differences in expression levels of the factors. Consistently, *SWI4* and *SWI6* in *C. albicans* were shown to be periodically expressed, with peak levels during G1/S transition [74], unlike *MBP1*. Although its role remains unclear, the results further suggest that Mbp1p is not a functional equivalent of Swi4p, and may play a less important role in hyphal vs. yeast cells.

3.4 Identification of possible Swi4p targets using genome-wide location analysis (ChIP-chip).

3.4.1 Global ChIP-chip results

In *S. cerevisiae*, Swi4p predominantly binds the Swi4/6-dependent cell cycle box (SCB) motif located in promoters of target genes important for polar growth of the bud, cell wall deposition, and other processes associated with the G1/S transition [31]. Mbp1p, on the other hand, binds *MluI* cell cycle box (MCB) elements of genes associated with DNA replication [31]. However, not all G1/S-associated genes contain SCB and/or MCB

motifs [31, 116], suggesting Swi4p and Mbp1p-independent regulation and/or that these factors can bind via alternate mechanisms. Cross-binding at SCB and MCB elements by Swi4p and Mbp1p is also known [32]. In *C. albicans*, promoters of G1/S-associated genes were enriched for MCB, but not SCB elements [74]. Although genetic and DNA expression data support a role for Swi4p and Swi6p in regulating the G1/S transition in *C. albicans* [77, 79], data that directly links these factors to G1/S-regulated genes is still lacking. Thus, we sought to identify the targets of Swi4p using genome-wide location analysis (ChIP-chip). Strains YC113 (*swi4::hisG/SWI4-HA-URA3*) and YC901 (*SWI4/SWI4, URA3+*) were grown to an O.D. _{600nm} of 0.8 in YPD medium at 30 °C, collected and processed for use with whole genome *C. albicans* oligonucleotide tiling arrays [104, 117]. Results from a single tiling array (P value of 0.01 and enriched binding ratio of ≥ 1.6 fold) (Fig. 25A) demonstrated 161 binding peaks located at single promoters, 36 located between promoters of two genes, 27 located at both a promoter and ORF, and 212 at ORF's alone. A further 62 were located at 3' ends of genes (Appendix I, Table S6, for complete results). Despite the fact that our results were obtained from a single tiling array, we analyzed them further to glean information on potential Swi4p function. Within the promoter-binding hits (Table 9), significant enrichment was noted for genes associated with budding pattern (*AXL2*), cell wall biogenesis (*PST1*), and cell cycle transitions (*CCN1, PCL2, CLB2, TOS1, YOX1, CUP9, HSL1, MIH1, RAD53*), similar to that seen for Swi4p in *S. cerevisiae* [31]. When the data set was analyzed for most enriched functional groups of genes, using the CGD Gene Ontology Slim Mapper function (<http://candidagenome.org/cgi-bin/GO/goTermMapper>), one of the most highly

represented biological processes was filamentous growth, including many core regulators of hyphal development (*EFG1*, *NRG1*, *TEC1*, *FGR*, *EHT1*, *RBT4*, *ESA1*, *RAS2*, for example) (Tables 9, 10). Overall, these results are consistent with the proposed functions of Swi4p in influencing the G1/S transition as well as hyphal differentiation [77]. Although these results require confirmation via qPCR, the binding pattern on the tiling array for many genes was consistent with that of true “hits” (Fig. 25B). Thus, the data provide the first *in vivo* glimpse of putative Swi4p targets on a genome-wide scale in *C. albicans*.

3.4.2 Comparison of location and expression data reveals some overlap and underscores putative Swi4p targets.

In order to gain additional information on potential Swi4p targets and function, we compared the Swi4p location results with DNA expression data associated with cells passing through G1/S cell cycle phase [74] as well as cells depleted of both Swi4p and Swi6p [77]. When comparing the Swi4p ChIP-chip data with genes that showed modulated expression at the G1/S transition [74], only 19 or 7.3% were common (Fig. 26A). These genes included several of the G1/S cell cycle-related factors such as G1 cyclins *PCL2* and *CCNI*, *YOX1*, *HSL1* and factors belonging to the FGR6 (Filamentous Growth Related) family (Appendix 1 Table S7). In contrast, only 0, 2 and 4 genes were in common when comparing with the M/G1, G2/M or S/G2 transition-associated groups, respectively, with histones *HT2A*, *HT2B*, *HHT2*, and *HHF22* constituting the latter common set (Fig. 26A). Thus, Swi4p may contribute to the regulation of expression of several G1/S associated genes, including G1/S cyclins and factors important for

filamentous growth. The fact that Swi4p was not located at the majority of genes whose expression is modulated at the G1/S transition could imply that Swi4p does not directly regulate these factors, or that the ChIP-chip screen for Swi4p enrichment was not saturated.

We next compared the Swi4p ChIP-chip data with DNA expression profiles of cells that were depleted of Swi6p and Swi4p [77]. In total, 19% (49/262) of the Swi4p-enriched targets were also modulated at the expression level in the absence of Swi4p and Swi6p (Fig. 26B). Intriguingly, common genes included cell cycle factors such as the G1 cyclin *PCL2*, *HCMI*, and *YOXI*, for example (Appendix 1 Table S7). That these genes are modulated at the expression level in the absence of Swi4p and Swi6p, and show enrichment of Swi4p at their promoters, suggests that they may be true Swi4p targets. The remaining large number of genes modulated in the absence of Swi4p and Swi6p that did not show Swi4p enrichment likely reflect indirect effects and possibly some independent function of Swi6p, which has not yet been ruled out [77]. On the other hand, the demonstration of Swi4p-enriched targets that did not change in expression in the absence of Swi4p and Swi6p might reflect technical issues leading to false positives in the ChIP-chip results or false negatives in the microarray data. Alternatively, it is possible that these factors require additional forms of regulation and/or are associated with specific processes/growth conditions. Notably, Swi4p-enriched targets associated with regulation of filamentous growth were not modulated in the absence of Swi4p/Swi6p [77].

3.4.3 A large proportion of Swi4p-enriched loci do not contain the predicted MCB element.

In order to help define the binding sequence for Swi4p, intergenic sequences that showed enriched binding at the promoter only on the tiling array were obtained for motif discovery via SCOPE (<http://genie.Dartmouth.edu/scope/>). The sequence showing the highest significance (147.9) and coverage (95%) was BGHSWC ((T/C/G)G(T/A/C)(C/G)(A/T)C) (Fig. 27), while the next highest in significance (44.1) and coverage (47.2%) was CACAAAA (Fig. 27), which bears close resemblance to the SCB motif, CRCGAAA. Intriguingly, the MCB (ACGCGT) motif was not identified. This was unexpected since genes whose expression was modulated at the G1/S transition showed enrichment of MCB, but not SCB, elements in *C. albicans* [74]. In order to determine whether any Swi4p-enriched intergenic loci contained the conserved MCB element, the same promoter sequences used in SCOPE were analyzed using fuzznuc software from EMBOSS (<http://emboss.bioinformatics.nl/>). Intriguingly, only 3 intergenic regions contained an MCB element, while 14 contained the SCB motif, including *CCNI* and *EFGI* (Table 11). In conclusion, the putative binding sequence of Swi4p does not appear to be MCB as predicted [74]. In order to confirm the presence of the motifs identified by SCOPE in putative Swi4p-enriched loci and determine whether they were truly enriched, we directly searched for these sequences in Swi4p intergenic targets vs. all intergenic regions of the genome using the fuzznuc software. The CACAAAA motif was present in 43.8% of the Swi4p targets (71/162) (Appendix I, Table S8) compared to 20.7% of all intergenic regions (1285/6218), or roughly double

the frequency. The less conserved BGHSCW sequence was 2.5% more frequent in Swi4p targets (850/162) vs. total intergenic regions (12827/6218). Thus, in contrast to many G1/S-associated genes [74], Swi4p putative targets are not enriched for the MCB element. This discrepancy may be due to a requirement for additional factors in G1/S regulation [77] and/or more technical aspects including the small sample size for ChIP-chip and possible lack of saturation. However, the fact that more Swi4p-enriched loci contained a conserved SCB element, and an even higher proportion (over 40%) contained a different motif with some similarity to SCB, questions the current model that there is one G1/S transcription factor complex in *C. albicans*, and its DNA-binding component, Swi4p, acts via the MCB motif [74].

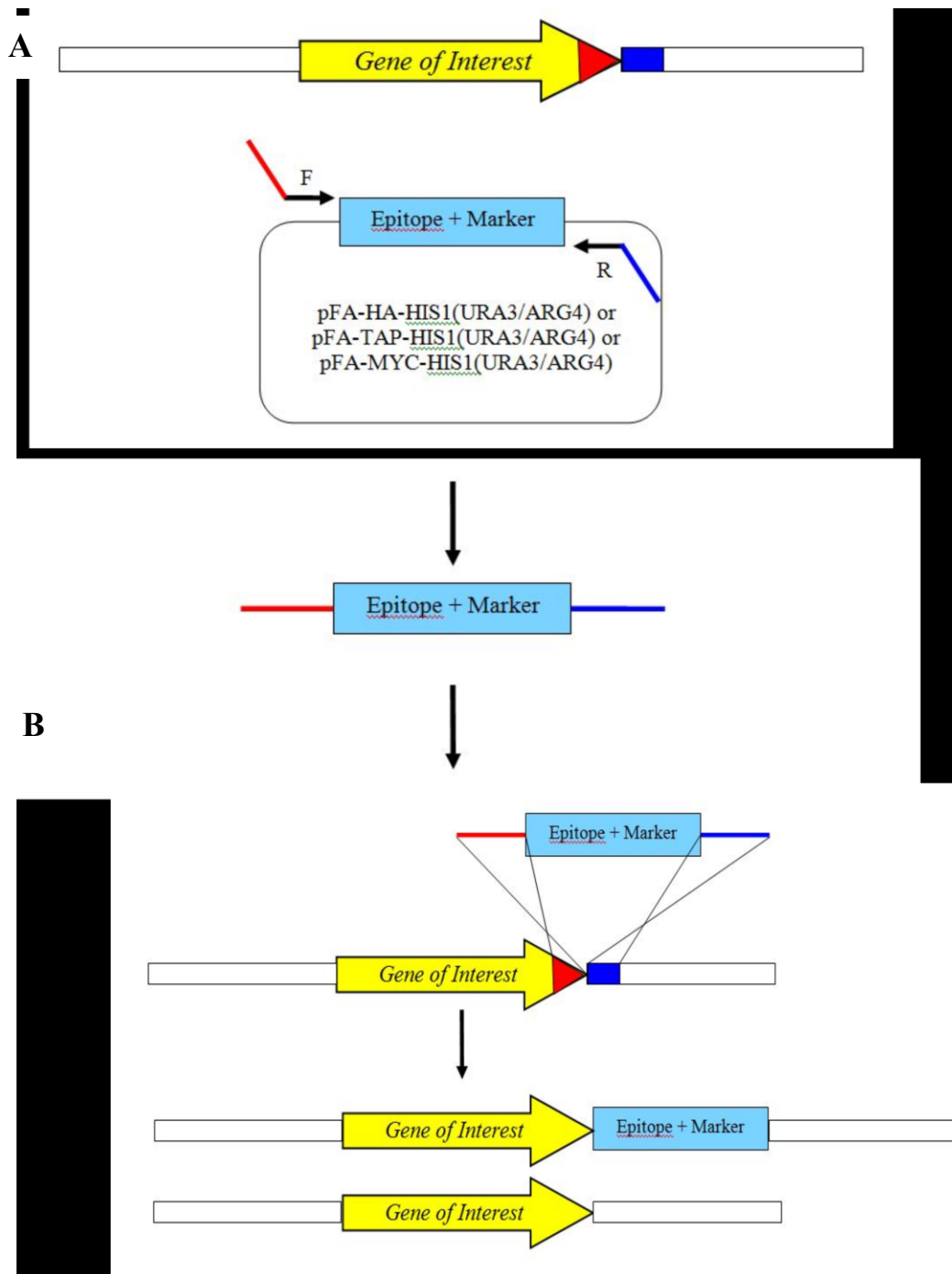


Figure 4. One-step PCR strategy for tagging a gene with HA, TAP or MYC.

(A) Oligonucleotides carrying 100 bp homology to target integration sites of the gene of interest and 20 bp homology to a tag and marker cassette were used to amplify a tagging construct. (B) The construct was transformed into strains for direct integration.

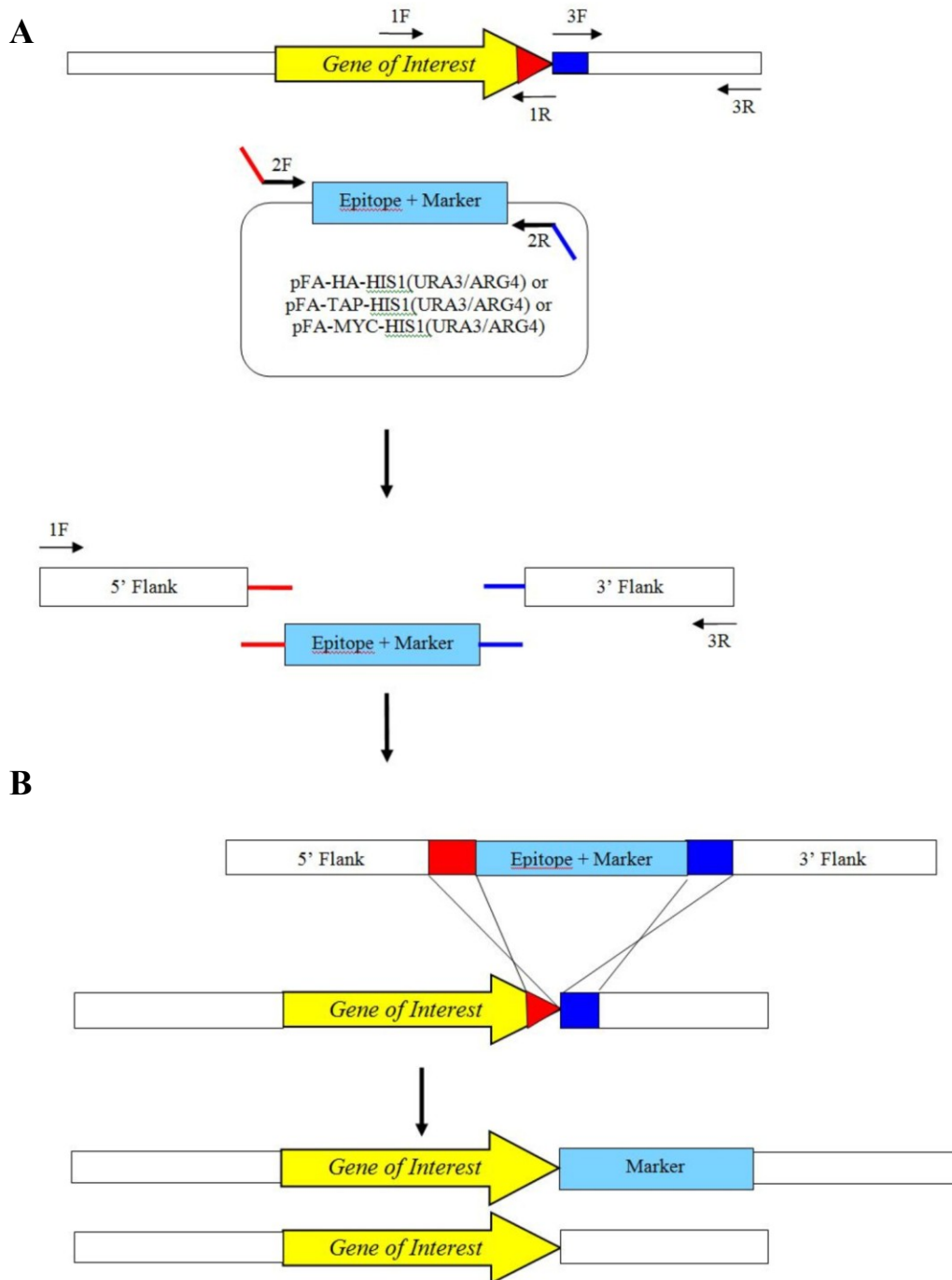
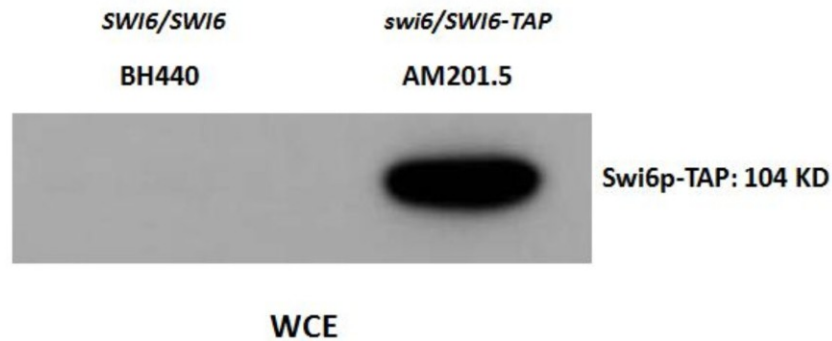


Figure 5. Two-step PCR strategy for tagging a gene with HA, TAP or MYC.

(A) Fragments corresponding to 5' and 3' flanking regions of target integration sites and a tag and marker cassette were amplified, then used in a fusion PCR to produce the integrating construct. (B) The construct was transformed into strains for direct integration.

A



B

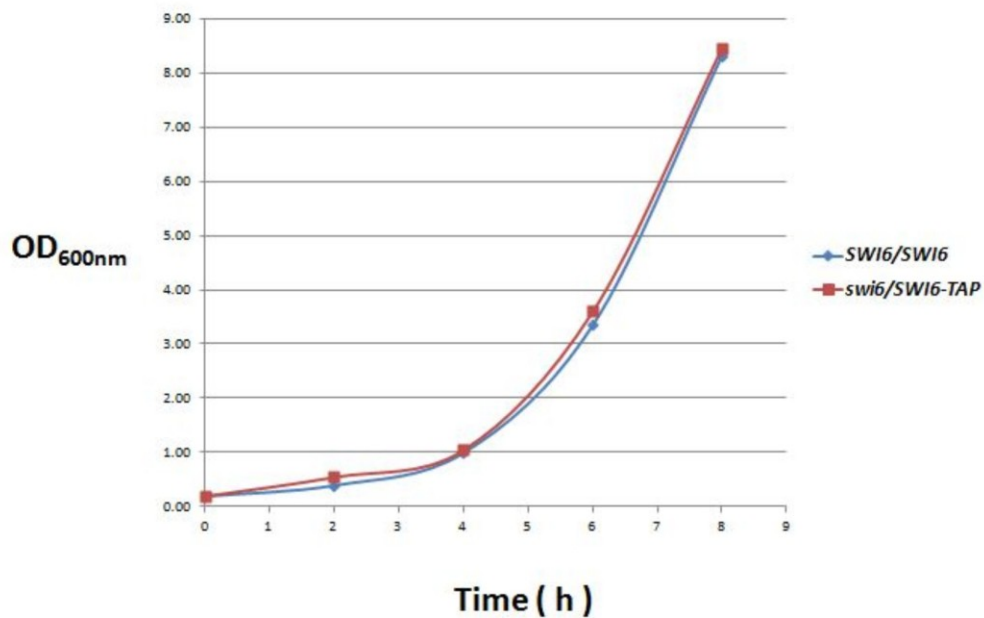


Figure 6. Western blot and growth curve confirming proper expression and function of Swi6p-TAP.

(A) Western blot containing 30 μ g of whole cell protein extracts from strains BH440 (*SWI6/SWI6*, *URA3*⁺, *HIS1*⁺) and AM201.5 (*swi6::HIS1/SWI6-TAP-URA3*) incubated with anti-TAP antibody. (B) Growth curve represented by O.D._{600nm} over time, utilizing strains BH440 and AM201.5.

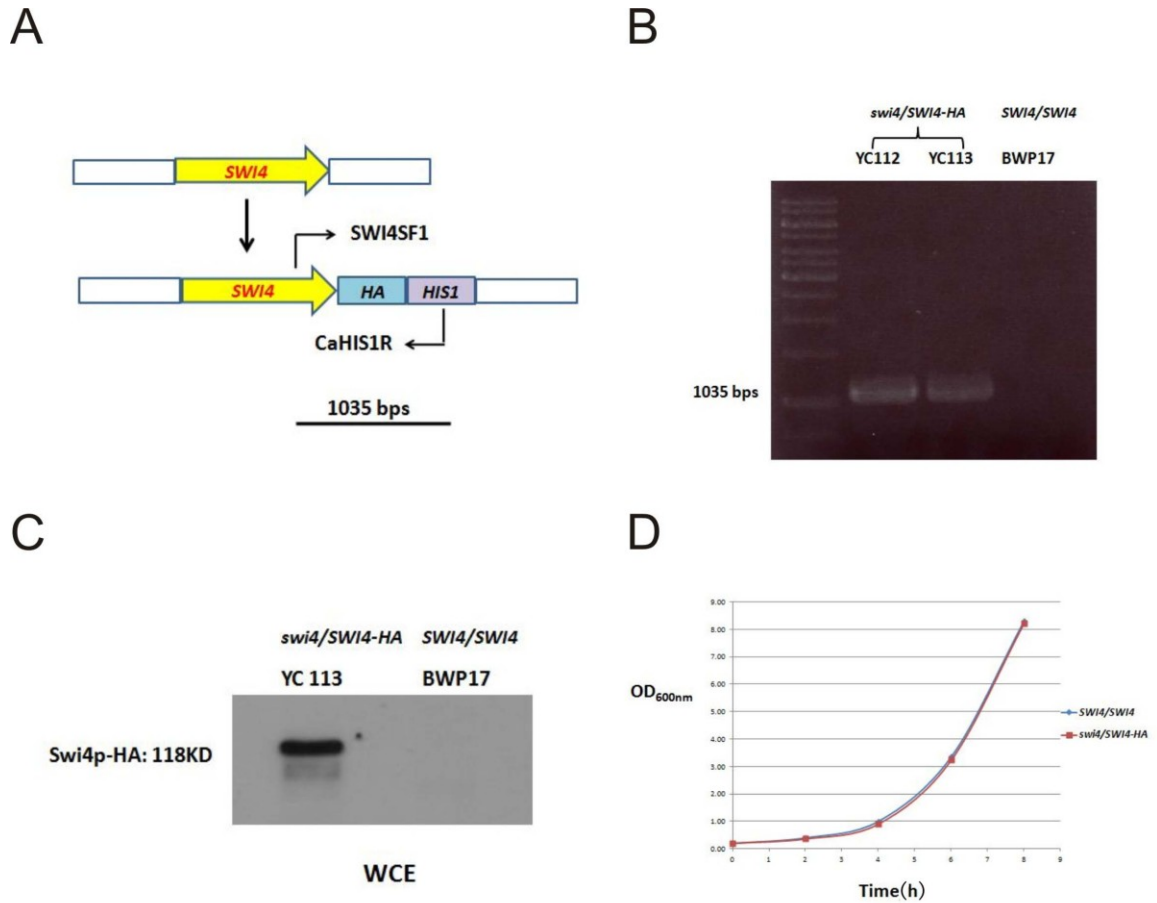


Figure 7. Confirmation of a *swi4* Δ /*SWI4-HA* strain.

(A) Map showing a PCR screening strategy to confirm correct integration of the HA-containing construct. Oligonucleotides SWI4SF1 and CaHIS1R generate a 1035 bp band for *SWI4-HA*. (B) Ethidium bromide-stained DNA gel showing positive strains YC112 and YC113 (*swi4::HIS1/SWI4-HA-URA3*) and the negative control strain BWP17. (C) Western blot containing 30 μ g of whole cell protein extracts from strains YC113 and BWP17 incubated with anti-HA antibody. (D) Growth curve of strains YC113 and BH440 (*SWI4/SWI4*, *URA3*⁺, *HIS1*⁺) represented by O.D. _{600nm} over time.

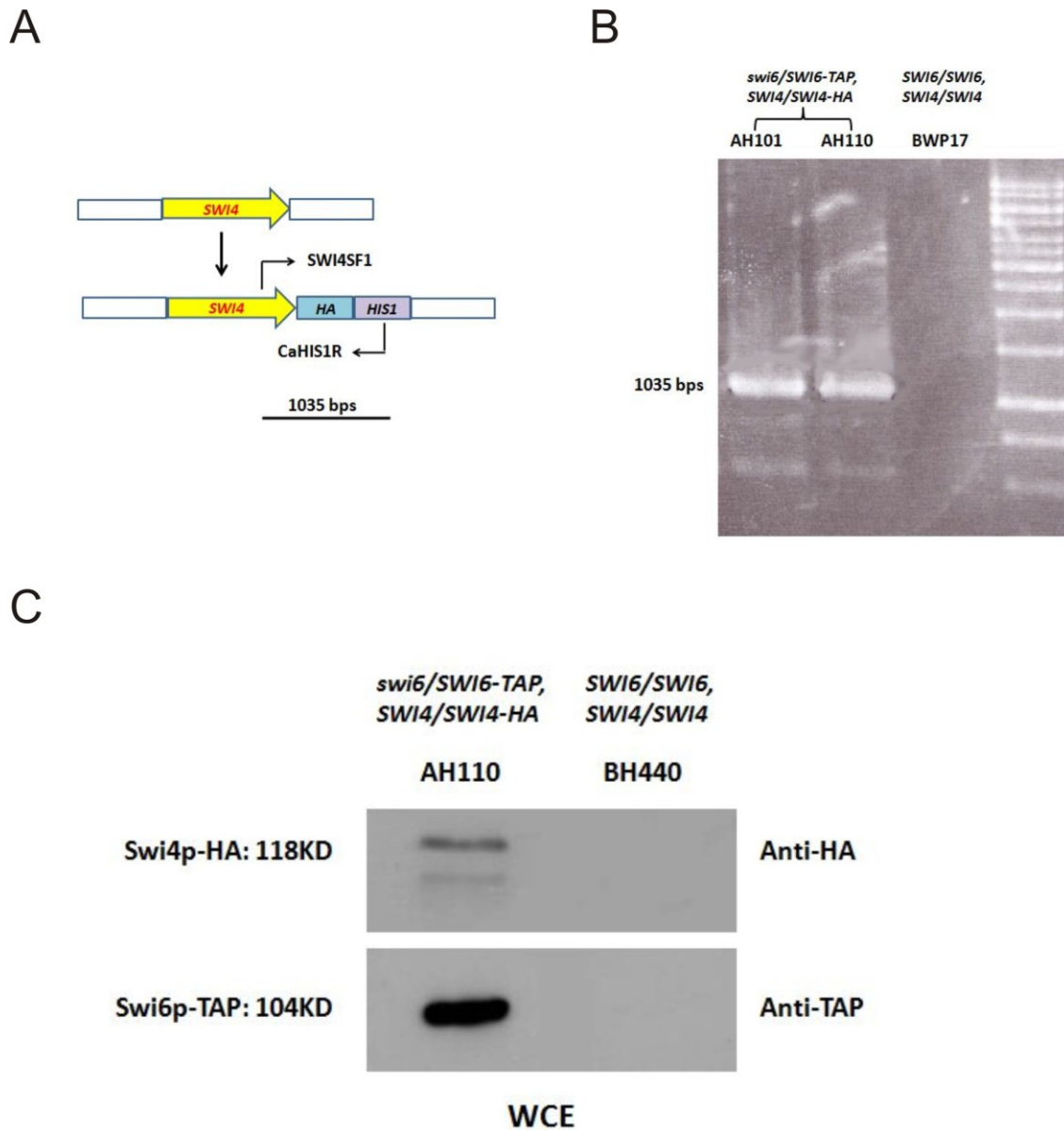


Figure 8. PCR and Western blot confirmation of tagging *SWI4* with HA in a strain carrying *SWI6-TAP*.

(A) Map showing a PCR screening strategy to confirm correct integration of the HA-containing construct. Oligonucleotides SWI4SF1 and CaHIS1R generate a 1035 bp band for *SWI4-HA*. (B) Ethidium-bromide-stained DNA gel showing positive strains AH101 and AH110 (*SWI4/SWI4-HA-HIS1*, *swi6Δ/SWI6-TAP*) and the negative control strain BWP17. (C) Western blot containing 30 μ g of whole cell protein extracts from strains AH110 and BH440 (*SWI4/SWI4*, *SWI6/SWI6*, *URA3+*, *HIS1+*) incubated with anti-HA and anti-TAP antibody, respectively.

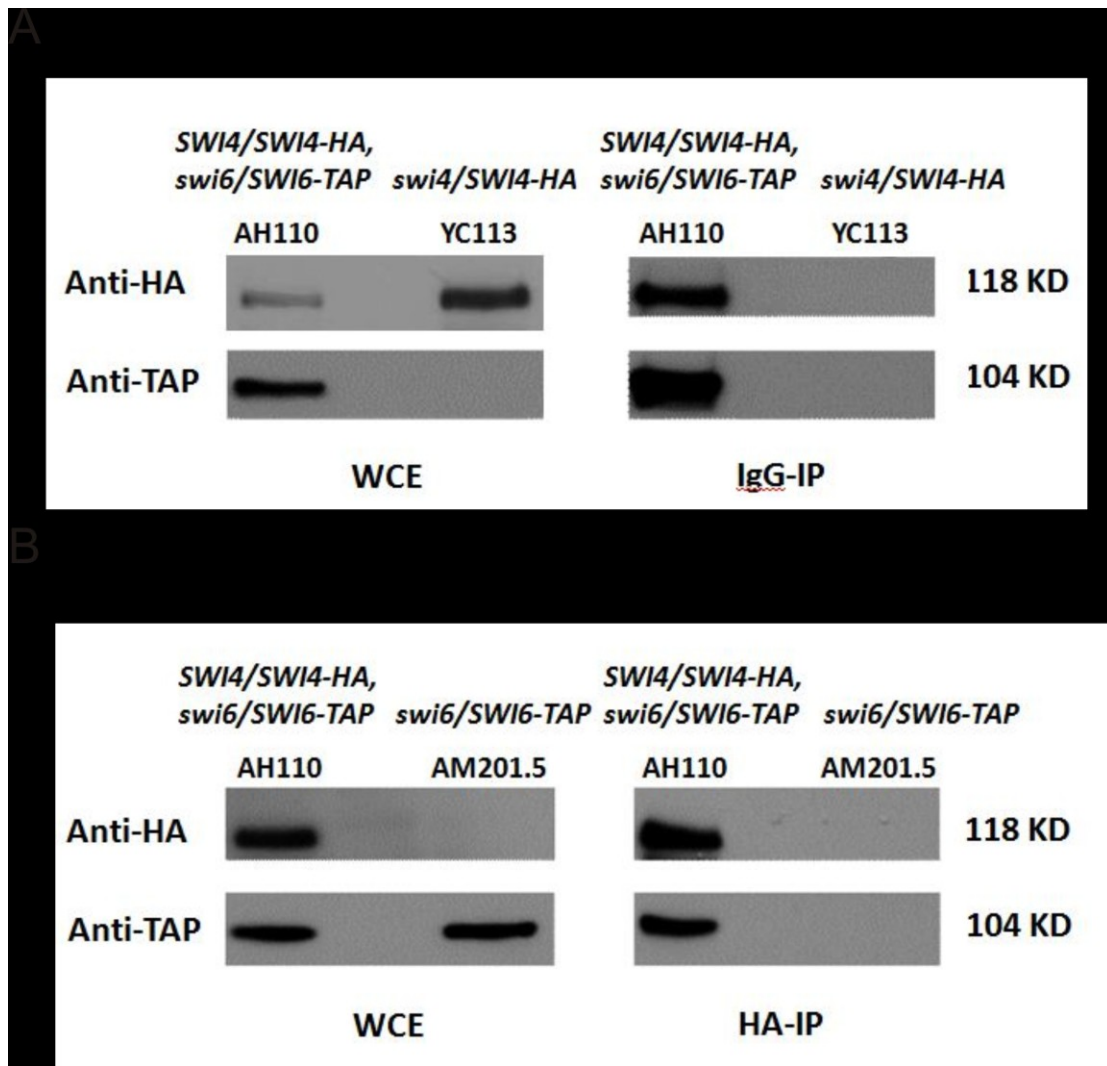


Figure 9. Co-immunoprecipitations demonstrate interactions between Swi4p and Swi6p.

Western blots of whole cell extracts (WCE) and immune-precipitates, using IgG sepharose (IgG-IP) (A) or anti-HA agarose (HA-IP) (B). 20 μ l of beads were incubated with 20 mg of protein overnight, washed, and boiled in SDS sample buffer to elute interacting proteins.

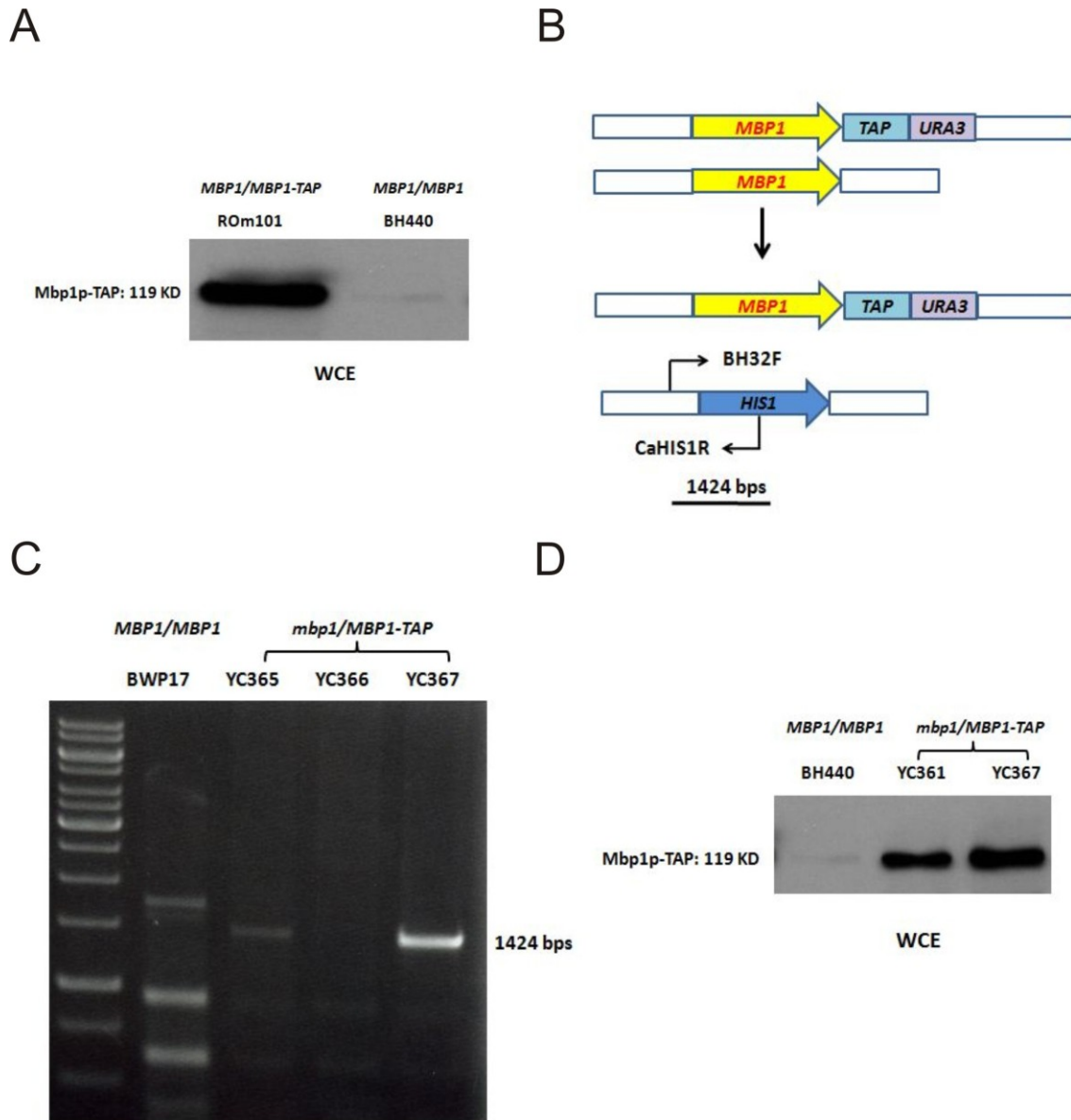


Figure 10. PCR and Western blot confirmation of an *mbp1* Δ /*MBP1-TAP* strain.

(A) Western blot containing 30 μ g of whole cell protein extracts from strains ROm101 and control untagged strain BH440, incubated with anti-TAP antibody. (B) Map showing a PCR screening strategy to confirm replacement of *MBP1* with *HIS1*, where oligonucleotides BH32F and CaHIS1R generate a 1424 bp band. (C) Ethidium-bromide-stained DNA gel showing positive strains YC365 and YC367 (*MBP1-TAP-URA3/mbp1::HIS1*) while YC366 is negative. BWP17 is the parental strain. (D) Western blot containing 30 μ g of whole cell protein extracts from strains YC361, YC367 and control untagged strain BH440, incubated with anti-TAP antibody.

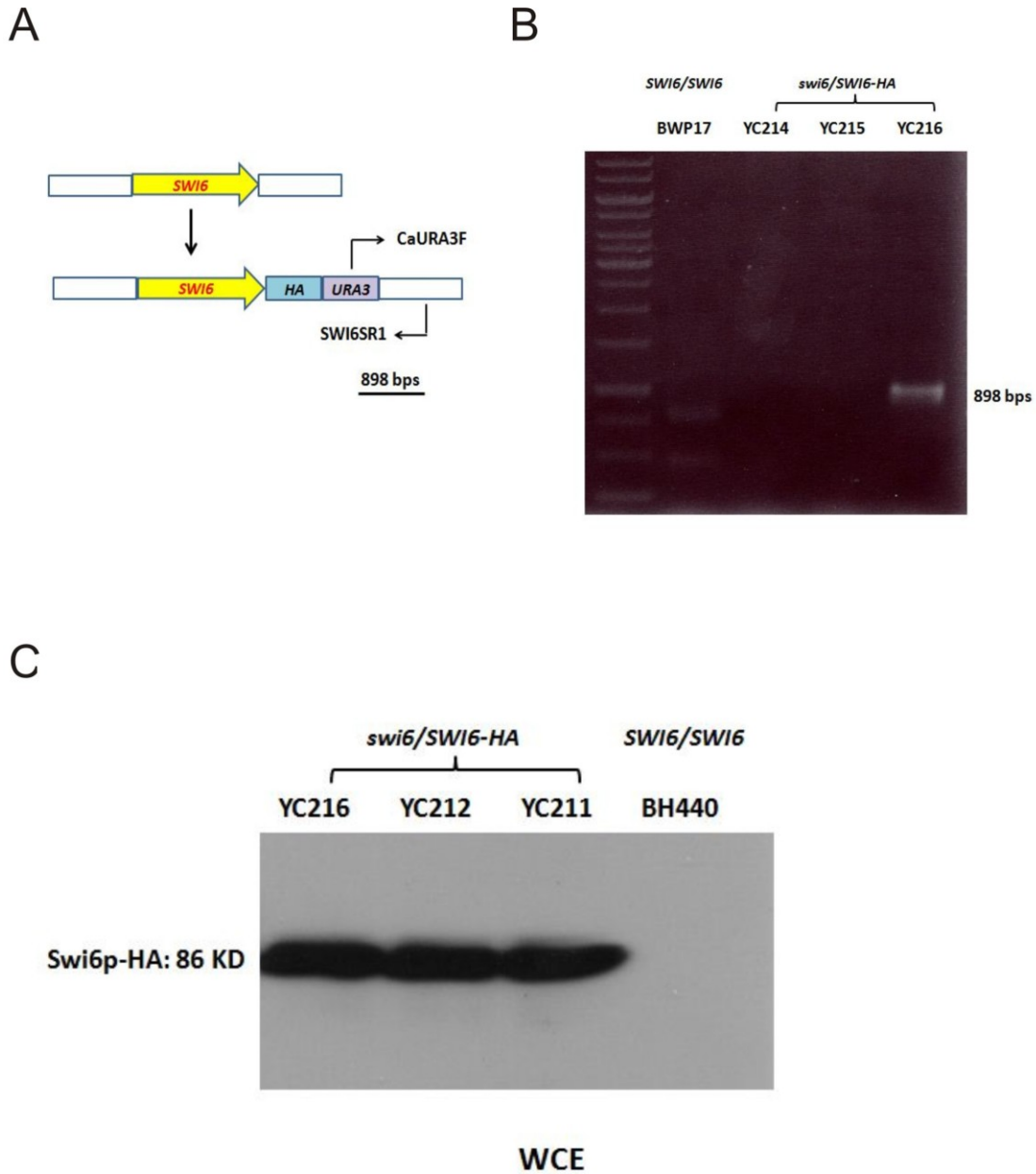


Figure 11. PCR and Western blot confirmation of a *swi6* Δ /*SWI6-HA* strain.

(A) Map showing a PCR screening strategy to confirm correct integration of the HA-containing construct at *SWI6*. Oligonucleotides CaURA3F and SWI6SR1 generate a 898 bp band for *SWI6-HA*. (B) Ethidium-bromide-stained DNA gel showing YC216 (*swi6::HIS1/SWI6-TAP-URA3*) as a positive strain while YC214 and YC215 are negative. BWP17 is the negative control strain. (C) Western blot containing 30 μ g of whole cell protein extracts from strains YC211, YC212 and YC216 and control untagged strain BH440, incubated with anti-HA antibody.

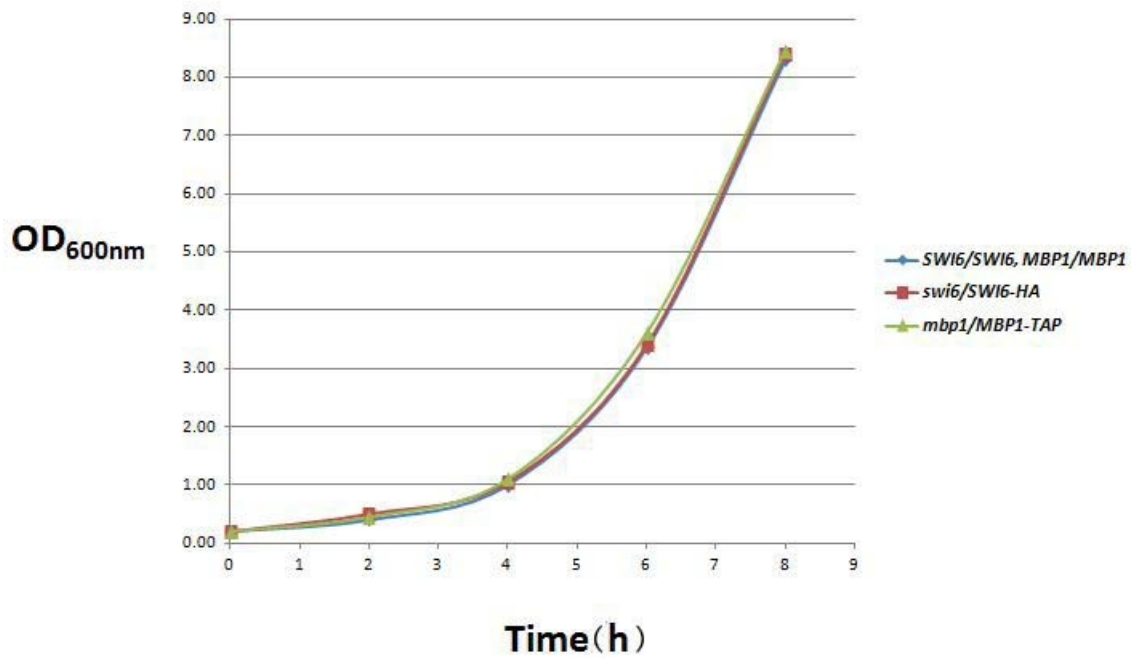


Figure 12. Growth curve of strains carrying a single copy of *SWI6-HA* or *MBP1-TAP*.

Overnight cultures of strains YC216 (*SWI6-HA-URA3/swi6Δ::HIS1*), YC367 (*MBP1-TAP-URA3/mbp1Δ::HIS1*) and control strain BH440 were diluted into 10 ml of fresh YPD medium to an OD_{600nm} of 0.2 and incubated at 30°C. Then OD_{600nm} was recorded every 2 h.

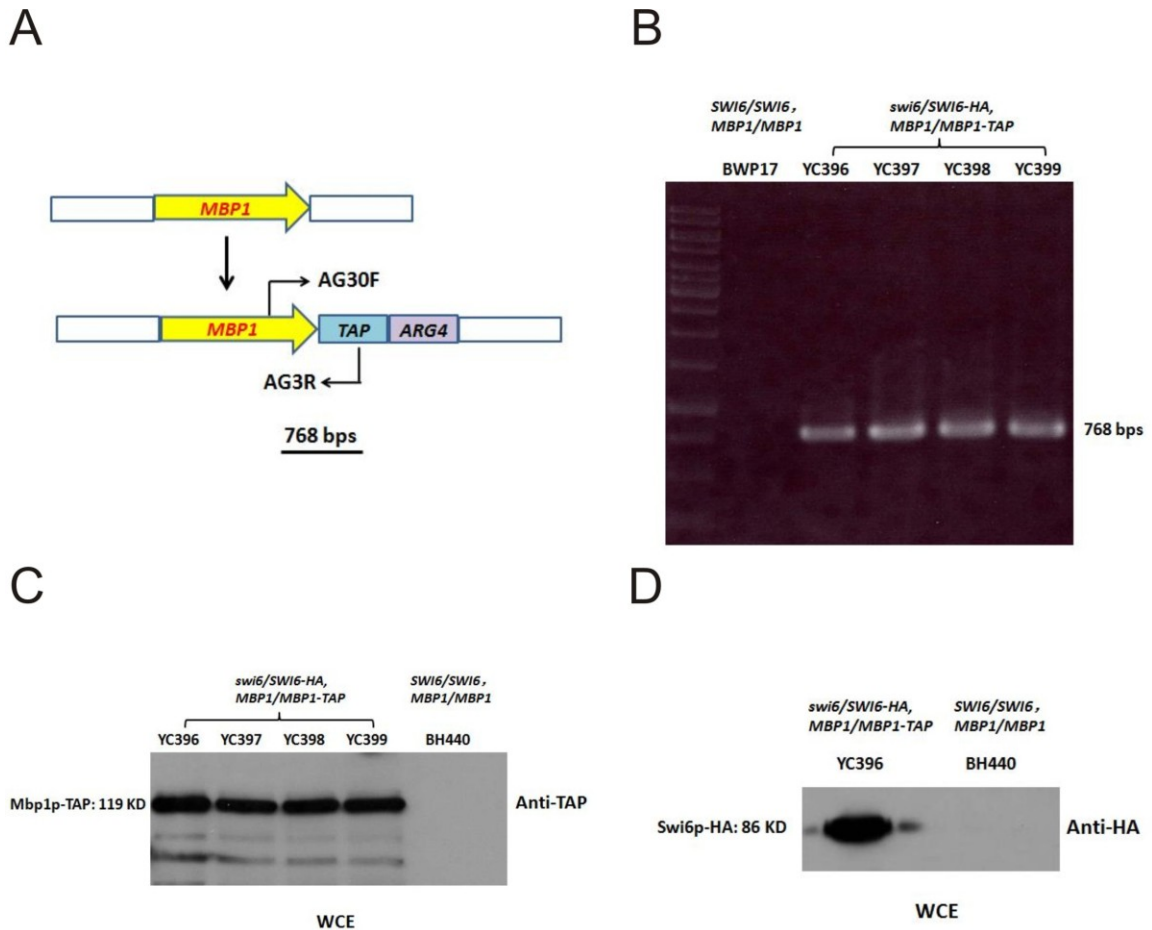
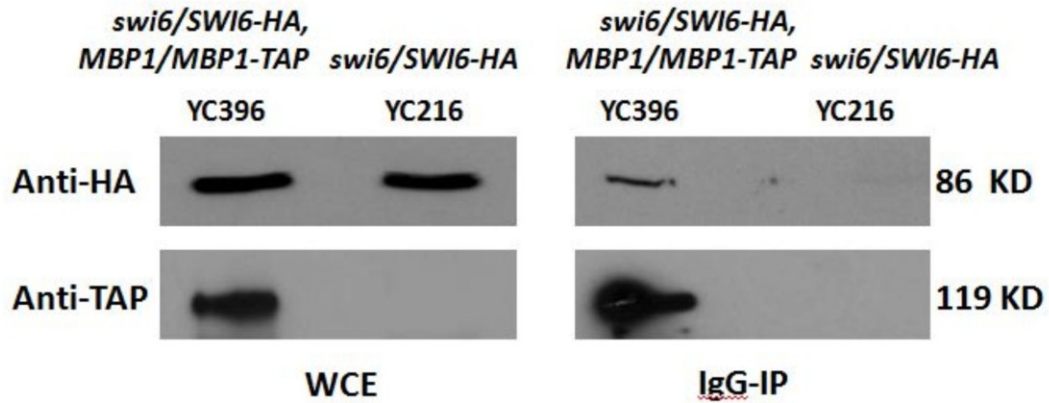


Figure 13. PCR and Western Blot confirmation of a *swi6* Δ /*SWI6-HA*, *MBP1/MBP1-TAP* strain.

(A) Map showing a PCR screening strategy to confirm correct integration of the TAP-containing construct. Oligonucleotides AG30F and AG3R generate a 768 bp band for *MBP1-TAP*. (B) Ethidium-bromide-stained DNA gel showing positive strains YC396, YC397, YC398 and YC399. BWP17 is the negative control strain. (C) Western blot containing 30 μ g of whole cell protein extracts from strains YC396, YC397, YC398 and YC399 (*MBP1/MBP1-TAP-ARG4, swi6::HIS1/SWI6-HA-URA3*) and control untagged strain BH440, incubated with anti-TAP antibody. (D) Western blot containing 30 μ g of whole cell protein extracts from strains YC396 and control untagged strain BH440, incubated with anti-HA antibody.

A



B

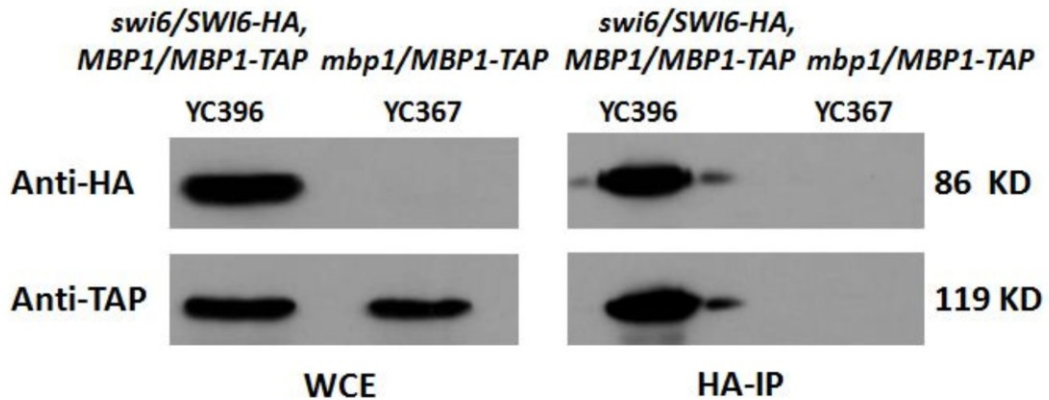


Figure 14. Co-immunoprecipitations demonstrate physical interactions between Mbp1p and Swi6p.

Western blots of whole cell extracts (WCE) and immune-precipitates, using IgG sepharose (IgG-IP) (A) or anti-HA agarose (HA-IP) (B). 20 μ l of beads were incubated with 20 mg of protein overnight, washed, and boiled in SDS sample buffer to elute interacting proteins.

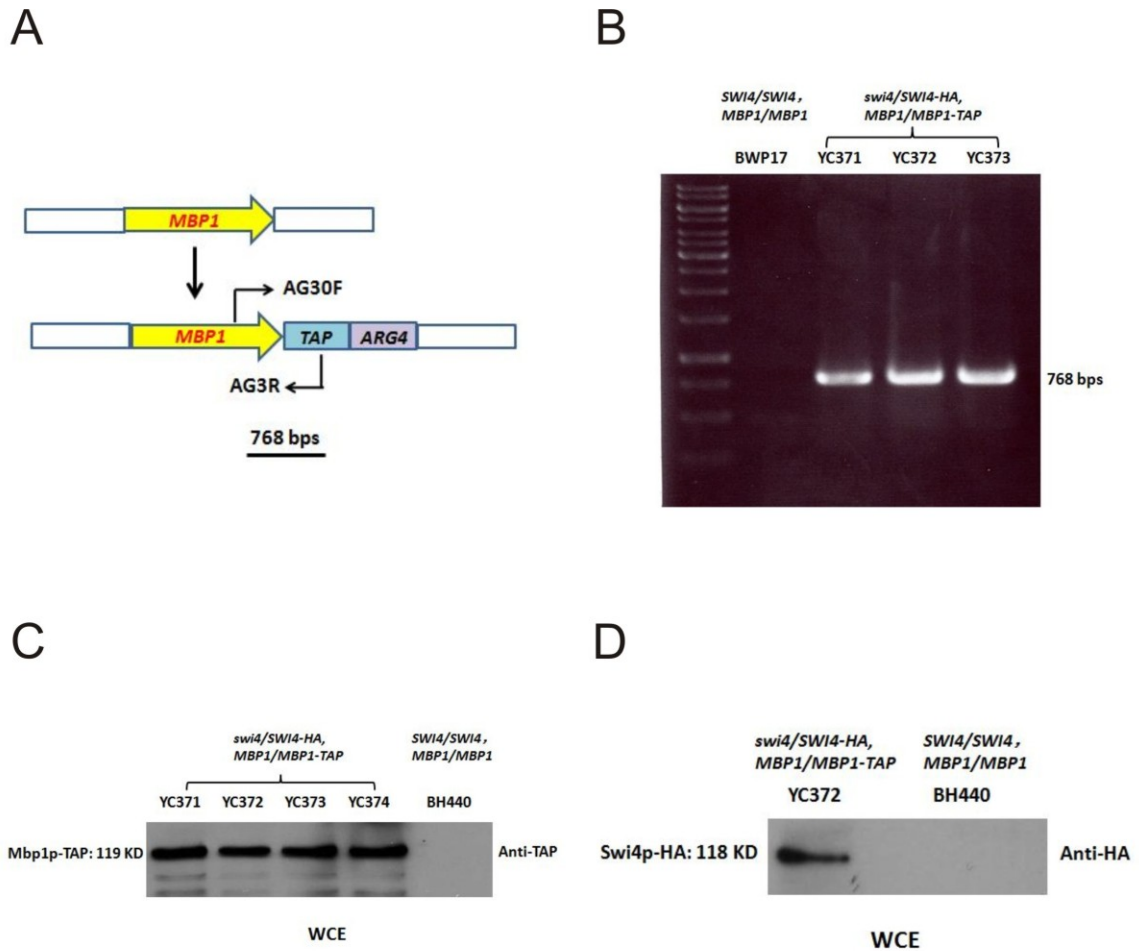
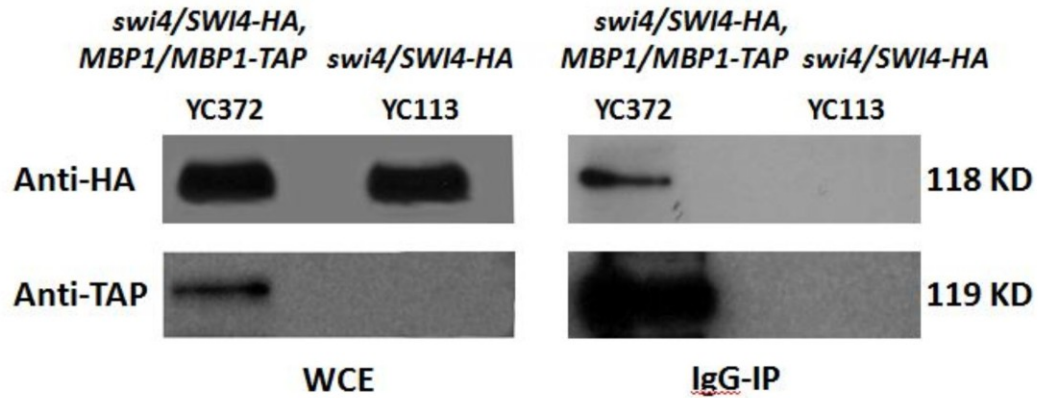


Figure 15. PCR and Western Blot confirmation of an *MBP1/MBP1-TAP swi4Δ/SWI4-HA* strain.

(A) Map showing a PCR screening strategy to confirm correct integration of the TAP-containing construct. Oligonucleotides AG30F and AG3R generate a 768 bp band for *MBP1-TAP*. (B) Ethidium-bromide-stained DNA gel showing YC371, YC372 and YC373 are positive strain. BWP17 is the negative control strain. (C) Western blot containing 30 μ g of whole cell protein extracts from strains YC371, YC372, YC373, YC374 (*swi4::hisG/SWI4-HA-HIS1, MBP1/MBP1-TAP-URA3*) and control untagged strain BH440, incubated with anti-TAP antibody. (D) Western blot containing 30 μ g of whole cell protein extracts from strains YC372 and control untagged strain BH440, incubated with anti-HA antibody.

A



B

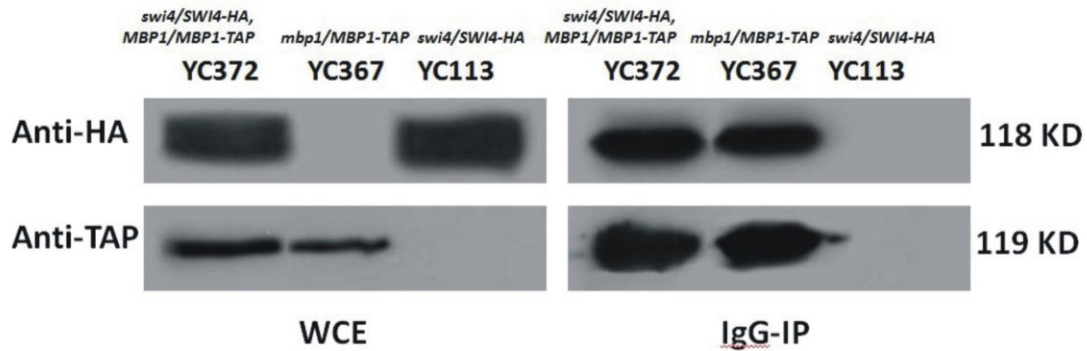


Figure 16. Co-immunoprecipitation of Swi4p and Mbp1p using IgG sepharose beads.

(A) Western blots of whole cell extracts (WCE) and immune-precipitates using IgG Sepharose beads. 40 ul of beads were incubated with 40 mg of protein overnight, washed, and boiled in SDS sample buffer to elute interacting proteins. (B) the procedure was repeated with the inclusion of an additional control, YC367 (*mbp1/MBP1-TAP*).

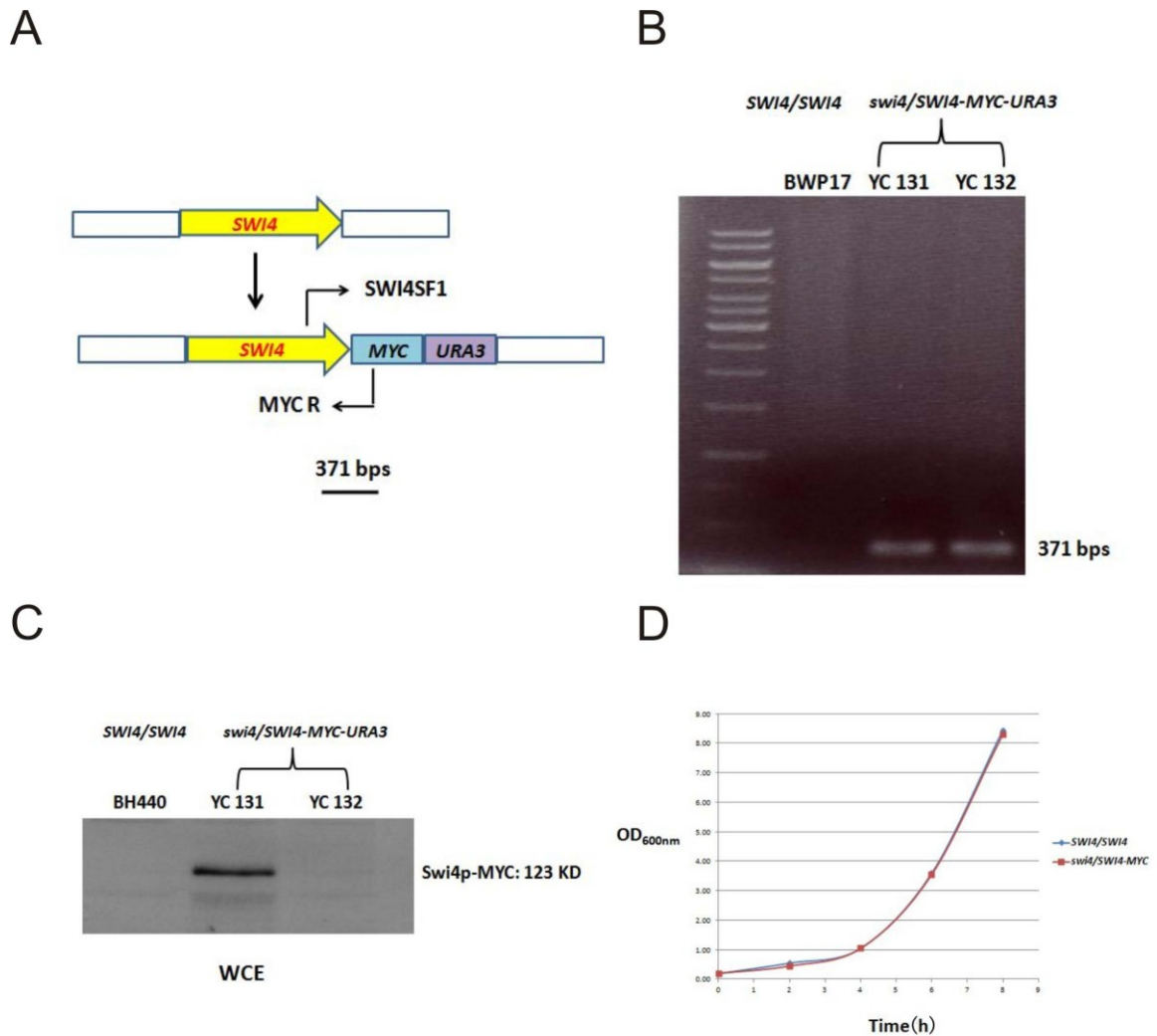


Figure 17. Confirmation of a *swi4Δ/SWI4-MYC* strain.

(A) Map showing a PCR screening strategy to confirm correct integration of the MYC-containing construct. Oligonucleotides SWI4SF1 and CaMYCR generate a 371 bp band for *SWI4-MYC*. (B) Ethidium-bromide-stained DNA gel showing positive strains YC131, YC132 and the negative control strain BWP17. (C) Western blot containing 30 μ g of whole cell protein extracts from strains YC131, YC132 (*swi4::HIS1/SWI4-MYC-URA3*) and BH440 incubated with anti-MYC antibody. (D) Growth assay supporting the notion that MYC-tagged Swi4p is functional.

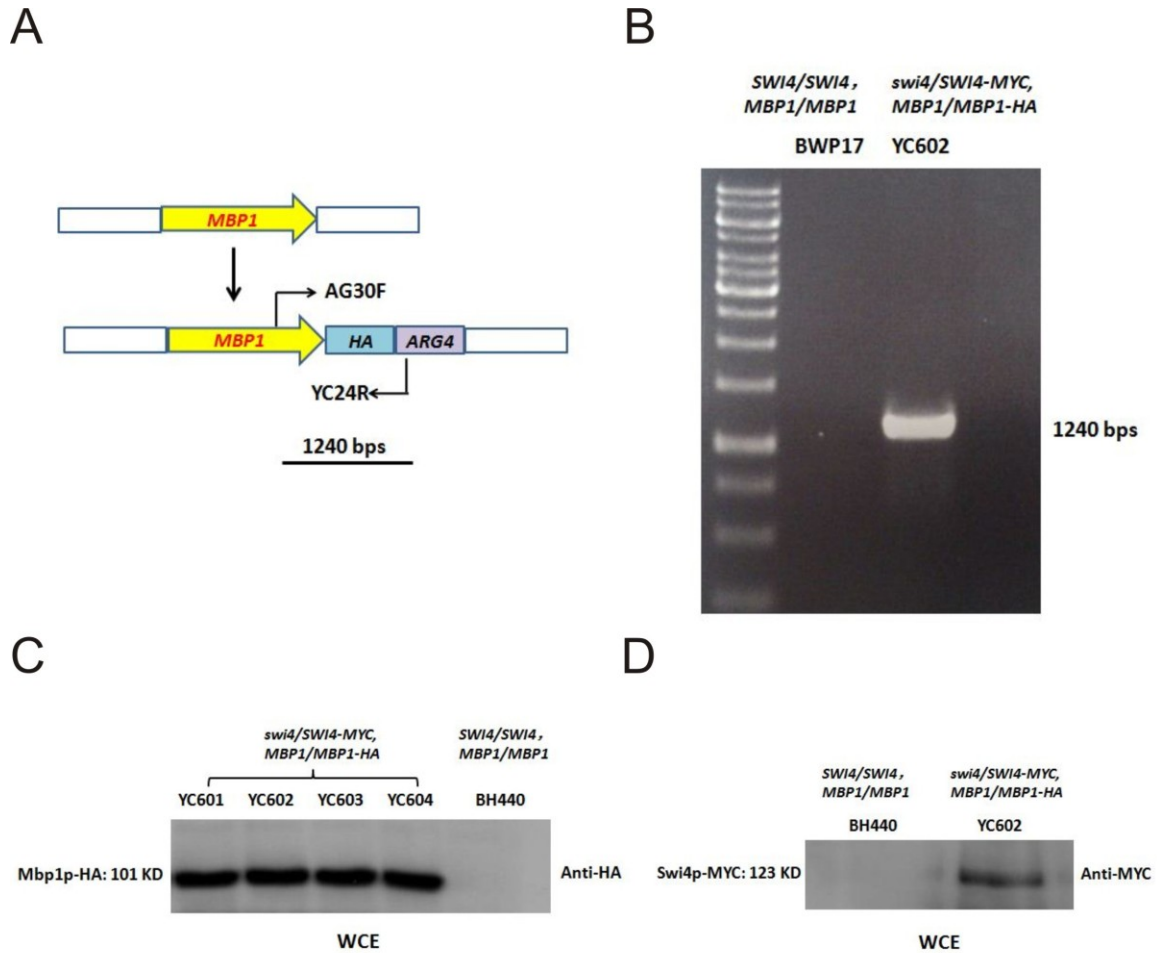


Figure 18. PCR and Western Blot confirmation of a *swi4*Δ/*SWI4-MYC*, *MBP1/MBP1-TAP* strain.

(A) Map showing a PCR screening strategy to confirm correct integration of the HA-containing construct. Oligonucleotides AG30F and YC24R generate a 1240 bp band for *MBP1-HA*. (B) Ethidium-bromide-stained DNA gel showing YC602 is positive strain. BWP17 is the negative control strain. (C) Western blot containing 30 μg of whole cell protein extracts from strains YC601, 602, 603, 604 (*swi4*::*HIS1/SWI4-MYC-URA3 MBP1/MBP1-HA-ARG4*) and control untagged strain BH440, incubated with anti-HA antibody. (D) Western blot containing 30 μg of whole cell protein extracts from strains YC602 and control untagged strain BH440, incubated with anti-MYC antibody.

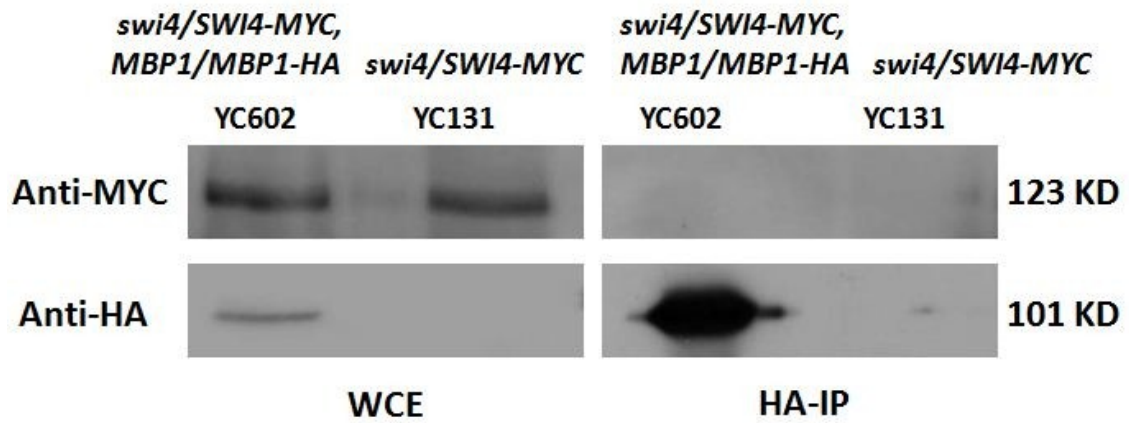
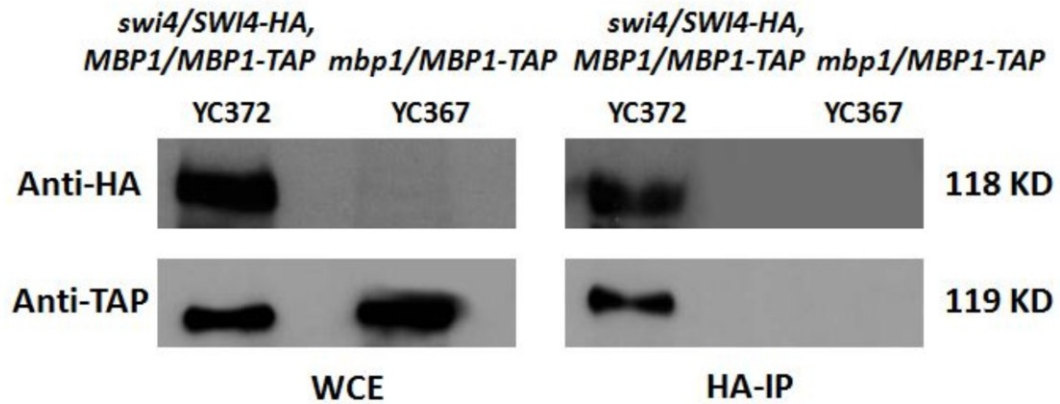


Figure 19. Co-immunoprecipitations on Swi4p-MYC and Mbp1p-HA using anti-HA beads.

Western blots of whole cell extracts (WCE) and immune-precipitates using anti-HA beads. 40 μ l of beads were incubated with 40 mg of protein overnight, washed, and boiled in SDS sample buffer to elute interacting proteins.

A



B

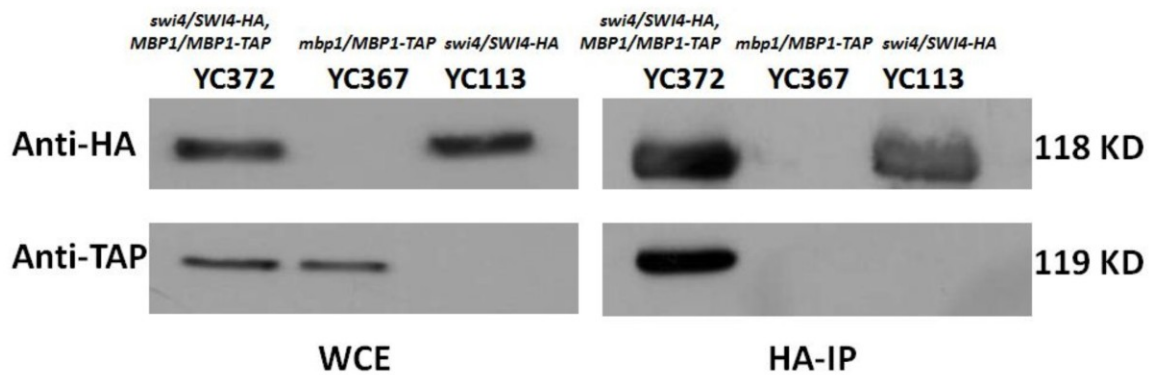


Figure 20. Co-immunoprecipitations of Swi4p and Mbp1p using anti-HA beads. (A) Western blots of whole cell extracts (WCE) and immune-precipitates using anti-HA beads. 40 ul of beads were incubated with 40 mg of protein overnight, washed, and boiled in SDS sample buffer to elute interacting proteins. (B) the procedure was repeated with the inclusion of an additional control, YC113 (*swi4/SWI4-HA*).

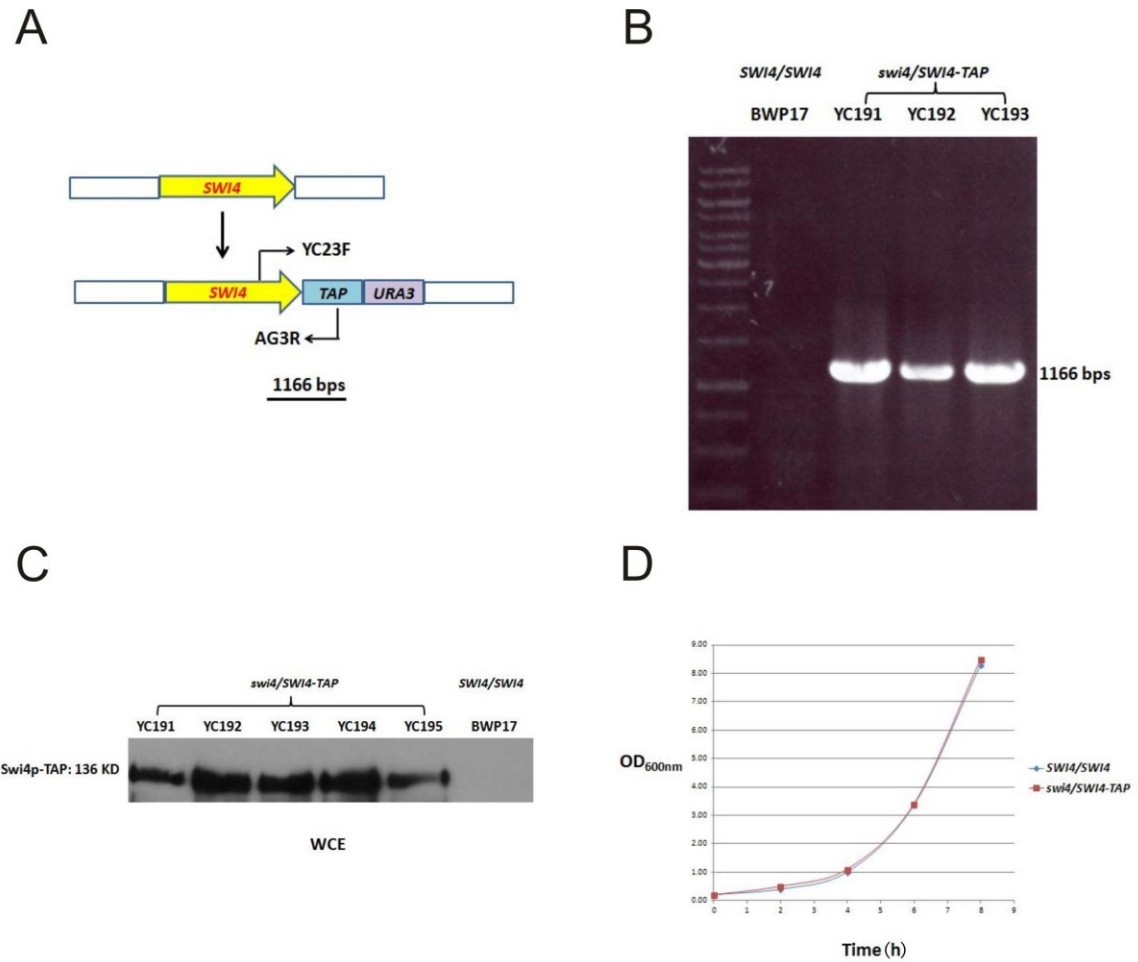


Figure 21. Confirmation of a *swi4*Δ/*SWI4-TAP* strain.

(A) Map showing a PCR screening strategy to confirm correct integration of the TAP-containing construct. Oligonucleotides YC23F and AG3R generate a 1166 bp band corresponding to *SWI4-TAP*. (B) Ethidium-bromide-stained DNA gel showing positive strains YC191, YC192 and YC193 (and the negative control strain BWP17). (C) Western blot containing 30 μ g of whole cell protein extracts from strains YC191, YC192, YC193, YC194 and YC195 (*swi4*::*HIS1/SWI4-TAP-URA3*) and BWP17 incubated with anti-TAP antibody. (D) Growth assay suggesting that Swi4p-TAP is functional.

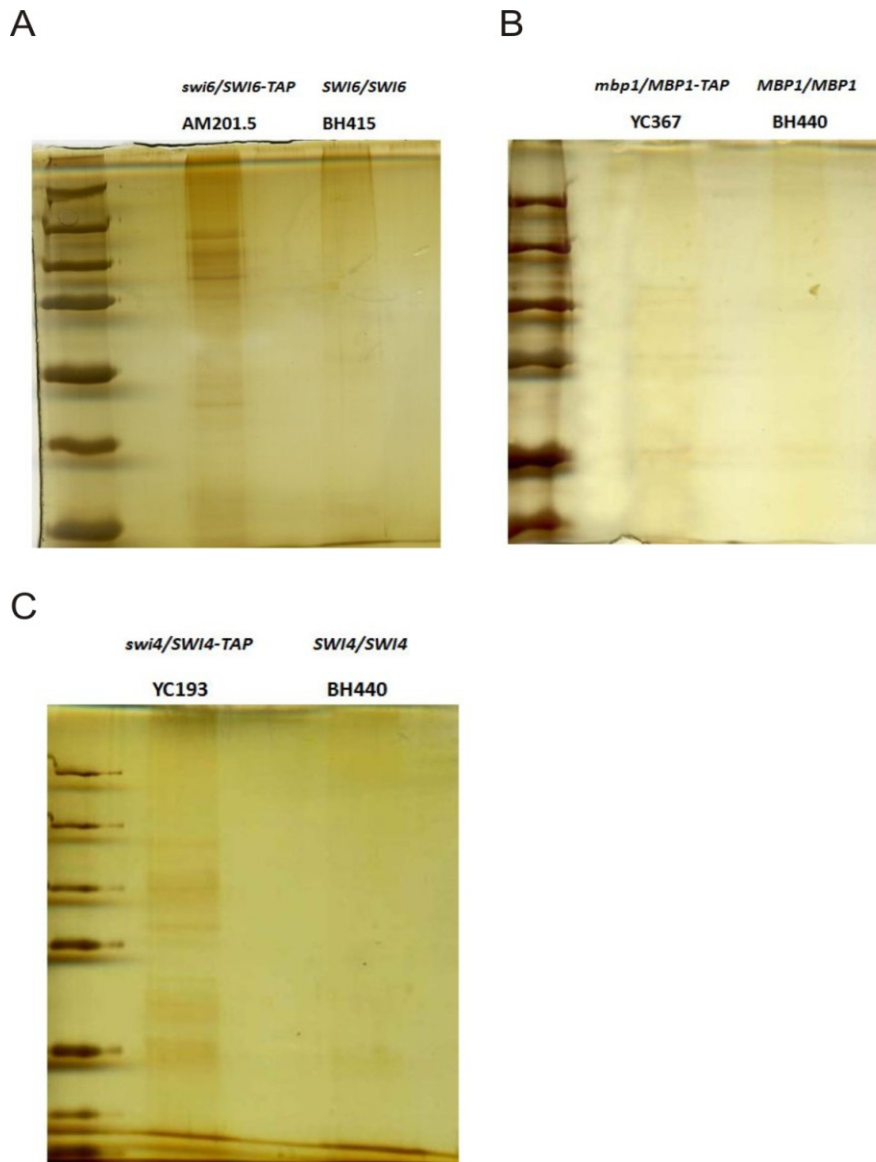


Figure 22: Tandem affinity purification of Swi6p, Mbp1p, and Swi4p

Protein extracted from 2 L cultures of strains AM201.5 (*swi6::URA3/SWI6-TAP-ARG4*) and BH415 (*SWI6/SWI6, URA3+*) (A), YC367 (*mbp1::HIS1/MBP1-TAP-URA3*) and BH440 (*URA3+, HIS1+*) (B), or YC193 (*swi4::HIS1/SWI4-TAP-URA3*) and BH440 (C) were subjected to tandem affinity purification [107]. Elutions were TCA precipitated, and run on SDS PAGE gels for silver staining.

Table 4: Orbitrap LC/MS analysis of putative Swi6p-interacting proteins ¹.

Protein ID	Number of Peptides ²	ORF Name	Present in Control ³	Protein Description
CAL0002762	52	SWI4/orf19.4545	N	Putative component of the SBF transcription complex involved in G1/S cell-cycle progression; periodic mRNA expression, peak at cell-cycle G1/S phase; predicted, conserved MBF binding sites upstream of G1/S-regulated genes
CAL0004400	28	SWI6/orf19.4725	N	Putative component of the MBF and SBF transcription complexes involved in G1/S cell-cycle progression; periodic mRNA expression, peak at cell-cycle G1/S phase
CAL0002380	22	MBP1/orf19.5855	N	Putative component of the MBF transcription complex involved in G1/S cell-cycle progression; non-periodic mRNA expression; predicted, conserved MBF binding sites upstream of G1/S-regulated genes
CAL0006140	5	SRB1/orf19.6190	N	Essential GDP-mannose pyrophosphorylase; synthesizes GDP-mannose for protein glycosylation; functional homolog of <i>S. cerevisiae</i> Psa1p; on yeast-form cell surface, not hyphal cells; alkaline upregulated; induced on adherence to polystyrene
CAL0001324	3	RPS1/orf19.3002	N	Putative ribosomal protein 10 of the 40S subunit, elicits a host antibody response during infection; transcription is induced during active growth
CAL0003773	3	RPL4B/orf19.7217	N	Ribosomal protein 4B; genes encoding cytoplasmic ribosomal subunits, translation
CAL0004511	3	TUB1/orf19.7308	N	Alpha-tubulin; gene has intron; complements cold-sensitivity of <i>S. cerevisiae</i> tub1 mutant; <i>C. albicans</i> has single alpha-tubulin gene, whereas <i>S. cerevisiae</i> has two (TUB1, TUB3); farnesol-upregulated in biofilm; sumoylation target
CAL0000340	2	SMC2/orf19.3623	N	Protein similar to <i>S. cerevisiae</i> Smc2p, which is a component of the condensin complex involved in mitotic chromosome condensation; induced under hydroxyurea treatment
CAL0001309	2	orf19.3793	N	ORF, Uncharacterized Putative protein of unknown function; mRNA binds to She3p; regulated by Nrg1p; greater mRNA abundance observed in a <i>cyr1</i> or <i>ras1</i> homozygous null mutant than in wild type
CAL0001362	2	orf19.3021	N	ORF, Uncharacterized Putative protein of unknown function; Hap43p-repressed gene; induced during planktonic growth
CAL0001506	2	UBI3/orf19.3087	N	Fusion of ubiquitin with the S34 protein of the small ribosomal subunit; mRNA decreases upon heat shock, appears to be degraded; functional homolog of <i>S. cerevisiae</i> RPS31; Hap43p-induced gene
CAL0003444	2	orf19.3295	N	ORF, Uncharacterized
CAL0004048	2	BRF1/orf19.6649	N	Component of the general transcription factor for RNA polymerase III (TFIIIB); possibly an essential gene, disruptants not obtained by UAU1 method
CAL0004119	2	RPS21/orf19.3334	N	Predicted ribosomal protein; genes encoding cytoplasmic ribosomal subunits, translation factors, and tRNA synthetases are downregulated upon phagocytosis by murine macrophage; transcription is positively regulated by Tbf1p
CAL0004587	2	CRP1/orf19.4784	N	Plasma membrane copper transporter; CPx P1-type ATPase; mediates Cu resistance; similar to proteins of Menkes and Wilson disease; copper-induced; Tbf1p-activated; suppresses Cu sensitivity of <i>S. cerevisiae</i> <i>cup1</i> mutant; biofilm-induced
CAL0004743	2	orf19.332	N	ORF, Uncharacterized Ortholog(s) have DNA replication origin binding, chromatin binding activity and role in cis assembly of pre-catalytic spliceosome, DNA-dependent DNA replication initiation
CAL0004922	2	orf19.6766	N	ORF, Uncharacterized Hap43p-induced gene; <i>S. cerevisiae</i> ortholog NOP13, a nucleolar protein found in preribosomal complexes
CAL0005202	2	PDC11/orf19.2877	N	Putative pyruvate decarboxylase; antigenic; at hyphal cell surface, not yeast-form cells; regulated by Hap43p, Gcn4p, Efg1p, Efh1p, Hsf1; fluconazole-, farnesol-, biofilm-induced; repressed upon amino acid starvation; sumoylation target

¹Approximately 295 mg protein extracts from 2 L cultures of AM201.5 (*swi6Δ/SWI6-TAP*) and BH415 (*SWI6/SWI6*) strains were subjected to tandem affinity purification [107]. Elutions were TCA-precipitated and run just into the resolving portion of an SDS PAGE gel [100]. The compressed bands were stained with Coomassie blue, cut from the gel, and analysed using an LTQ-OrbitrapElite with nano-ESI. ²Proteins represented by 1 peptide were excluded from the table but can be found in the Appendix Table S1. ³Peptides identified in both the tagged strain and the untagged control strain were excluded from the results.

Table 5: Orbitrap LC/MS analysis of putative Swi4p-interacting proteins¹.

Protein ID	Number of Peptides ²	ORF Name	Present in Control ³	Protein Description
CAL0002762	142	SWI4/orf19.4545	N	Verified ORF; Putative component of the SBF transcription complex involved in G1/S cell-cycle progression
CAL0004400	85	SWI6/orf19.4725	N	Verified ORF; Putative component of the MBF and SBF transcription complexes involved in G1/S cell-cycle progression
CAL0005797	20	ATP1/orf19.6854	N	Verified ORF; ATP synthase alpha subunit; antigenic in human/mouse; at hyphal surface not yeast; induced by ciclopirox ketoconazole flucytosine
CAL0006140	20	SRB1/orf19.6190	N	Verified ORF; Essential GDP-mannose pyrophosphorylase; synthesizes GDP-mannose for protein glycosylation; functional homolog of <i>S. cerevisiae</i> Psa1p
CAL0001324	19	RPS1/orf19.3002	N	Uncharacterized ORF; Putative ribosomal protein 10 of the 40S subunit elicits a host antibody response during infection
CAL0001639	18	orf19.2489	N	Uncharacterized ORF; Putative karyopherin beta; repressed by nitric oxide
CAL0001208	17	SSA2/orf19.1065	N	Verified ORF; HSP70 family chaperone; found in cell wall fractions; antigenic; role in import of beta-defensin peptides; ATPase domain binds histatin 5
CAL0005500	16	MIR1/orf19.4885	N	Verified ORF; Putative mitochondrial phosphate transporter; caspofungin repressed; expression is increased in a fluconazole-resistant isolate
CAL0000146	16	TFP1/orf19.1680	N	Uncharacterized ORF; Subunit of vacuolar H ⁺ -ATPase; stationary phase enriched protein; sumoylation target
CAL0004700	16	DED81/orf19.6702	N	Uncharacterized ORF; Putative tRNA-Asn synthetase
CAL0001367	15	SSB1/orf19.6367	N	Verified ORF; HSP70 family heat shock protein; mRNA in yeast cells and germ tubes; at surface of yeast cells not hyphae; antigenic in human mouse system
CAL0005977	14	CDC19/orf19.3575	N	Verified ORF; Pyruvate kinase; on yeast cell surface; Gcn4p Hog1p regulated; induced on polystyrene adherence
CAL0006017	14	RPL10/orf19.2935	N	Verified ORF; Ribosomal protein L10; intron in 5'-UTR; genes encoding cytoplasmic ribosomal subunits translation factors and tRNA synthetases
CAL0000759	14	URA2/orf19.2360	N	Uncharacterized ORF; Putative bifunctional carbamoylphosphate synthetase-aspartate transcarbamylase; flucytosine induced
CAF0006912	13	RPS9B/orf19.838.1	N	Uncharacterized ORF; Predicted ribosomal protein; genes encoding cytoplasmic ribosomal subunits translation factors and tRNA synthetases are downregulated
CAL0004511	13	TUB1/orf19.7308	N	Verified ORF; Alpha-tubulin; gene has intron; complements cold-sensitivity of <i>S. cerevisiae</i> tub1 mutant; <i>C. albicans</i> has single alpha-tubulin gene
CAL0003655	12	PET9/orf19.930	N	Verified ORF; Mitochondrial ADP/ATP carrier protein involved in ATP biosynthesis; possible lipid raft component; 3 predicted transmembrane helices
CAL0006304	12	RPL3/orf19.1601	N	Verified ORF; Putative ribosomal protein large subunit; induced by ciclopirox olamine treatment; genes encoding cytoplasmic ribosomal subunits are downre
CAL0005101	12	TUB2/orf19.6034	N	Verified ORF; Beta-tubulin; functional homolog of ScTub2p; hyphal-induced; fluconazole-induced; gene has two introns
CAL0001524	11	RNR1/orf19.5779	N	Verified ORF; Ribonucleotide reductase large subunit; expression greater in low iron; transposon mutation affects filamentous growth
CAL0000663	11	ATP2/orf19.5653	N	Verified ORF; F1 beta subunit of F1F0 ATPase complex; antigenic in human mouse; induced by ciclopirox olamine; flucytosine; caspofungin repressed
CAF0006970	11	RPS16A/orf19.2994.1	N	Uncharacterized ORF; Putative 40S ribosomal subunit; macrophage/pseudohyphal-induced after 16 h
CAL0001726	11	LSC2/orf19.1860	N	Uncharacterized ORF; Putative succinate-CoA ligase beta subunit; transcription regulated by Mig1p and Tup1p; transcriptionally regulated by iron
CAL0006334	10	RPN1/orf19.4956	N	Uncharacterized ORF; Putative 19S regulatory particle of the 26S proteasome; regulated by Gcn2p and Gcn4p
CAL0006022	10	RPT6/orf19.3593	N	Uncharacterized ORF; Putative ATPase of the 19S regulatory particle of the 26S proteasome; transcription is regulated by Mig1p; regulated by Gcn2p and Gcn
CAL0006335	10	ILV2/orf19.1613	N	Verified ORF; Putative acetolactate synthase; regulated by Gcn4p; induced by amino acid starvation (3-AT treatment); stationary phase enriched protein
CAL0002245	10	RNR21/orf19.5801	N	Uncharacterized ORF; Ribonucleoside-diphosphate reductase; regulated by tyrosol and cell density; transcription upregulated in response to ciclopirox olamin
CAL0003957	10	RPL9B/orf19.236	N	Uncharacterized ORF; Ribosomal protein L9; downregulated upon phagocytosis by murine macrophages; repressed by nitric oxide

CAL0001552	9	PR26/orf19.5793	N	Uncharacterized ORF; Protein with similarity to proteasomal 26S regulatory subunit of <i>S. cerevisiae</i> <i>H. sapiens</i> <i>Methanobacterium thermoautotrophicum</i>
CAL0000516	9	GLT1/orf19.6257	N	Uncharacterized ORF; Putative glutamate synthase; alkaline downregulated; transcription is downregulated in both intermediate and mature biofilms
CAL0006344	9	GFA1/orf19.1618	N	Verified ORF; Glucosamine-6-phosphate synthase homotetrameric enzyme of chitin/hexosamine biosynthesis
CAL0000732	8	CDC48/orf19.2340	N	Verified ORF; Putative microsomal ATPase; plasma membrane-localized; regulated by Gcn2p and Gcn4p; induced by amino acid starvation (3-AT treatment)
CAL0000989	7	RPS5/orf19.4336	N	Verified ORF; Ribosomal protein S5; macrophage/pseudohyphal-induced after 16 h; genes encoding cytoplasmic ribosomal subunits translation factors
CAL0005300	7	RPS24/orf19.5466	N	Uncharacterized ORF; Predicted ribosomal protein; hyphal downregulated; genes encoding cytoplasmic ribosomal subunits translation factors and tRNA synthetases
CAL0000855	7	ACS1/orf19.1743	N	Uncharacterized ORF; Putative acetyl-CoA synthetase; upregulated by human neutrophils; fluconazole-downregulated; regulated by Nrg1p and Mig1p
CAL0005660	7	GRS1/orf19.437	N	Uncharacterized ORF; Putative tRNA-Gly synthetase; genes encoding ribosomal subunits translation factors tRNA synthetases are downregulated upon phagocytosis
CAL0004953	7	ENO1/orf19.395	N	Verified ORF; Enolase enzyme of glycolysis and gluconeogenesis; major cell-surface antigen; binds host plasmin/plasminogen; immunoprotective
CAL0002164	6	NOP5/orf19.1199	N	Verified ORF; Protein similar to <i>S. cerevisiae</i> Nop5p protein of small nucleolar ribonucleoprotein complex; transposon mutation affects filamentous growth
CAF0007002	6	orf19.4149.1	N	Uncharacterized ORF; Ortholog(s) have structural constituent of ribosome activity and role in maturation of SSU-rRNA from tricistronic rRNA transcript
CAL0005242	6	CCT8/orf19.6099	N	Verified ORF; Chaperonin-containing T-complex subunit; involved in hyphal morphogenesis particularly starvation-induced
CAL0000756	6	RPS7A/orf19.1700	N	Verified ORF; Ribosomal protein S7; genes encoding cytoplasmic ribosomal subunits translation factors
CAF0006944	6	RPL2/orf19.2309.2	N	Uncharacterized ORF; Putative 60S ribosomal protein L2; Hap43p-induced gene; shows downregulation in infected rabbit kidney in SC5314
CAL0005536	6	TCP1/orf19.401	N	Uncharacterized ORF; Chaperonin-containing T-complex subunit transcription induced by alpha pheromone in SpiderM medium; stationary phase enriched protein
CAL0005346	6	CDC46/orf19.5487	N	Uncharacterized ORF; Putative hexameric MCM complex subunit with a predicted role in control of cell division
CAL0002415	6	LYS12/orf19.2525	N	Uncharacterized ORF; Putative mitochondrial homoisocitrate dehydrogenase; clade-associated gene expression; protein level decreases in stationary phase
CAF0006992	6	orf19.3690.2	N	Uncharacterized ORF; Ortholog(s) have RNA binding structural constituent of ribosome activity role in cytoplasmic translation and cytosolic large ribosome
CAL0001433	6	RPN3/orf19.3054	N	Uncharacterized ORF; Putative non-ATPase regulatory subunit of the 26S proteasome lid; amphotericin B repressed; oxidative stress-induced via Cap1p
CAL0001714	6	ADE5,7/orf19.5061	N	Verified ORF; Phosphoribosylamine-glycine ligase and phosphoribosylformylglycinamide cyclo-ligase; interacts with Vps34p
CAL0005360	6	GSP1/orf19.5493	N	Verified ORF; Small RAN G-protein; essential; prenylation not predicted; overproduction complements viability of <i>S. cerevisiae</i> <i>gsp1</i> mutant;

¹Approximately 224 mg protein extracts from 2 L cultures of YC193 (*swi4Δ/SWI4-TAP*) and BH440 (*SWI4/SWI4*) strains were subjected to tandem affinity purification [107]. Elutions were TCA-precipitated and run just into the resolving portion of an SDS PAGE gel [100]. Remove words of ref if just put number-see above. The compressed bands were stained with Coomassie blue, cut from the gel, and analysed using an LTQ-OrbitrapElite with nano-ESI. ²Peptides less than 6 were excluded from the results but can be found in Appendix Table S2. ³Peptides identified in both the tagged strain and the untagged control strain were excluded from the results.

Table 6: 1st Orbitrap LC/MS analysis of putative Mbp1p-interacting proteins¹.

Protein ID	Number of Peptides ²	ORF Name	Present in Control ³	Protein Description
CAL0002380	50	MBP1/orf19.5855	N	Verified ORF; Putative component of the MBF transcription complex involved in G1/S cell-cycle progression; non-periodic mRNA expression
CAL0005069	6	orf19.6022	N	Uncharacterized ORF; Predicted ORF in Assemblies 19 20 and 21; downregulated during core stress response
CAL0004400	4	SWI6/orf19.4725	N	Verified ORF; Putative component of the MBF and SBF transcription complexes involved in G1/S cell-cycle progression
CAL0005867	3	RPS8A/orf19.6873	N	Verified ORF; Small 40S ribosomal subunit protein; gene is induced by ciclopirox olamine
CAL0001571	2	ACT1/orf19.5007	N	Verified ORF; Actin; gene has intron; transcriptionally regulated by growth phase and by starvation; localizes to polarized growth site in budding and hyphal growth.

¹Approximately 240 mg protein extracts from 2 L cultures of YC367 (*mbp1Δ/MBP1-TAP*) and BH440 (*MBP1/MBP1*) strains were subjected to tandem affinity purification [107]. Elutions were TCA-precipitated and washed 3 times with 80% acetone then sent for analysis via mass spectrometry. ²Peptides at a frequency of 1 were excluded from the results but can be found in the Appendix Table S3. ³Peptides identified in both the tagged strain and the untagged control strain were excluded from the results.

Table 7: Orbitrap LC/MS analysis of putative Mbp1p-interacting proteins¹ from larger cultures.

Protein ID	Number of Peptides ²	ORF Name	Present in Control ³	Protein Description
CAL0003773	11	RPL4B/orf19.7217	N	Verified ORF; Ribosomal protein 4B
CAF0006966	10	RPL28/orf19.2864.1	N	Uncharacterized ORF; Putative ribosomal protein; Plc1p-regulated
CAL0002295	9	NOP1/orf19.3138	N	Verified ORF; Nucleolar protein; flucytosine induced; Hap43p-induced gene
CAL0005867	6	RPS8A/orf19.6873	N	Verified ORF; Small 40S ribosomal subunit protein; gene is induced by ciclopirox olamine; genes encoding cytoplasmic ribosomal subunits are downregulated
CAL0001571	4	ACT1/orf19.5007	N	Verified ORF; Actin; gene has intron; transcriptionally regulated by growth phase and by starvation; localizes to polarized growth site in budding and hyphal growth
CAL0000142	4	SIK1/orf19.7569	N	Verified ORF; Putative U3 snoRNP protein; Hap43p-induced gene; physically interacts with TAP-tagged Nop1p
CAL0005657	4	TDH3/orf19.6814	N	Verified ORF; NAD-linked glyceraldehyde-3-phosphate dehydrogenase; enzyme of glycolysis; binds fibronectin and laminin; at surface of yeast and hyphae
CAF0006998	4	RPL24A/orf19.3789	N	Uncharacterized ORF; Predicted ribosomal protein
CAL0003531	3	orf19.2684	N	Uncharacterized ORF
CAL0000513	3	RPS23A/orf19.6253	N	Uncharacterized ORF; Putative ribosomal protein
CAL0000006	3	HSP70/orf19.4980	N	Verified ORF; Putative hsp70 chaperone; role in entry into host cells; heat-shock amphotericin B cadmium ketoconazole-induced
CAF0007074	3	RPS14B/orf19.6265.1	N	Uncharacterized ORF; Putative ribosomal protein
CAL0004400	3	SWI6/orf19.4725	N	Verified ORF; Putative component of the MBF and SBF transcription complexes involved in G1/S cell-cycle progression
CAL0003748	3	RPS6A/orf19.4660	N	Verified ORF; Ribosomal protein 6A
CAL0003255	3	SMC6/orf19.6568	N	Uncharacterized ORF; Putative structural maintenance of chromosomes (SMC) protein; Hap43p-induced gene; cell-cycle regulated periodic mRNA expression
CAL0006157	2	RPL13/orf19.2994	N	Verified ORF; Putative ribosomal subunit; antigenic during murine systemic infection
CAL0001506	2	UBI3/orf19.3087	N	Verified ORF; Fusion of ubiquitin with the S34 protein of the small ribosomal subunit; mRNA decreases upon heat shock appears to be degraded
CAL0004332	2	KAR2/orf19.2013	N	Verified ORF; Similar to chaperones of Hsp70p family; role in translocation of proteins into the ER; transcriptionally regulated by iron
CAL0005202	2	PDC11/orf19.2877	N	Verified ORF; Putative pyruvate decarboxylase; antigenic; at hyphal cell surface not yeast-form cells; regulated by Hap43p Gcn4p Efg1p Efh1p Hsf1
CAL0002380	2	MBP1/orf19.5855	N	Verified ORF; Putative component of the MBF transcription complex involved in G1/S cell-cycle progression; non-periodic mRNA expression
CAL0005153	2	orf19.2852	N	Uncharacterized ORF; Has domain(s) with predicted structural constituent of ribosome activity role in translation and ribosome localization
CAL0006017	2	RPL10/orf19.2935	N	Verified ORF; Ribosomal protein L10; intron in 5'-UTR
CAL0006403	2	orf19.1634	N	Uncharacterized ORF; Has domain(s) with predicted fatty-acyl-CoA binding activity
CAL0001324	2	RPS1/orf19.3002	N	Uncharacterized ORF; Putative ribosomal protein 10 of the 40S subunit elicits a host antibody response during infection
CAL0000756	2	RPS7A/orf19.1700	N	Verified ORF; Ribosomal protein S7
CAL0002668	2	TRY3/orf19.1971	N	Uncharacterized ORF; Has domain(s) with predicted zinc ion binding activity

¹Approximately 550 mg protein extracts from 4 L cultures of YC367 (*mbp1Δ/MBP1-TAP*) and BH440 (*MBP1/MBP1*) strains were subjected to tandem affinity purification [107]. Elutions were TCA-precipitated and washed 3 times with 80% acetone then sent for analysis via mass spectrometry. ²Peptides with a frequency one were excluded from the results but can be found in the Appendix Table S4. ³Peptides identified in both the tagged strain and the untagged control strain were excluded from the results.

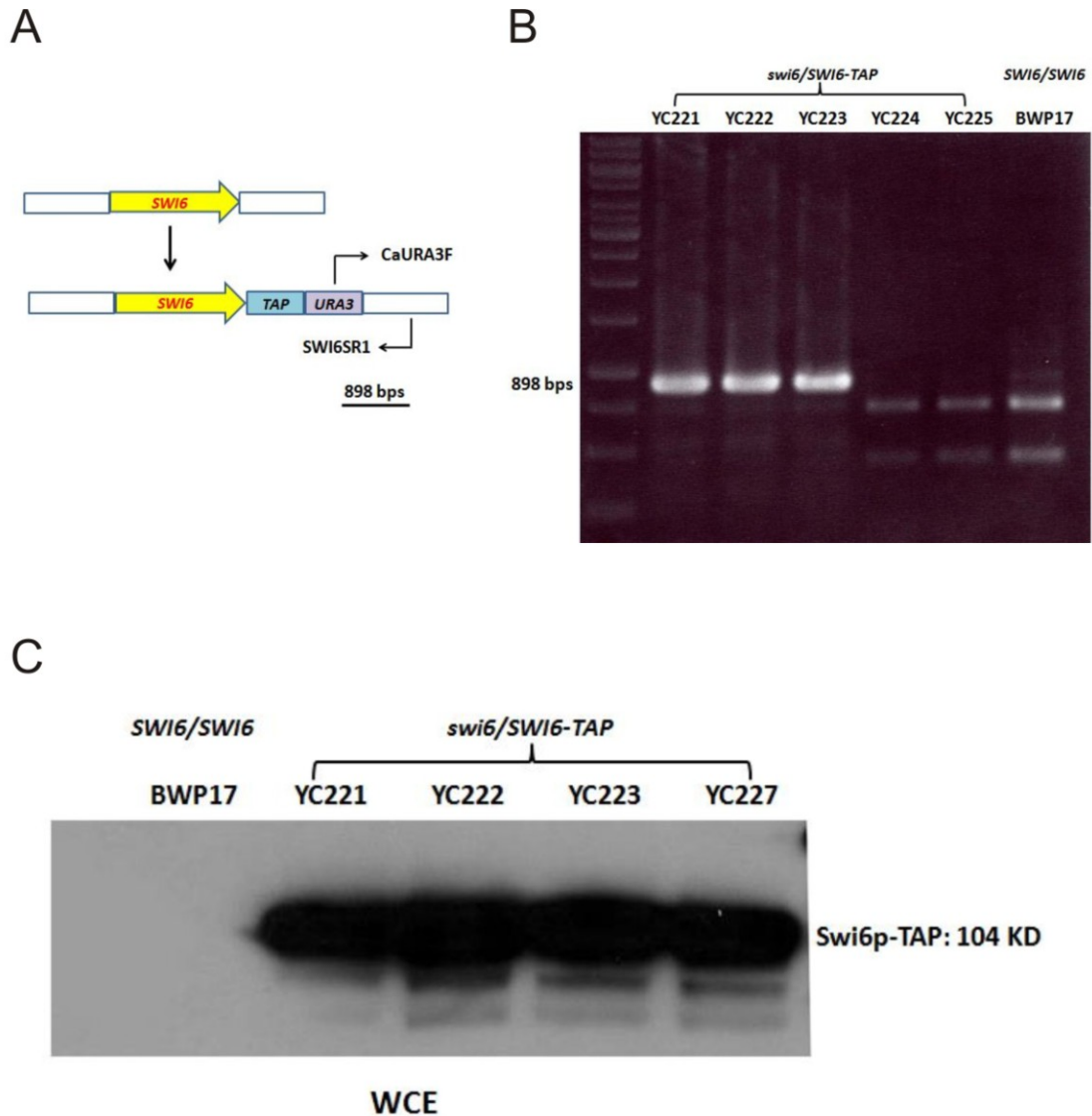


Figure 23. PCR and Western confirmation of tagging of *SWI6* with TAP in a *cln3Δ/MET3::CLN3* strain.

(A) Map showing a PCR screening scheme with oligonucleotides CaURA3F and SWI6SR1, which generate a 898 nt band for *SWI6-TAP*. (B) DNA gel showing positive strains YC221, YC222 and YC223 (*SWI6-TAP-URA3/SWI6 cln3::hisG/MET3p-CLN3-ARG4*) while YC224 and YC225 are negative. (C) Western blot confirming expression of Swi6p-TAP.

Table 8: Orbitrap LC/MS analysis of putative Swi6p-interacting proteins in cells blocked in G1 phase ¹.

Protein ID	Number of Peptides ²	ORF Name	Present in Control ³	Protein Description
CAL0002762	48	SWI4/orf19.4545	N	Verified ORF; Putative component of the SBF transcription complex involved in G1/S cell-cycle progression; periodic mRNA expression peak at cell-cycle G1/S phase
CAL0006304	19	RPL3/orf19.1601	N	Verified ORF; Putative ribosomal protein large subunit; induced by ciclopirox olamine treatment
CAL0003235	17	RPL19A/orf19.5904	N	Verified ORF; Ribosomal protein L19; genes encoding cytoplasmic ribosomal subunits translation factors
CAF0006944	14	RPL2/orf19.2309.2	N	Uncharacterized ORF; Putative 60S ribosomal protein L2; Hap43p-induced gene
CAL0005300	14	RPS24/orf19.5466	N	Uncharacterized ORF; Predicted ribosomal protein; hyphal downregulated; genes encoding cytoplasmic ribosomal subunits
CAL0006017	13	RPL10/orf19.2935	N	Verified ORF; Ribosomal protein L10; intron in 5'-UTR
CAL0002164	12	NOP5/orf19.1199	N	Verified ORF; Protein similar to <i>S. cerevisiae</i> Nop5p protein of small nucleolar ribonucleoprotein complex; transposon mutation affects filamentous growth;
CAL0003748	11	RPS6A/orf19.4660	N	Verified ORF; Ribosomal protein 6A; localizes to cell surface of yeast cells but not hyphae
CAL0000513	11	RPS23A/orf19.6253	N	Uncharacterized ORF; Putative ribosomal protein; genes encoding cytoplasmic ribosomal subunits translation factors and tRNA synthetases are downregulate
CAL0004688	11	RPS26A/orf19.1470	N	Uncharacterized ORF; Predicted ribosomal protein; regulated by Nrg1p Tup1p; genes encoding cytoplasmic ribosomal subunits translation factors
CAL0000756	10	RPS7A/orf19.1700	N	Verified ORF; Ribosomal protein S7; genes encoding cytoplasmic ribosomal subunits translation factors
CAL0004084	10	RPS25B/orf19.6663	N	Uncharacterized ORF; Ribosomal protein; macrophage/pseudohyphal-induced after 16 h; downregulated upon phagocytosis by murine macrophage
CAL0004119	10	RPS21/orf19.3334	N	Uncharacterized ORF; Predicted ribosomal protein; genes encoding cytoplasmic ribosomal subunits translation factors
CAF0006992	10	orf19.3690.2	N	Uncharacterized ORF; Ortholog(s) have RNA binding structural constituent of ribosome activity role in cytoplasmic translation and cytosolic large ribosoma
CAL0005156	9	SRP40/orf19.2859	N	Uncharacterized ORF; Putative chaperone of small nucleolar ribonucleoprotein particles; macrophage/pseudohyphal-induced
CAF0007002	8	orf19.4149.1	N	Uncharacterized ORF; Ortholog(s) have structural constituent of ribosome activity and role in maturation of SSU-rRNA
CAL0002028	8	RPL17B/orf19.4490	N	Verified ORF; Ribosomal protein L17; mutation confers hypersensitivity to 5-FU tubercidin; genes encoding cytoplasmic ribosomal subunits
CAL0002747	7	RPL21A/orf19.840	N	Uncharacterized ORF; Putative ribosomal protein
CAL0001395	7	orf19.5722	N	Uncharacterized ORF; Has domain(s) with predicted DNA binding activity and role in regulation of transcription DNA-dependent
CAF0007036	7	RPL27A/orf19.5225.2	N	Verified ORF; Ribosomal protein L27
CAL0005866	7	RPL15A/orf19.493	N	Uncharacterized ORF; Putative ribosomal protein; genes encoding cytoplasmic ribosomal subunits translation factors
CAL0004009	7	VMMA2/orf19.6634	N	Verified ORF; Vacuolar H(+)-ATPase; protein present in exponential and stationary growth phase yeast cultures; plasma membrane localized
CAL0004400	6	SWI6/orf19.4725	N	Verified ORF; Putative component of the MBF and SBF transcription complexes involved in G1/S cell-cycle progression
CAL0003843	6	NPL3/orf19.7238	N	Verified ORF; Putative RNA-binding protein; required for normal biofilm growth; nuclear export is facilitated by Hmt1p
CAF0006953	6	orf19.2478.1	N	Verified ORF; 60S ribosomal protein L7; snoRNA snR39b encoded within the 2nd intron
CAL0002245	6	RNR21/orf19.5801	N	Uncharacterized ORF; Ribonucleoside-diphosphate reductase; regulated by tyrosol and cell density; transcription upregulated in response to ciclopirox olamin
CAL0006140	6	SRB1/orf19.6190	N	Verified ORF; Essential GDP-mannose pyrophosphorylase; synthesizes GDP-mannose for protein glycosylation; functional homolog of <i>S. cerevisiae</i> Psa1p
CAL0002678	5	HSP21/orf19.822	N	Verified ORF; Similar to heat-shock protease protein; protein detected in some not all biofilm extracts; fluconazole-downregulated
CAL0004487	5	FRE10/orf19.1415	N	Verified ORF; Major cell-surface ferric reductase under low-iron conditions; 7 transmembrane regions and a secretion signal predicted;
CAL0001208	5	SSA2/orf19.1065	N	Verified ORF; HSP70 family chaperone; found in cell wall fractions; antigenic; role in import of beta-defensin peptides; ATPase domain binds histatin 5;
CAL0001259	5	RPS3/orf19.6312	N	Uncharacterized ORF; Ribosomal protein S3; Hog1p- Hap43p-induced; genes encoding cytoplasmic ribosomal subunits translation factors
CAL0005797	5	ATP1/orf19.6854	N	Verified ORF; ATP synthase alpha subunit; antigenic in human/mouse; at hyphal surface not yeast; induced by ciclopirox ketoconazole flucytosine
CAF0006947	5	RPS17B/orf19.2329.1	N	Uncharacterized ORF; Ribosomal protein 17B
CAF0006907	5	RPL37B/orf19.667.1	N	Uncharacterized ORF; Ribosomal protein L37; Hap43p-induced gene
CAL0006335	5	ILV2/orf19.1613	N	Verified ORF; Putative acetolactate synthase; regulated by Gcn4p; induced by amino acid starvation (3-AT treatment); stationary phase enriched protein
CAF0006939	5	RPS10/orf19.2179.2	N	Verified ORF; Ribosomal protein S10; downregulated in the presence of human whole blood or polymorphonuclear (PMN) cells
CAF0007010	5	RPS30/orf19.4375.1	N	Uncharacterized ORF; Putative 40S ribosomal protein S30; shows colony morphology-related gene regulation by Ssn6p

CAL0004436	4	MSS116/orf19.4739	N	Uncharacterized ORF; Putative DEAD-box protein required for efficient splicing of mitochondrial Group I and II introns; Hap43p-induced gene
CAL0005042	4	CDC5/orf19.6010	N	Verified ORF; Polo-like kinase; member of conserved Mcm1p regulon; depletion causes defects in spindle elongation and Cdc35p-dependent filamentation
CAF0007090	4	orf19.6882.1	N	Uncharacterized ORF; Ortholog(s) have structural constituent of ribosome activity role in cytoplasmic translation and cytosolic large ribosomal subunit I
CAL0006157	4	RPL13/orf19.2994	N	Verified ORF; Putative ribosomal subunit; antigenic during murine systemic infection
CAL0003176	4	ADH1/orf19.3997	N	Verified ORF; Alcohol dehydrogenase; oxidizes ethanol into acetaldehyde; at yeast but not hyphal cell surface; soluble in hyphae
CAL0003449	4	RPL18/orf19.5982	N	Uncharacterized ORF; Predicted ribosomal protein; Plc1p-regulated Tbf1p-activated

¹Approximately 112 mg protein extracts from 3 L cultures of strains YC221 (*SWI6/SWI6-TAP, cln3Δ/MET3::CLN3*) and BH253 (*SWI6/SWI6, cln3Δ/MET3::CLN3*) incubated in SD+MC medium for 2.5 h were subjected to tandem affinity purification [107]. Elutions were TCA-precipitated and directly analysed using an LTQ-OrbitrapElite with nano-ESI. ²Peptides less than 4 were excluded from the results but can be found in the Appendix Table S5. ³Peptides identified in both the tagged strain and the untagged control strain were excluded from the results.

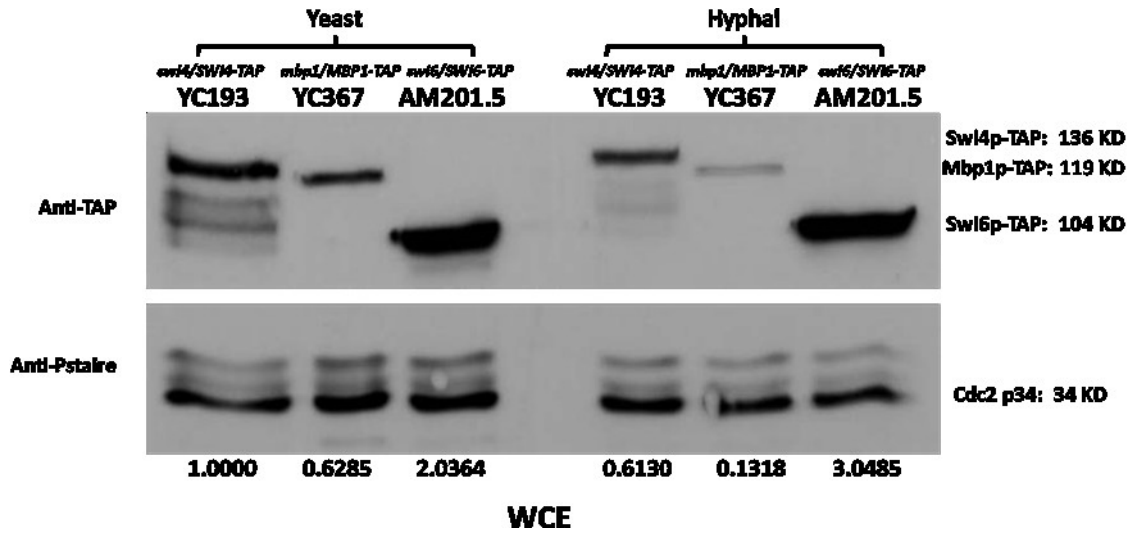


Figure 24: Protein expression levels of Swi4p, Swi6p and Mbp1p under yeast and hyphal growth conditions.

Strains YC193, AM201.5 and YC367 were incubated in YPD medium until they reached an O.D._{600nm} of 1.0, Cells for the hyphal condition was incubated in the 10% FBS contained YPD medium and with the temperature of 37°C for 2 hours. Adjusted density was obtained using ImageJ software (<http://rsb.info.nih.gov/ij/index.html>) [114].

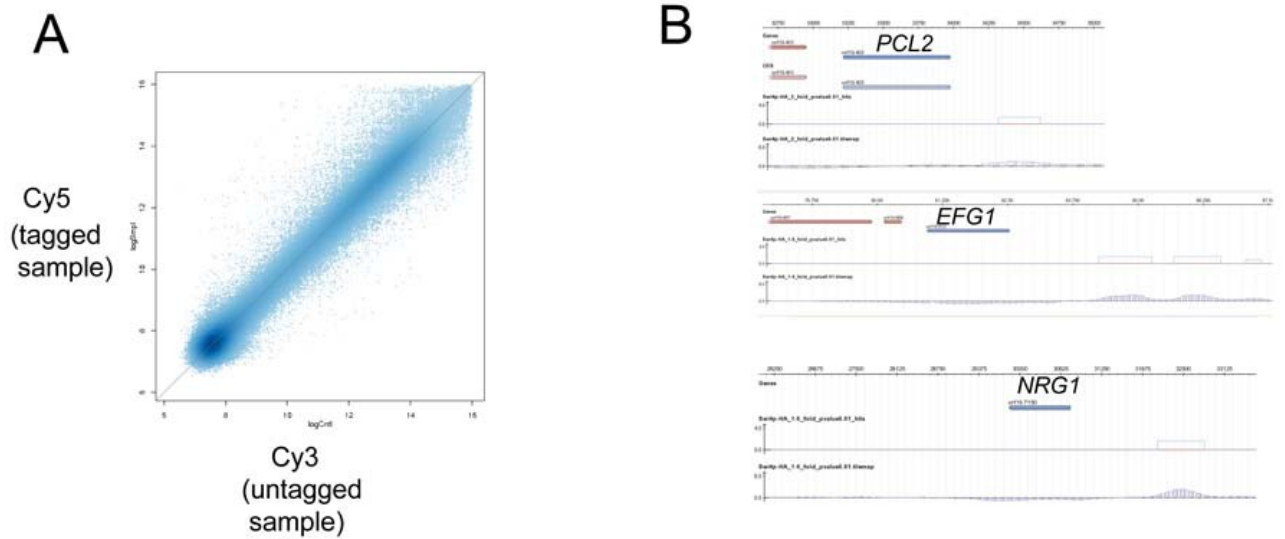


Figure 25: Genome-wide location analysis of Swi4p-HA.

(A) Scatterplot showing Cy5 (*swi4Δ/Swi4p-HA*) and Cy3 (*SWI4/SWI4*) intensities on a single *C. albicans* whole genome oligonucleotide tiling array [106]. (B) Swi4p-HA binding at select promoters. Signal intensities (log₂ transformed) are represented on the y axis, and gene location on the x axis. Genes *PCL2*, *EFG1* and *NRG1* are represented.

Table 9. Selected Swi4p-enriched targets ¹

Systematic name ²	CGD/NRC name ³	CandidaDB name ⁴	<i>S.cerevisiae</i> ortholog ⁵	GO terminology ⁶	BR ⁷
orf19.7017	YOX1	IPF2351	YOX1		1.386
orf19.403	PCL2	IPF26921	PCL2		0.94
orf19.4308	HSL1	IPF23021	HSL1		1.105
orf19.6936	RAD53	IPF20181	RAD53		0.871
orf19.6514	CUP9	IPF20614	TOS8		0.765
orf19.1446	CLB2	IPF25776	CLB2		0.71
orf19.1690	TOS1	IPF25628	TOS1		1.5
orf19.4853	HCM1	IPF22406	HCM1	Cell cycle regulators	0.697
orf19.4867	SWE1	IPF10223	SWE1		0.735
orf19.3071	MIH1	IPF19027	MIH1		1.149
orf19.1868	RNR22	IPF25438	RNR2		2.082
orf19.548	CDC10	IPF26797	CDC10		1.11
orf19.1853	HHT2	IPF25478	HHT2		0.892
orf19.1854	HHF22	IPF25481	HHF2		0.892
orf19.1051	HTA2	IPF26275	HTA1		1.258
orf19.1052	orf19.1052	IPF26276	HTB1		1.258
orf19.3207	CCN1	IPF24117	CLB3		0.735
orf19.610	EFG1	IPF3577	SOK2		1.516
orf19.6021	IHD2	IPF21083	N/A		0.87
orf19.5902	RAS2	IPF21239	RAS1		0.94
orf19.4621	orf19.4621	IPF22563	PBY1		1.359
orf19.3669	SHA3	IPF23589	SKS1		1.345
orf19.2241	PST1	IPF17954	PST2		1.2
orf19.5416	ESA1	IPF21714	ESA1	Filament associated activity	0.93
orf19.396	EAF6	IPF26924	EAF6		0.735
orf19.7150	NRG1	IPF1932	SCR1		1.465
orf19.5908	TEC1	IPF21178	TEC1		1.03
orf19.6965	FGR30	IPF4269	N/A		1.07
orf19.5741	ALS1	IPF21498	SAG1		1.025
orf19.2531	CSP37	IPF24765	OM45		1.01
orf19.1944	GPR1	IPF11281	GPR1		0.967
orf19.6734	TCC1	IPF20318	CYC8		0.925
orf19.3302	orf19.3302	IPF23920	GAC1		0.9
orf19.2659	orf19.2659	IPF200561	N/A	0.88	
orf19.4459	orf19.4459	IPF22769	YNL234W	0.865	
orf19.3997	ADH1	IPF13058	ADH3	0.837	

orf19.3325	orf19.3325	IPF83211	GLG2		0.817
orf19.4246	orf19.4246	IPF22957	YKR070W		0.783
orf19.1189	orf19.1189	IPF19121	N/A		0.765
orf19.5992	WOR2	IPF21214	UME6		0.689
orf19.2241	PST1	IPF17954	PST2		1.2
orf19.5292	AXL2	IPF21817	AXL2		1.321
orf19.3040	EHT1	IPF24309	EHT1	Mating process associated activity	1.367
orf19.7020	orf19.7020	IPF2356	KEX1		1.342
orf19.3369	MOH1	IPF10404	MOH1		1.195
orf19.1907	EMC9	IPF144683	NNF2		1.025
orf19.4390	orf19.4390	IPF22884	YPL014W		0.787
orf19.1027	PDR16	IPF15777	PDR16	response to drugs	0.775
orf19.5604	MDR1	IPF21587	FLR1		1.291
orf19.5079	CDR4	IPF22170	PDR5		1.903
orf19.5292	AXL2	IPF21817	AXL2	Budding related	1.321
orf19.2122	ALS12	IPF18994	N/A		1.03
orf19.2531	CSP37	IPF24765	OM45		1.01
orf19.3010.1	ECM33	IPF24311	ECM33		0.81
orf19.4246	orf19.4246	IPF22957	YKR070W	Cell wall related protein	0.783
orf19.3672	GAL10	IPF23585	GAL10		1.44
orf19.54	RHD1	IPF27198	N/A		1.095
orf19.2765	PGA62	IPF20161	FLO1		0.785
orf19.691	GPD2	IPF26632	GDP1		1.305
orf19.3651	PGK1	IPF23636	PGK1		1.291

¹ Complete list of Swi4p enriched promoters are in the Appendix, S1

² orf19 nomenclature according to the assembly 19 version.

³ Gene name according to the CGD (<http://www.candidagenome.org/>).

⁴ Gene name at CandidaDB (<http://genolist.pasteur.fr/CandidaDB/>).

⁵ Ortholog in *S. cerevisiae* (<http://www.candidagenome.org/>).

⁶ GO annotation found at CGD (<http://www.candidagenome.org/>).

⁷ BR, binding ratios represented in log₂ form.

Table 10: GO slim analysis of Swi4p-enriched targets¹

<u>GO category²</u>	<u>P value³</u>	<u>GO genes in set⁴</u> (236 total)	<u>GO genes in genome⁵</u> (6803 total)
Regulation of biological process	4.9E-3	56	1764
Filamentous growth	1.0E-4	38	560
Response to stress	4.0E-3	43	798
Carbohydrate metabolism	4.0E-4	21	256
Interspecies interaction between organisms	1.0E-4	18	127
Pathogenesis	1.2E-3	18	217
RNA metabolic process	9.2E-3	13	727
Biofilm formation	6.8E-3	11	128
Growth of unicellular organism as a thread of attached cells	2.4E-3	9	78
Cell adhesion	6.0E-4	8	49

¹ Gens that showed significant enrichment of Swi4p at promoters on the tiling array used for ChIP-chip.

² GO type: Biological process

³ Enrichment of GO category represented in Swi4p ChIP-chip data based on Fisher Exact Test.

⁴ Number of genes within total set of Swi4p-enriched targets that are associated with the select GO category.

⁵ Total number of genes within the genome that associate with select GO category.

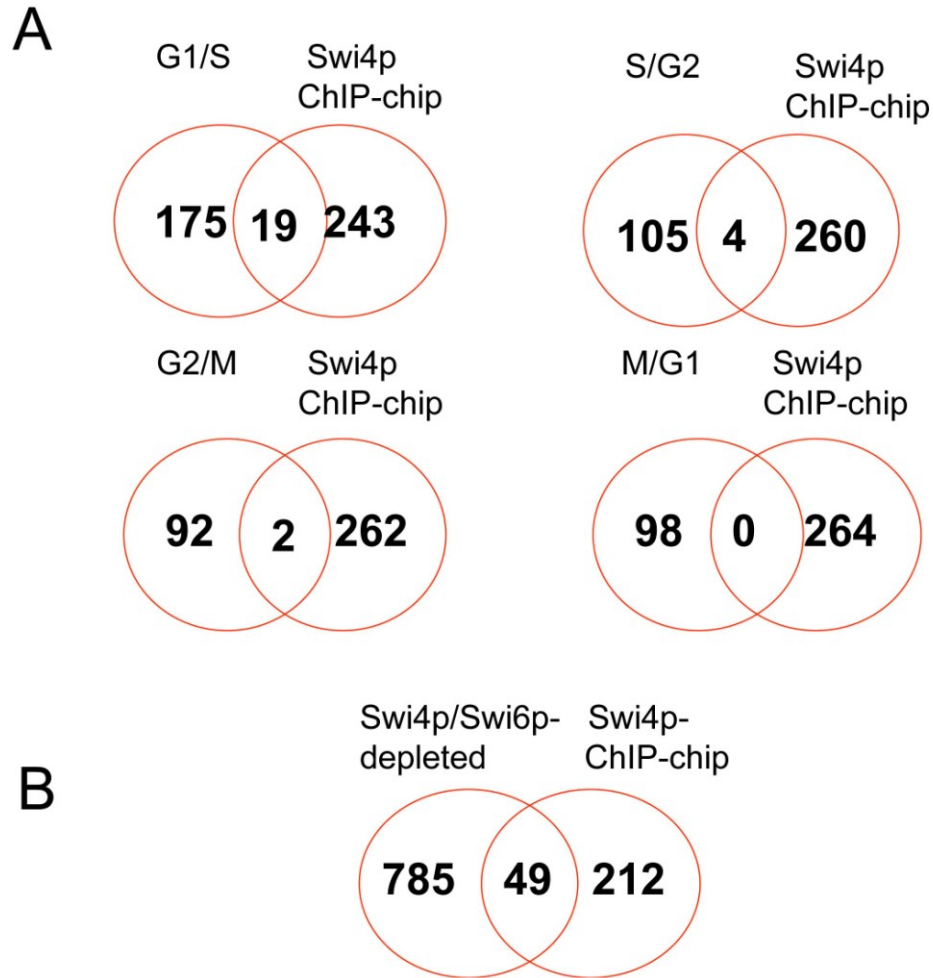


Figure 26: Comparison of ChIP-chip location and DNA expression data.

Venn diagrams comparing Swi4p ChIP-chip data with transcription profiles of *C. albicans* cells passing through different cell cycle stages (**A**) (taken from Cote *et al.*, 2009) [74] or cells depleted of Swi4p and Swi6p (**B**) (Hussein *et al.*, 2011) [77]. Modulated genes in Swi4p/Swi6p-depleted cells include both up and down-regulated.

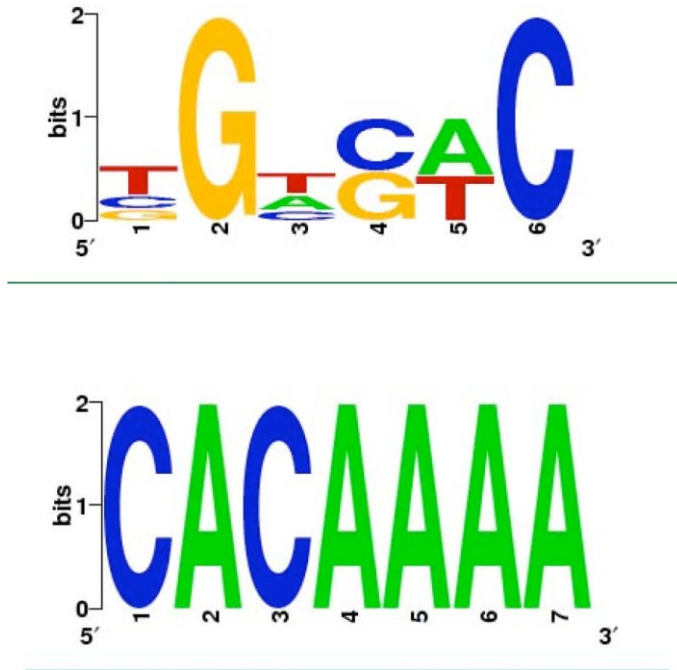


Figure 27: Motifs enriched in promoters of genes bound by Swi4p-HA.
Binding regions of Swi4p-HA in promoters of genes obtained from a single tiling array were analyzed with SCOPE (<http://genie.dartmouth.edu/scope/>).

Table 11. Swi4p-HA enriched promoters containing SCB (CNCGAAA) or MCB (ACGCGT) elements¹

Element contained	Systematic name ²	CGD/NRC name ³	CandidaDB name ⁴	<i>S.cerevisiae</i> ortholog ⁵	GO terminology ⁶	BR ⁷
SCB	orf19.4485	deleted				0.755
	orf19.4712	FGR6-3	IPF12868		FGR6-related genes; transposon mutation affects filamentous growth	0.745
	orf19.727	orf19.727	IPF26578	N/A	FGR6-related genes	0.705
	orf19.5315	FGR6	IPF21845	N/A	transposon mutation affects filamentous growth	0.718
	orf19.3207	CCN1	IPF24117	CLB3	G1 cyclin; required for hyphal growth maintenance	0.735
	orf19.610	EFG1	IPF3577	SOK2	transcriptional regulator required for white-phase cell type; hyphal growth, metabolism, cell-wall gene regulator; roles in adhesion, virulence	0.757
	orf19.734	GLK1	IPF27232	GLK1	Putative glucokinase; transcription regulated upon yeast-hyphal switch; regulated by Efg1p	0.69
	orf19.3965	orf19.3965	IPF18603	N/A	meiotic gene conversion, reciprocal meiotic recombination	1.847
	orf19.4304	GAP1	IPF22960	GAP1	GlcNAc, phagocytosis, biofilm induced	0.73
	orf19.4390	orf19.4390	IPF22884	YPL014W	repressed in response to alpha pheromone in SpiderM medium	0.787
	orf19.4579	orf19.4579	IPF22619	ERV29	Putative SURF4 family member; plasma membrane-localized	0.702
	orf19.4783	orf19.4783	IPF19867	N/A	ORF, Uncharacterized	1.782
	orf19.6501	orf19.6501	IPF3931	YJU3	ORF, Uncharacterized	0.745
	orf19.7458	orf19.7458	IPF2906	N/A	ORF, Uncharacterized	0.928
MCB	orf19.1907	EMC9	IPF144683	NNF2	Induced during the mating process	1.025
	orf19.2926	orf19.2926	IPF24250	PSO2	5'-3' exonuclease activity, role in DNA repair and nucleus localization	0.987
	orf19.4552	deleted				0.928

¹ whole list of Swi4p enriched promoters are in the appendix.

² orf19 nomenclature according to the assembly 19 version

³ Gene name according to the CGD (<http://www.candidagenome.org/>)

⁴ Gene name at CandidaDB (<http://genolist.pasteur.fr/CandidaDB/>).

⁵ Ortholog in *S. cerevisiae* (<http://www.candidagenome.org/>).

⁶ GO annotation found at CGD (<http://www.candidagenome.org/>).

⁷ BR, binding ratio.

4. Discussion

Elucidating the regulation of the G1/S transition in *C. albicans* has important implications for understanding and controlling cell proliferation, as well as hyphal development, both of which are important for virulence. Previously, *C. albicans* Swi4p and Swi6p were suggested to be the core components of a single MBF-like G1/S transcription complex in *C. albicans* [77, 79]. However, biochemical evidence supporting complex formation between these factors was lacking, the precise DNA binding sequence was not known, and direct targets had not yet been explored. Further, previous data suggested that additional factors may contribute to G1/S control in *C. albicans* [77], but their identity was not known. Our results demonstrate that Swi4p and Swi6p can physically interact to form a complex, in support of the model. However, Mbp1p also interacted with Swi6p, suggesting that it may be another core component of the complex. Affinity purification/mass spectrometry underscored interactions between the factors but did not reveal additional abundant proteins. Finally, ChIP-chip analysis identified putative Swi4p targets involved in G1/S control, as predicted, but also hyphal development. In summary, our results provide new insights on G1/S regulation in *C. albicans* but raise important new questions on the functions of Swi6p, Swi4p and Mbp1p.

4.1 Physical interactions between Swi6p, Swi4p and Mbp1p: implications for G1/S transcription complex composition.

Based on previous results [77, 79], Swi4p and Swi6p were proposed to be the major components of a G1/S transcription complex in *C. albicans*, while the role of Mbp1p was less clear [77]. In utilizing co-immunoprecipitation and affinity purification/mass spectrometry approaches, we provide the first demonstration that Swi4p and Swi6p in *C. albicans* physically interact, supporting the model that these factors may function as a complex. However, we also demonstrated that another predominant interacting protein of Swi6p is Mbp1p. Mbp1p was not present when Swi6p was affinity-purified from cells blocked in G1 phase, suggesting that the interaction may be cell cycle stage-specific, but this requires confirmation via co-immunoprecipitation. In exponential-growing cells, at least, Swi6p and Mbp1p were dominant binding partners, suggesting that Mbp1p may in fact be another core complex factor. This raises questions on the composition and number of G1/S transcription complexes. One possibility is that *C. albicans* contains two complexes, composed of Swi6p and Mbp1p or Swi6p and Swi4p, as seen with MBF and SBF, respectively, in *S. cerevisiae*. However, absence of *MBP1* had little effect on *C. albicans* growth, unlike absence of *SWI4* or *SWI6*, and was not synthetically lethal with *SWI4* [77]. In contrast, Mbp1p can be redundant with Swi4p in *S. cerevisiae*, and absence of both is lethal [78] as is absence of Res1 and Res2 in *S. pombe* [44]. Moreover, Swi4p and Mbp1p are at similar levels in *S. cerevisiae* [115], but we showed that Mbp1p levels are significantly less than that of Swi4p or Swi6p in *C. albicans*. Thus, if Mbp1p forms a separate complex with Swi6p, this is not predicted to

act as a dominant co-regulator of the G1/S transition as its MBF counterpart in *S. cerevisiae*.

The interaction between Swi6p and Mbp1p may alternatively suggest that all three factors exist in a single heteromeric complex, similar to the situation with MBF in *S. pombe*. We addressed this possibility by determining whether Mbp1p could interact with Swi4p. Although Mbp1p-TAP co-purified with immunoprecipitated Swi4p-HA, co-purification was not observed between Swi4p-MYC and Mbp1p-HA. The latter may be due to issues with MYC tagging and a lower signal for Swi4p tagged with MYC vs. other tags. However, Swi4p-TAP-interacting factors did not include Mbp1p, and Mbp1p-interacting factors did not include Swi4p. It is possible that Swi4p and Mbp1p indirectly interact via association via Swi6p, allowing detection via co-immunoprecipitation, but the weaker interactions were lost during preparation for mass spectrometry. Current investigations aimed at clarifying this issue include tagging Swi4p correctly with a 13 vs. 5 copies of MYC and repeating co-immunoprecipitation with Mbp1p-HA.

If Mbp1p is a G1/S transcription complex(es) component in *C. albicans*, its function remains unclear. In *S. pombe*, one of the two DNA-binding factors of MBF, Res2p, is exclusively utilized during DNA replication in premeiotic cells [41]. Thus, Mbp1p in *C. albicans* could play a more dominant role in different cell forms or under specific conditions. Notably, Mbp1p was significantly reduced in *C. albicans* hyphal vs. yeast cells, unlike Swi4p and Swi6p, underscoring the potential for cell type-specific features. We also can not rule out the possibility that Mbp1p regulates a subset of G1/S

genes, has functions outside of G1/S, or that Swi4p, Swi6p and Mbp1p can also function independently. Notably, absence of both *SWI6* and *MBP1* orthologues in the filamentous fungus *Aspergillus nidulans* has no effect on growth [118], demonstrating the potential for alternative functions and/or the need for additional factors in G1/S control in different fungi. Future experiments will include ChIP-chip with Mbp1p, gel shift assays, and cell-cycle stage-specific co-immunoprecipitation to help distinguish Mbp1p, Swi4p and Swi6p function, and provide further insights on G1/S complex composition in *C. albicans*.

4.2 Systematic affinity purifications of Swi6p, Swi4p and Mbp1p reveal few other predominant interacting proteins.

Since absence of both Swi4p and Mbp1p in *C. albicans* was not lethal [77], in contrast to the situations in *S. cerevisiae* and *S. pombe*, G1/S regulation was proposed to involve additional core factors [77]. We attempted to identify these factors and glean more information on Swi4p, Swi6p and Mbp1p function and regulation through systematic tandem-affinity purification/mass spectrometry. Predicted interacting proteins were highly abundant, such as Swi4p and Mbp1p in immune complexes of Swi6p, validating the technique in our hands. However, few additional abundant factors were present. Nrm1p was previously shown to bind Swi4p in *C. albicans* through co-immunoprecipitation [79], but this was accomplished by first cross-linking the cells. Nrm1p was not present in our putative Swi4p-interacting data set, but was enriched in one trial of affinity purification of Mbp1p. This remains to be confirmed through co-

immunoprecipitation, but if true, further suggests that Mbp1p may be playing a more significant role in G1/S regulation in *C. albicans*. Absence of other interacting factors could be due to affinity purifying from exponential-growing cells. However, our results were not significantly enhanced by utilizing cells blocked in G1 phase (for Swi6p). Additional co-regulatory components are predicted to exist, but may function under specific conditions and/or have weaker interactions. Future attempts at their identification could incorporate chemical cross-linking [79], different growth conditions/treatments or increasing the input protein. In summary, our results provide the first systematic identification of putative Swi4p, Swi6p and Mbp1p-interacting factors in *C. albicans*, and reinforce the notion that these proteins predominantly bind each other.

4.3 ChIP-chip analysis identifies putative Swi4p targets involved in G1/S progression and filamentous growth.

Although previous genetic and DNA expression data implied a role for Swi4p and Swi6p in regulating the G1/S transition in *C. albicans* [77, 79], direct targets had not been identified. We addressed this question using genome-wide location analysis (ChIP-chip). The results were based on a single tiling array, and have not yet been confirmed with qPCR, but provide the first *in vivo* glimpse of putative Swi4p targets on a genome-wide scale in *C. albicans*. Intriguingly, the results are consistent with the expected functions of Swi4p, based on the phenotype of *swi4Δ/Δ* cells and transcription profiles of cells lacking Swi4p and Swi6p [77]. First, promoters of G1 cyclins (*CCN1*, *PCL2*) and other

G1, S phase cell cycle regulatory factors (*YOX1*, *HSL1* and *RAD53*, for example) showed enriched Swi4p binding. Since many of these factors also show modulated expression in cells lacking Swi4p and Swi6p [77] or during the G1/S transition [74], they are candidates for true Swi4p targets. Intriguingly, genes associated with filamentous growth constituted the most abundant group of putative Swi4p targets, and included regulators of hyphal development, including Efg1p. Previous work demonstrated that depletion of the G1 cyclin Cln3p in *C. albicans* yeast cells resulted in a G1 phase arrest, followed by development of true hyphae and pseudohyphae in an Ras1p and Efg1p-dependent manner [73, 76]. Absence of Swi4p and/or Swi6p also resulted in a high proportion of yeast cells switching to hyphal growth, raising the possibility that these factors may lie in pathway linking G1 phase to hyphal differentiation [77, 79]. Alternatively, filamentation may be an indirect response to G1 phase arrest or delay. If Swi4p binds regulators of the hyphal program, this provides a mechanism by which G1 phase progression may be directly linked to development. One possible model could involve Swi4p-dependent induction of G1/S genes in proliferating yeast, and simultaneous Swi4p-mediated repression of development genes with the assistance of loci-specific co-repressors. Hyphal regulators such as *EFG1* were not induced in the absence of Swi4p and Swi6p but hyphal-specific genes normally regulated by Efg1p were strongly induced [77].

The set of putative Swi4p-enriched targets only partially overlapped with genes are expressed at the G1/S transition [74]. This could imply that the ChIP-chip data consisted of false positives. However, the targets were consistent with Swi4p function.

Further, not all SBF/MBF targets in *S. cerevisiae* are periodically expressed [31]. The screen is likely not saturated given the use of a single tiling array, but it is also possible that Swi4p does not directly regulate all of the G1/S-associated genes; they may require other forms of regulation or be indirect targets [119].

Collectively this data supports the model that Swi4p is part of a transcription factor complex in *C. albicans* that regulates G1/S progression, and provides insights on possible mechanisms of action. The results further suggest that Swi4p may also directly regulate aspects of the hyphal development program. Future work will involve increasing the sample size for ChIP-chip, and using qPCR to confirm select targets.

4.4 Swi4p may not function exclusively through the conserved MCB element.

Unexpectedly, few of the putative Swi4p target promoters contained the MBF-binding MCB element. In *S. cerevisiae*, Swi4p predominantly binds the Swi4/6-dependent cell cycle box (SCB) motif located in promoters of target genes associated with the G1/S transition [31], while Mbp1p binds *MluI* cell cycle box (MCB) elements of genes associated with DNA replication [31]. However, promoters of *C. albicans* G1/S-associated genes were enriched for MCB, but not SCB elements [74]. This discrepancy may be due to technical aspects associated with a small sample size for ChIP-chip. However, not all G1/S-associated genes in *C. albicans* contained the MCB element. Consistently, in *S. cerevisiae*, 51% of Swi4p targets lacked SCB elements while 45% of Mbp1p targets lacked MCB motifs [31, 116]. Alternatively, we found that over 40% of

the putative Swi4p target promoters contained the sequence CACAAAA, which is similar to the SCB motif, CRCGAAA, and was 2-fold enriched in Swi4p promoters relative to all intergenic regions. Notably, more Swi4p putative targets contained an SCB (8.6%) vs. MCB (1.9%) element. However, many SCB/MBF targets in *S. cerevisiae* contain both motifs, and cross-binding by Swi4p and Mb1p1p is also known [32]. Although we can not rule out an interaction between Swi4p and the MCB motif, the data in hand suggests that Swi4p may show promiscuous binding and/or function through alternate sequences/mechanisms. Further, many of the G1/S-regulated genes may require additional or different factors for regulation. Future work will involve direct investigation of binding to CACAAAA vs. MCB and SCB motifs.

In summary, our results provide several new insights on G1/S regulation in *C. albicans*, specifically the composition and possible mechanisms of action of the G1/S transcription complex. Since this complex is important for cell proliferation, and possibly linked to hyphal development, the results have important implications for controlling growth and virulence of an important fungal pathogen of humans.

References:

1. Correia, I., R. Alonso-Monge, and J. Pla, *MAPK cell-cycle regulation in Saccharomyces cerevisiae and Candida albicans*. Future Microbiol, 2010. **5**(7): p. 1125-41.
2. Suryadinata, R., M. Sadowski, and B. Sarcevic, *Control of cell cycle progression by phosphorylation of cyclin-dependent kinase (CDK) substrates*. Biosci Rep, 2010. **30**(4): p. 243-55.
3. Jensen, L.J., et al., *Co-evolution of transcriptional and post-translational cell-cycle regulation*. Nature, 2006. **443**(7111): p. 594-7.
4. Morgan, D.O., *The Cell Cycle: Principles of Control*. 2007: New Science Press Ltd.
5. Gerard, C. and A. Goldbeter, *From quiescence to proliferation: Cdk oscillations drive the mammalian cell cycle*. Front Physiol, 2012. **3**: p. 413.
6. Merrick, K.A. and R.P. Fisher, *Why minimal is not optimal: driving the mammalian cell cycle--and drug discovery--with a physiologic CDK control network*. Cell Cycle, 2012. **11**(14): p. 2600-5.
7. Elledge, S.J., *Cell cycle checkpoints: preventing an identity crisis*. Science (New York, N.Y.), 1996. **274**(5293): p. 1664-72.
8. Sanchez, Y., et al., *Conservation of the Chk1 checkpoint pathway in mammals: linkage of DNA damage to Cdk regulation through Cdc25*. Science (New York, N.Y.), 1997. **277**(5331): p. 1497-501.
9. Levine, K., A.H. Tinkelenberg, and F. Cross, *The CLN gene family: central regulators of cell cycle Start in budding yeast*. Prog Cell Cycle Res, 1995. **1**: p. 101-14.
10. Blagosklonny, M.V. and A.B. Pardee, *The restriction point of the cell cycle*. Cell Cycle, 2002. **1**(2): p. 103-10.
11. Friedman, A., B. Hu, and C.Y. Kao, *Cell cycle control at the first restriction point and its effect on tissue growth*. J Math Biol, 2010. **60**(6): p. 881-907.
12. Pfeuty, B., T. David-Pfeuty, and K. Kaneko, *Underlying principles of cell fate determination during G1 phase of the mammalian cell cycle*. Cell Cycle, 2008. **7**(20): p. 3246-57.
13. Csikasz-Nagy, A., et al., *Analysis of a generic model of eukaryotic cell-cycle regulation*. Biophys J, 2006. **90**(12): p. 4361-79.
14. Johnson, D.G., K. Ohtani, and J.R. Nevins, *Autoregulatory control of E2F1 expression in response to positive and negative regulators of cell cycle progression*. Genes Dev, 1994. **8**(13): p. 1514-25.
15. Iaquinta, P.J. and J.A. Lees, *Life and death decisions by the E2F transcription factors*. Curr Opin Cell Biol, 2007. **19**(6): p. 649-57.
16. Nevins, J.R., *E2F: a link between the Rb tumor suppressor protein and viral oncoproteins*. Science (New York, N.Y.), 1992. **258**(5081): p. 424-9.
17. Dyson, N., *The regulation of E2F by pRB-family proteins*. Genes Dev, 1998. **12**(15): p. 2245-62.
18. Magnaghi-Jaulin, L., et al., *Retinoblastoma protein represses transcription by recruiting a histone deacetylase*. Nature, 1998. **391**(6667): p. 601-5.
19. Dimova, D.K. and N.J. Dyson, *The E2F transcriptional network: old acquaintances with new faces*. Oncogene, 2005. **24**(17): p. 2810-26.
20. Costanzo, M., et al., *CDK activity antagonizes Whi5, an inhibitor of G1/S transcription in yeast*. Cell, 2004. **117**(7): p. 899-913.

21. Takahata, S., Y. Yu, and D.J. Stillman, *The E2F functional analogue SBF recruits the Rpd3(L) HDAC, via Whi5 and Stb1, and the FACT chromatin reorganizer, to yeast G1 cyclin promoters*. EMBO J, 2009. **28**(21): p. 3378-89.
22. Breeden, L., *Start-specific transcription in yeast*. Curr Top Microbiol Immunol, 1996. **208**: p. 95-127.
23. de Bruin, R.A., et al., *Clb3 activates G1-specific transcription via phosphorylation of the SBF bound repressor Whi5*. Cell, 2004. **117**(7): p. 887-98.
24. Wagner, M.V., et al., *Whi5 regulation by site specific CDK-phosphorylation in Saccharomyces cerevisiae*. PLoS One, 2009. **4**(1): p. e4300.
25. Siegmund, R.F. and K.A. Nasmyth, *The Saccharomyces cerevisiae Start-specific transcription factor Swi4 interacts through the ankyrin repeats with the mitotic Clb2/Cdc28 kinase and through its conserved carboxy terminus with Swi6*. Mol Cell Biol, 1996. **16**(6): p. 2647-55.
26. Wittenberg, C. and S.I. Reed, *Cell cycle-dependent transcription in yeast: promoters, transcription factors, and transcriptomes*. Oncogene, 2005. **24**(17): p. 2746-55.
27. Bahler, J., *Cell-cycle control of gene expression in budding and fission yeast*. Annu Rev Genet, 2005. **39**: p. 69-94.
28. de Bruin, R.A., et al., *Constraining G1-specific transcription to late G1 phase: the MBF-associated corepressor Nrm1 acts via negative feedback*. Mol Cell, 2006. **23**(4): p. 483-96.
29. Sanchez, Y., et al., *Control of the DNA damage checkpoint by chk1 and rad53 protein kinases through distinct mechanisms*. Science (New York, N.Y.), 1999. **286**(5442): p. 1166-71.
30. Travesa, A., et al., *DNA replication stress differentially regulates G1/S genes via Rad53-dependent inactivation of Nrm1*. EMBO J, 2012. **31**(7): p. 1811-22.
31. Iyer, V.R., et al., *Genomic binding sites of the yeast cell-cycle transcription factors SBF and MBF*. Nature, 2001. **409**(6819): p. 533-8.
32. Bean, J.M., E.D. Siggia, and F.R. Cross, *High functional overlap between MluI cell-cycle box binding factor and Swi4/6 cell-cycle box binding factor in the G1/S transcriptional program in Saccharomyces cerevisiae*. Genetics, 2005. **171**(1): p. 49-61.
33. Koch, C., et al., *A role for the transcription factors Mbp1 and Swi4 in progression from G1 to S phase*. Science (New York, N.Y.), 1993. **261**(5128): p. 1551-1557.
34. Ferrezuelo, F., M. Aldea, and B. Futcher, *Bck2 is a phase-independent activator of cell cycle-regulated genes in yeast*. Cell Cycle, 2009. **8**(2): p. 239-52.
35. Wijnen, H. and B. Futcher, *Genetic analysis of the shared role of CLN3 and BCK2 at the G(1)-S transition in Saccharomyces cerevisiae*. Genetics, 1999. **153**(3): p. 1131-1143.
36. Di Como, C.J., H. Chang, and K.T. Arndt, *Activation of CLN1 and CLN2 G1 cyclin gene expression by BCK2*. Mol Cell Biol, 1995. **15**(4): p. 1835-46.
37. Wijnen, H. and B. Futcher, *Genetic analysis of the shared role of CLN3 and BCK2 at the G(1)-S transition in Saccharomyces cerevisiae*. Genetics, 1999. **153**(3): p. 1131-43.
38. Kasten, M.M. and D.J. Stillman, *Identification of the Saccharomyces cerevisiae genes STB1-STB5 encoding Sin3p binding proteins*. Mol Gen Genet, 1997. **256**(4): p. 376-86.
39. Silverstein, R.A. and K. Ekwall, *Sin3: a flexible regulator of global gene expression and genome stability*. Curr Genet, 2005. **47**(1): p. 1-17.
40. Martin-Castellanos, C., et al., *The pu1 cyclin regulates the G1 phase of the fission yeast cell cycle in response to cell size*. Mol Biol Cell, 2000. **11**(2): p. 543-54.

41. Tanaka, K. and H. Okayama, *A pcl-like cyclin activates the Res2p-Cdc10p cell cycle "start" transcriptional factor complex in fission yeast*. Mol Biol Cell, 2000. **11**(9): p. 2845-62.
42. Ayte, J., et al., *The Schizosaccharomyces pombe MBF complex requires heterodimerization for entry into S phase*. Mol Cell Biol, 1995. **15**(5): p. 2589-99.
43. Primig, M., et al., *Anatomy of a transcription factor important for the start of the cell cycle in Saccharomyces cerevisiae*. Nature, 1992. **358**(6387): p. 593-7.
44. Miyamoto, M., K. Tanaka, and H. Okayama, *res2+, a new member of the cdc10+/SWI4 family, controls the 'start' of mitotic and meiotic cycles in fission yeast*. EMBO J, 1994. **13**(8): p. 1873-80.
45. Gordon, C.B. and P.A. Fantes, *The cdc22 gene of Schizosaccharomyces pombe encodes a cell cycle-regulated transcript*. EMBO J, 1986. **5**(11): p. 2981-5.
46. Kelly, T.J., et al., *The fission yeast cdc18+ gene product couples S phase to START and mitosis*. Cell, 1993. **74**(2): p. 371-82.
47. Hofmann, J.F. and D. Beach, *cdt1 is an essential target of the Cdc10/Sct1 transcription factor: requirement for DNA replication and inhibition of mitosis*. EMBO J, 1994. **13**(2): p. 425-34.
48. Peng, X., et al., *Identification of cell cycle-regulated genes in fission yeast*. Mol Biol Cell, 2005. **16**(3): p. 1026-42.
49. Aligianni, S., et al., *The fission yeast homeodomain protein Yox1p binds to MBF and confines MBF-dependent cell-cycle transcription to G1-S via negative feedback*. PLoS Genet, 2009. **5**(8): p. e1000626.
50. Caetano, C., S. Klier, and R.A. de Bruin, *Phosphorylation of the MBF repressor Yox1p by the DNA replication checkpoint keeps the G1/S cell-cycle transcriptional program active*. PLoS One, 2011. **6**(2): p. e17211.
51. White, J. and S. Dalton, *Cell cycle control of embryonic stem cells*. Stem Cell Rev, 2005. **1**(2): p. 131-8.
52. Wittenberg, C. and R. La Valle, *Cell-cycle-regulatory elements and the control of cell differentiation in the budding yeast*. Bioessays, 2003. **25**(9): p. 856-67.
53. Gari, E., et al., *Whi3 binds the mRNA of the G1 cyclin CLN3 to modulate cell fate in budding yeast*. Genes Dev, 2001. **15**(21): p. 2803-8.
54. Loeb, J.D., et al., *Saccharomyces cerevisiae G1 cyclins are differentially involved in invasive and pseudohyphal growth independent of the filamentation mitogen-activated protein kinase pathway*. Genetics, 1999. **153**(4): p. 1535-46.
55. Chong, J.L., et al., *E2f3a and E2f3b contribute to the control of cell proliferation and mouse development*. Mol Cell Biol, 2009. **29**(2): p. 414-24.
56. Iwanaga, R., et al., *Identification of novel E2F1 target genes regulated in cell cycle-dependent and independent manners*. Oncogene, 2006. **25**(12): p. 1786-98.
57. Humbert, P.O., et al., *E2f3 is critical for normal cellular proliferation*. Genes Dev, 2000. **14**(6): p. 690-703.
58. De Falco, G., F. Comes, and C. Simone, *pRb: master of differentiation. Coupling irreversible cell cycle withdrawal with induction of muscle-specific transcription*. Oncogene, 2006. **25**(38): p. 5244-5249.
59. Anandakumar, S., et al., *Phage displayed short peptides against cells of Candida albicans demonstrate presence of species, morphology and region specific carbohydrate epitopes*. PLoS One, 2011. **6**(2): p. e16868.
60. Owotade, F.J., et al., *Prevalence of oral disease among adults with primary HIV infection*. Oral Dis, 2008. **14**(6): p. 497-9.

61. Hoehamer, C.F., et al., *Changes in the proteome of Candida albicans in response to azole, polyene, and echinocandin antifungal agents*. Antimicrob Agents Chemother, 2010. **54**(5): p. 1655-64.
62. Cateau, E., J.M. Berjeaud, and C. Imbert, *Possible role of azole and echinocandin lock solutions in the control of Candida biofilms associated with silicone*. Int J Antimicrob Agents, 2011. **37**(4): p. 380-4.
63. Ruhnke, M., et al., *Anidulafungin for the treatment of candidaemia/invasive candidiasis in selected critically ill patients*. Clin Microbiol Infect, 2012. **18**(7): p. 680-7.
64. Whiteway, M. and C. Bachewich, *Morphogenesis in Candida albicans (*)*. Annual Review of Microbiology, 2007. **61**: p. 529-553.
65. Li, D., J. Bernhardt, and R. Calderone, *Temporal expression of the Candida albicans genes CHK1 and CSSK1, adherence, and morphogenesis in a model of reconstituted human esophageal epithelial candidiasis*. Infect Immun, 2002. **70**(3): p. 1558-65.
66. Rocha, C.R., et al., *Signaling through adenylyl cyclase is essential for hyphal growth and virulence in the pathogenic fungus Candida albicans*. Mol Biol Cell, 2001. **12**(11): p. 3631-43.
67. Gow, N.A., A.J. Brown, and F.C. Odds, *Fungal morphogenesis and host invasion*. Curr Opin Microbiol, 2002. **5**(4): p. 366-71.
68. Thompson, D.S., P.L. Carlisle, and D. Kadosh, *Coevolution of morphology and virulence in Candida species*. Eukaryot Cell, 2011. **10**(9): p. 1173-82.
69. Romani, L., F. Bistoni, and P. Puccetti, *Adaptation of Candida albicans to the host environment: the role of morphogenesis in virulence and survival in mammalian hosts*. Curr Opin Microbiol, 2003. **6**(4): p. 338-43.
70. Lo, H.J., et al., *Nonfilamentous C. albicans mutants are avirulent*. Cell, 1997. **90**(5): p. 939-49.
71. Frade, J.P. and B.A. Arthington-Skaggs, *Effect of serum and surface characteristics on Candida albicans biofilm formation*. Mycoses, 2011. **54**(4): p. e154-62.
72. Doedt, T., et al., *APSES proteins regulate morphogenesis and metabolism in Candida albicans*. Mol Biol Cell, 2004. **15**(7): p. 3167-80.
73. Sudbery, P.E., *Growth of Candida albicans hyphae*. Nat Rev Microbiol, 2011. **9**(10): p. 737-48.
74. Cote, P., H. Hogues, and M. Whiteway, *Transcriptional analysis of the Candida albicans cell cycle*. Molecular biology of the cell, 2009. **20**(14): p. 3363-3373.
75. Chapa y Lazo, B., S. Bates, and P. Sudbery, *The G1 cyclin Cln3 regulates morphogenesis in Candida albicans*. Eukaryot Cell, 2005. **4**(1): p. 90-4.
76. Bachewich, C. and M. Whiteway, *Cyclin Cln3p links G1 progression to hyphal and pseudohyphal development in Candida albicans*. Eukaryot Cell, 2005. **4**(1): p. 95-102.
77. Hussein, B., et al., *G1/S transcription factor orthologues Swi4p and Swi6p are important but not essential for cell proliferation and influence hyphal development in the fungal pathogen Candida albicans*. Eukaryot Cell, 2011. **10**(3): p. 384-97.
78. Koch, C., et al., *A role for the transcription factors Mbp1 and Swi4 in progression from G1 to S phase*. Science (New York, N.Y.), 1993. **261**(5128): p. 1551-7.
79. Ofir, A., et al., *Role of a Candida albicans Nrm1/Whi5 homologue in cell cycle gene expression and DNA replication stress response*. Mol Microbiol, 2012. **84**(4): p. 778-94.
80. Levin, D.E., *Regulation of cell wall biogenesis in Saccharomyces cerevisiae: the cell wall integrity signaling pathway*. Genetics, 2011. **189**(4): p. 1145-75.
81. Zhao, X., R. Mehrabi, and J.R. Xu, *Mitogen-activated protein kinase pathways and fungal pathogenesis*. Eukaryot Cell, 2007. **6**(10): p. 1701-14.

82. LaFayette, S.L., et al., *PKC signaling regulates drug resistance of the fungal pathogen Candida albicans via circuitry comprised of Mkc1, calcineurin, and Hsp90*. PLoS Pathog, 2010. **6**(8): p. e1001069.
83. Lew, D.J. and S.I. Reed, *Cell cycle control of morphogenesis in budding yeast*. Curr Opin Genet Dev, 1995. **5**(1): p. 17-23.
84. Hazan, I., M. Sepulveda-Becerra, and H. Liu, *Hyphal elongation is regulated independently of cell cycle in Candida albicans*. Mol Biol Cell, 2002. **13**(1): p. 134-45.
85. Bachewich, C., A. Nantel, and M. Whiteway, *Cell cycle arrest during S or M phase generates polarized growth via distinct signals in Candida albicans*. Molecular microbiology, 2005. **57**(4): p. 942-959.
86. Soll, D.R., M.A. Herman, and M.A. Staebell, *The involvement of cell wall expansion in the two modes of mycelium formation of Candida albicans*. J Gen Microbiol, 1985. **131**(9): p. 2367-75.
87. Zheng, X., Y. Wang, and Y. Wang, *Hgc1, a novel hypha-specific G1 cyclin-related protein regulates Candida albicans hyphal morphogenesis*. EMBO J, 2004. **23**(8): p. 1845-56.
88. Loeb, J.D., et al., *A G1 cyclin is necessary for maintenance of filamentous growth in Candida albicans*. Mol Cell Biol, 1999. **19**(6): p. 4019-27.
89. Feng, Q., et al., *Ras signaling is required for serum-induced hyphal differentiation in Candida albicans*. J Bacteriol, 1999. **181**(20): p. 6339-46.
90. Fonzi, W.A. and M.Y. Irwin, *Isogenic strain construction and gene mapping in Candida albicans*. Genetics, 1993. **134**(3): p. 717-28.
91. Wilson, R.B., D. Davis, and A.P. Mitchell, *Rapid hypothesis testing with Candida albicans through gene disruption with short homology regions*. J Bacteriol, 1999. **181**(6): p. 1868-74.
92. Gola, S., et al., *New modules for PCR-based gene targeting in Candida albicans: rapid and efficient gene targeting using 100 bp of flanking homology region*. Yeast (Chichester, England), 2003. **20**(16): p. 1339-47.
93. Care, R.S., et al., *The MET3 promoter: a new tool for Candida albicans molecular genetics*. Mol Microbiol, 1999. **34**(4): p. 792-8.
94. Kelly, R., S.M. Miller, and M.B. Kurtz, *One-step gene disruption by cotransformation to isolate double auxotrophs in Candida albicans*. Mol Gen Genet, 1988. **214**(1): p. 24-31.
95. Chen, D.C., B.C. Yang, and T.T. Kuo, *One-step transformation of yeast in stationary phase*. Curr Genet, 1992. **21**(1): p. 83-4.
96. Gietz, R.D., et al., *Studies on the transformation of intact yeast cells by the LiAc/SS-DNA/PEG procedure*. Yeast (Chichester, England), 1995. **11**(4): p. 355-60.
97. Gietz, R.D. and R.A. Woods, *Genetic transformation of yeast*. BioTechniques, 2001. **30**(4): p. 816-20, 822-6, 828 passim.
98. Rose, M.D., F. Winston, and P. Hieter, *Methods in Yeast Genetics: A Laboratory Course Manual*. Cold Spring Harbor Laboratory Press, 1990.
99. Bensen, E.S., et al., *The mitotic cyclins Clb2p and Clb4p affect morphogenesis in Candida albicans*. Mol Biol Cell, 2005. **16**(7): p. 3387-400.
100. Liu, H.L., et al., *Single-step affinity purification for fungal proteomics*. Eukaryot Cell, 2010. **9**(5): p. 831-3.
101. Bradford, M.M., *A rapid and sensitive method for the quantitation of microgram quantities of protein utilizing the principle of protein-dye binding*. Anal Biochem, 1976. **72**: p. 248-54.

102. Rigaut, G., et al., *A generic protein purification method for protein complex characterization and proteome exploration*. Nat Biotechnol, 1999. **17**(10): p. 1030-2.
103. Znaidi, S., et al., *Identification of the Candida albicans Cap1p regulon*. Eukaryot Cell, 2009. **8**(6): p. 806-20.
104. Liu, X., et al., *Bayesian hierarchical model for transcriptional module discovery by jointly modeling gene expression and ChIP-chip data*. BMC Bioinformatics, 2007. **8**: p. 283.
105. Wu, J., et al., *ChIP-chip comes of age for genome-wide functional analysis*. Cancer Res, 2006. **66**(14): p. 6899-902.
106. Srikantha, T., et al., *TOS9 regulates white-opaque switching in Candida albicans*. Eukaryot Cell, 2006. **5**(10): p. 1674-87.
107. Lavoie, H., et al., *A toolbox for epitope-tagging and genome-wide location analysis in Candida albicans*. BMC Genomics, 2008. **9**: p. 578.
108. Costanzo, M., O. Schub, and B. Andrews, *G1 transcription factors are differentially regulated in Saccharomyces cerevisiae by the Swi6-binding protein Stb1*. Mol Cell Biol, 2003. **23**(14): p. 5064-77.
109. Whitehall, S., et al., *Cell cycle-regulated transcription in fission yeast: Cdc10-Res protein interactions during the cell cycle and domains required for regulated transcription*. Mol Biol Cell, 1999. **10**(11): p. 3705-15.
110. Ashe, M., et al., *The SBF- and MBF-associated protein Msa1 is required for proper timing of G1-specific transcription in Saccharomyces cerevisiae*. J Biol Chem, 2008. **283**(10): p. 6040-9.
111. Collins, S.R., et al., *Functional dissection of protein complexes involved in yeast chromosome biology using a genetic interaction map*. Nature, 2007. **446**(7137): p. 806-10.
112. Breitskreutz, A., et al., *A global protein kinase and phosphatase interaction network in yeast*. Science (New York, N.Y.), 2010. **328**(5981): p. 1043-6.
113. Tye, B.K., *MCM proteins in DNA replication*. Annu Rev Biochem, 1999. **68**: p. 649-86.
114. Chou, H., A. Glory, and C. Bachewich, *Orthologues of the anaphase-promoting complex/cyclosome coactivators Cdc20p and Cdh1p are important for mitotic progression and morphogenesis in Candida albicans*. Eukaryot Cell, 2011. **10**(5): p. 696-709.
115. Gallego, C., et al., *The Cln3 cyclin is down-regulated by translational repression and degradation during the G1 arrest caused by nitrogen deprivation in budding yeast*. EMBO J, 1997. **16**(23): p. 7196-206.
116. Simon, I., et al., *Serial regulation of transcriptional regulators in the yeast cell cycle*. Cell, 2001. **106**(6): p. 697-708.
117. Cottier, F., et al., *Carbonic anhydrase regulation and CO2 sensing in the fungal pathogen Candida glabrata involves a novel Rca1p ortholog*. Bioorg Med Chem, 2013. **21**(6): p. 1549-54.
118. Fujioka, T., et al., *MpkA-Dependent and -independent cell wall integrity signaling in Aspergillus nidulans*. Eukaryot Cell, 2007. **6**(8): p. 1497-510.
119. Horak, C.E., et al., *Complex transcriptional circuitry at the G1/S transition in Saccharomyces cerevisiae*. Genes & development, 2002. **16**(23): p. 3017-3033.

Appendix I: Full list of Orbitrap LC/MS and Swi4p ChIP-chip data (See excel files in attached CD).

Appendix Table S1: Orbitrap LC/MS analysis of putative Swi6p-interacting proteins

Appendix Table S2: Orbitrap LC/MS analysis of putative Swi4p-interacting proteins

Appendix Table S3: 1st Orbitrap LC/MS analysis of putative Mbp1p-interacting proteins

Appendix Table S4: Orbitrap LC/MS analysis of putative Mbp1p-interacting proteins from larger cultures.

Appendix Table S5: Orbitrap LC/MS analysis of putative Swi6p-interacting proteins in cells blocked in G1 phase

Appendix Table S6: Swi4p ChIP-chip data analysis

Appendix Table S7: VENN result of comparison of location and expression data

Appendix Table S8: Swi4p-HA enriched promoters containing CACAAA motif

Appendix II: Identification of additional factors that contribute to G1/S regulation using a directed approach: Characterization of orf19.5961 (See word file in attached CD).